IDENTIFICATION AND CHARACTERIZATION OF NOVEL CILIOGENIC MACHINERY

Presented by

Ryan Luis Huizar

Undergraduate Thesis

In Partial Fulfillment

of the Requirements

for Graduation with a Degree in

Biochemistry, Honors

The University of Texas at Austin

May, 2017

John Wallingford Supervising Professor	Date
Jeff Barrick Honors Advisor in Biochemistry	Date

This thesis is composed of original research undertaken by myself, and where the work of others is included, their contributions have been duly acknowledged.

Ryan Huizar
May 2017

Acknowledgements

First and foremost, I would like to thank John Wallingford for taking me in as an undergraduate and giving me the opportunity to take on my own projects in the lab. Your passion for developmental biology has rubbed off on me and inspired me to pursue the subject in graduate school. I am greatly appreciative for your patience, time, and effort in guiding me through parts of projects I have been involved in and helping me to understand unfamiliar scientific concepts. Thank you for investing your time in my growth as a scientist over the past two years.

Thanks also to Chanjae Lee for taking so much of her own time to guide me through my experiments during my early stages in the lab and teaching me almost every technique I know. Thanks for always answering my questions when I had them, no matter how simple or irrelevant they were. Your help with designing and conducting experiments, as well as data analysis and interpretation has been invaluable during my time in the lab. Without your time and effort, I would not have been able to develop the set of skills I have today.

Finally, thanks to Mitch Butler, Fan Tu, Jaime Hibbard, Caitlin Devitt, Austin Baldwin, Robert Huebner, Elle Roberson, Jakub Sedzinski, Jacqui Tabler, Rebecca Fitch, and all other members of the Wallingford Lab who have been here during my time. Your helpful input into my projects during lab meetings and journal clubs have helped me immensely.

IDENTIFICATION AND CHARACTERIZATION OF NOVEL CILIOGENIC MACHINERY

Ryan Luis Huizar

The University of Texas at Austin, 2017

Supervisor: John Wallingford

Cilia are microtubule-based structures that project from almost every cell in the vertebrate body. In humans, there are two types of cilia, motile, which generate fluid flow across tissues of the ventricles, airway, and oviduct, as well as in propulsion in single cells, such as sperm, and primary, which are responsible for transducing many signaling pathways, such as Hedgehog. Primary and motile cilia are dependent on a bidirectional trafficking process called intraflagellar transport (IFT) in order to bring material into the cilium, which governs their growth, maintenance, and signaling. IFT is mediated by two distinct protein complexes called IFT-A and IFT-B, which function in anterograde and retrograde transport, respectively. In motile cilia, an organization of multiple large protein complexes within the axoneme allow for wave-like motion to be produced. Instrumental to this motility are axonemal dynein arms, large motor protein complexes that slide along microtubule doublets in a coordinated manner to generate bending.

Here, using the *Xenopus laevis* epidermis as a model ciliated tissue, I describe two studies regarding ciliogenesis in multiciliated cells, a highly-specialized cell type decorated with dozens of motile cilia. First, using a computationally-curated human protein complex map, I identify ANKRD55 as an IFT-B interactor. I demonstrate that this protein traffics through multiciliated cell axonemes and results in severe

developmental defects in its absence. In addition, I describe early insights into the potential role this gene plays in cilia-related human disease. Together, these data suggest that ANKRD55 is a novel member of IFT-B.

Second, I characterize the cell biological processes that underlie the cytoplasmic assembly of axonemal dynein arms, wherein various chaperones and cytoplasmic factors work in unison to fold and complex dynein arm subunits prior to ciliary transport. Using various imaging methods, I show that the factors responsible for dynein arm assembly localize to non-membrane bound cytoplasmic phase-separations in multiciliated cells, which we term DynAPs (Dynein Assembly Particles). I then demonstrate that machinery involved in phase separation of stress granules, ubiquitous cellular structures, is required for formation of DynAPs as well as downstream recruitment of dynein arms to axonemes. This is the first report of cell-type-specific phase separation being utilized as a means of compartmentalization to carry out chaperone-mediated assembly of large protein complexes.

Table of Contents

List of Figures

List of Tables

Chapter 1: Introduction

1.1 - Cilia structure and function

Cilia are microtubule-based protrusions that hold a special place in cell biology: they are among the first described organelles identified by Antoni Van Leeuwenhoek in the 17th century. Since their initial discovery, vast advances have been made in understanding the functions they carry out in biological processes. There are two main types of cilia, motile and primary (immotile) that are built upon a conserved structure. The axoneme of each type consists of nine microtubule doublets that project from a modified centriolar structure called a basal body (Hoyer-Fender, 2010). Surrounding these doublets is a modified plasma membrane that plays various roles in sensation and signaling (Rohatgi and Snell, 2010). Motile cilia also contain two central singlet microtubules that constitute the central pair (a so-called 9+2 structure), which is absent from primary cilia (9+0 structure) (Figure 1.1). Motile cilia are responsible for driving fluid flow across a range of tissues in the human body, including the lungs, ventricles, fallopian tubes, embryonic node, as well as sperm, where they drive either fluid flow or propulsion. Primary cilia, on the other hand, are found on virtually every cell-type in the human body. This importance of these organelles is highlighted by a variety of human diseases collectively termed ciliopathies that manifest in phenotypes ranging from respiratory ailments to neural tube closure defects (Hildebrandt et al., 2011).

At the core of each ciliary axoneme lies a set of nine microtubule doublets, which are nucleated from a docked basal body at the cell membrane. The basal

body itself is composed of a core structure containing nine microtubule triplets (A, B, and C fibers). The A and B fibers serve as nucleation sites of ciliary microtubules and give rise to the A and B tubules of microtubule doublets found within axonemes (Carvalho-Santos et al., 2011). Surrounding this core centriolar structure is a pericentriolar region, which also contains centriolar components, but also serves as a site of triage for many proteins involved in the formation and maintenance of cilia (Kobayashi and Dynlacht, 2011). The region that bridges the basal body to the main axoneme is known as the transition zone (TZ), which may serve as a regulator of entry into and exit from the cilium (Czarnecki and Shah, 2012).

The formation of both primary and motile cilia (ciliogenesis) is dependent on a bidirectional trafficking process called intraflagellar transport (IFT), which is responsible for movement of axonemal precursor molecules such as tubulin to the tip of the axoneme (Rosenbaum and Witman, 2002). This process is dependent on two protein complexes: the IFT-A complex and the IFT-B complex, which work in a coordinated manner with microtubule-binding motor proteins to transport material from the cell body to the distal tip of the cilium (Hao and Scholey, 2009).

1.1.1 - Structure of motile cilia

Motile cilia exist in numerous capacities. In the respiratory tract, ventricles of the brain, as well as the female reproductive tract, dozens of motile cilia project from the surface of a highly-specialized epithelial cell type called multiciliated cells. Here, cilia of multiciliated cells beat in a coordinated, polarized manner to drive directional fluid flow (Brooks and Wallingford, 2014). At the embryonic node,

certain cells are monociliated (nodal cilia), where they beat in a rotational manner to specify left-right patterning in the early embryo (Essner *et al.*, 2002). Motile cilia are also inherently important for movement in unicellular organisms (such as the green algae *Chlamydomonas reinhardtii*) as well as in gametes of species across eukaryotes (Mitchell, 2007).

The motility of cilia is dependent on a concerted action of a variety of protein complexes within the axoneme. However, the behavior is ultimately due to the existence of two rows of dynein motor protein complexes docked along the A-tubule of doublets called the inner dynein arms (IDA) and outer dynein arms (ODA). These complexes interact with the B-tubule of adjacent doublets in an ATP-dependent manner to produce a sliding force, which results in the bending of microtubules (and thus, bending of the axoneme). As this force is propagated along the cilium, a waveform-motion is produced that allows for motility in single cells or propulsion of fluid. The formation and function of these dynein arm complexes will be discussed further in section 1.3.2.

Working in concert with these dynein arms are a number of regulatory structures, including t-shaped structures called radial spokes, protein complexes surrounding the central pair as well as nexin-dynein regulatory complexes (N-DRC) that link microtubule doublets (Isikawa, 2017). EM tomography studies have revealed that these components are placed along microtubules throughout the axoneme in a pattern repeating every 96 nm, which contains an IDA, four ODA, three radial spokes, and a N-DRC (see figure 1.5; Nicastro *et al*, 2006).

Throughout nature, there are also types of motile cilia that deviate significantly from the structure found in cilia of multiciliated cells. Cilia found at the mouse node lack a central pair as well as radial spokes, but retain dynein arms and N-DRC, which likely allows for rotational beating rather than planar beating observed in airway cilia (Shinohara *et al.*, 2015; Woolley, 1998). The Monogenean gill worm *Pseudodactylogyrus* possesses cilia that contain nine outer doublets radial to a single central microtubule (9+1 structure) (Arfa and Reda, 2012). Even further removed from this odd ultrastructure of gametic cilia found in the Cecidomyiinae fly, which can contain hundreds of microtubule doublets with outer dynein arms which form sheets as opposed to cylinders (Baccetti and Dallai, 1976).

1.1.2 - Structure of primary cilia

The structure of the primary cilia was initially described through electron microscopy (EM) studies, and were long thought to be vestigial structures with no importance (Sorokin, 1962; Wheatley, 1969). The functional role of primary cilia was not appreciated until recent studies highlighted the importance of these structures in an array of developmental and homeostatic signaling pathways, including transduction of Hedgehog(Hh), Wnt, and platelet derived growth factor receptor α (PDGFR-α) signals to the cell body. This role has given rise to the analogy that the primary cilium serves as a cell's antenna (Singla and Reiter, 2006).

Because these sensory organelles do not need to generate force like their motile counterparts, they are typically very short (on the order of about one micron). Additionally, a myriad of structural components found in motile cilia are absent in primary cilia. Their microtubule architecture consists of nine microtubule doublets with no central pair. Further, primary cilia lack motility-enabling structures including radial spokes, dynein arms, and N-DRC (Goetz and Anderson, 2010).

Similar to deviations in structure between motile cilia, primary cilia also deviate significantly in structure, even from cell type to cell type in humans. In many circumstances, the primary cilium has evolved to meet specific sensory functions (Zimmerman and Yoder, 2015). The outer segments of photoreceptor cells -- rods and cones -- are modified primary cilia that contain tens of membranous discs that sense light (Pugh, 2015; Wheway et al., 2014). The plasma membrane of primary cilia is also significantly different from that of motile cilia in its protein composition. The primary ciliary membrane is enriched for various signaling components specific to sensory or signalling roles (Pazour and Bloodgood, 2008). One example of this is the localization of polycystin calcium channels to primary cilia in epithelial cells, where they function in mechanosensation (Khayyeri et al., 2015; Nauli *et al.*, 2003).

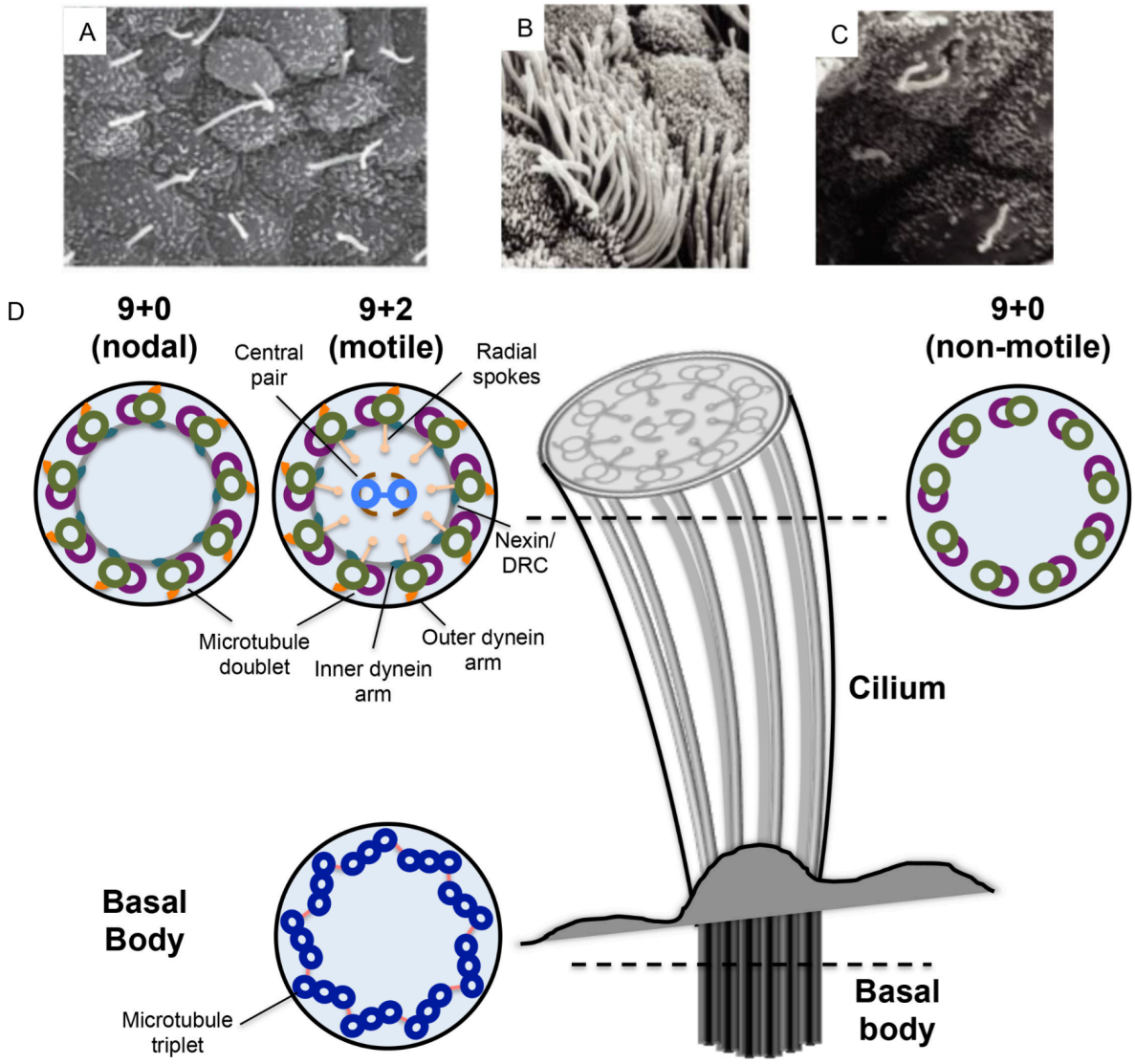

Figure 1.1 – Structures of three types of vertebrate cilia. Throughout the vertebrate body, there are several different types of cilia that carry out distinct functions in development and homeostasis. (A) Scanning electron micrograph (SEM) of cilia at the embryonic node, where cilia drive fluid flow to pattern the left-right axis. (B) SEM of multiciliated cell in a mammalian trachea, where dozens of cilia coordinate to drive fluid flow. (C) SEM of non-motile primary cilia that play key roles in many signal transduction pathways. (D) Schematic of ciliary ultrastructure across various types. All types contain 9 outer microtubule doublets. Motile cilia contain motility machinery including dynein arms, central pair, and radial spokes (The latter two components not found in nodal cilia). (Taken from Praveen et al., 2015)

1.1.3 - Cilia in vertebrate development and homeostasis

As stated previously, cilia serve a multitude of functions in both adult and embryonic tissues, where they play major roles in transduction of signaling pathways, sensation, and motility. At the root of ciliary function is the formation and maintenance of the organelle, which is carried out by sets of genes conserved from algae to humans. These genes often function in basal body integrity, intraflagellar transport, transition zone formation, or a plethora of other integral components of the organelle. As a result, widespread vertebrate mutations can lead to the manifestation of similar disorders all stemming from loss of ciliary function, including skeletal malformation, obesity, polycystic kidneys, among many others (Figure 1.2).

Developmental diseases and disorders rooted in ciliary formation are often tied to failed transduction of particular signaling pathways. For example, loss of cilia often results in neural tube and limb patterning defects, which stem from a failure of hedgehog signals to be transduced. Normally, an integral membrane protein called Patched is localized to the ciliary membrane, where it serves as a receptor for extracellular sonic hedgehog (Shh) ligand. Once bound to Shh, patched is moved out of the ciliary membrane and a seven-pass transmembrane protein called Smoothened is shuttled in via intraflagellar transport. This movement results in release of Gli family transcription factors from the cilium to the cell body, where they transcribe downstream genes (Jiang and Hui, 2008). This pathway is essential for the dorsal-ventral patterning of the vertebrate neural tube, as well as

specification of identity and number of digits on limbs. As a result of the dysregulation of this pathway in loss of cilia, the neural tube fails to close properly, resulting in disorders such as exencephaly and holoprosencephaly; and limbs fail to specify the correct number of digits, resulting in polydactyly (Hildebrandt et al., 2011). In humans, disorders stemming from hedgehog signaling defects underlie the etiology of many ciliopathies, including Joubert's syndrome, which is characterized by mental retardation and ataxia; Meckel-Gruber syndrome, characterized by perinatal death as a result of malformation of many organs; and Bardet-Biedl syndromes, characterized by retinal degeneration, cystic kidneys, obesity, and cognitive impairment (Hildebrandt et al., 2011).

Motile cilia play critical roles in development and homeostasis as well, though not through a direct role in signaling. At the embryonic node, they contribute to the establishment of left-right patterning of an embryo by driving leftward fluid flow to drive downstream signaling events (Norris et al., 2012). Perturbation of any of the components involved in ciliary beating and motility, for example dynein arm components, typically results in *situs inversus*, a condition characterized by randomization of left-right axis of the body (organs normally on the left side of the body now on the right and vice versa).

Motile cilia also play critical roles in homeostasis of various tissues in the body through propelling fluids in a polarized manner. In the brain, multiciliated cells line the ventricles, where they beat in a coordinated fashion to circulate cerebrospinal fluid. In the airway, they drive mucociliary clearance to clear debris from lungs. In the oviduct, multiciliated cells are responsible for guiding ovulated

oocytes to the uterus. Similar to nodal cilia, defects in motility machinery drives pathogenesis of many defects related to these tissues, including persistent respiratory infection, hydrocephalus, and infertility (Afzelius, 1976; Praveen et al., 2015).

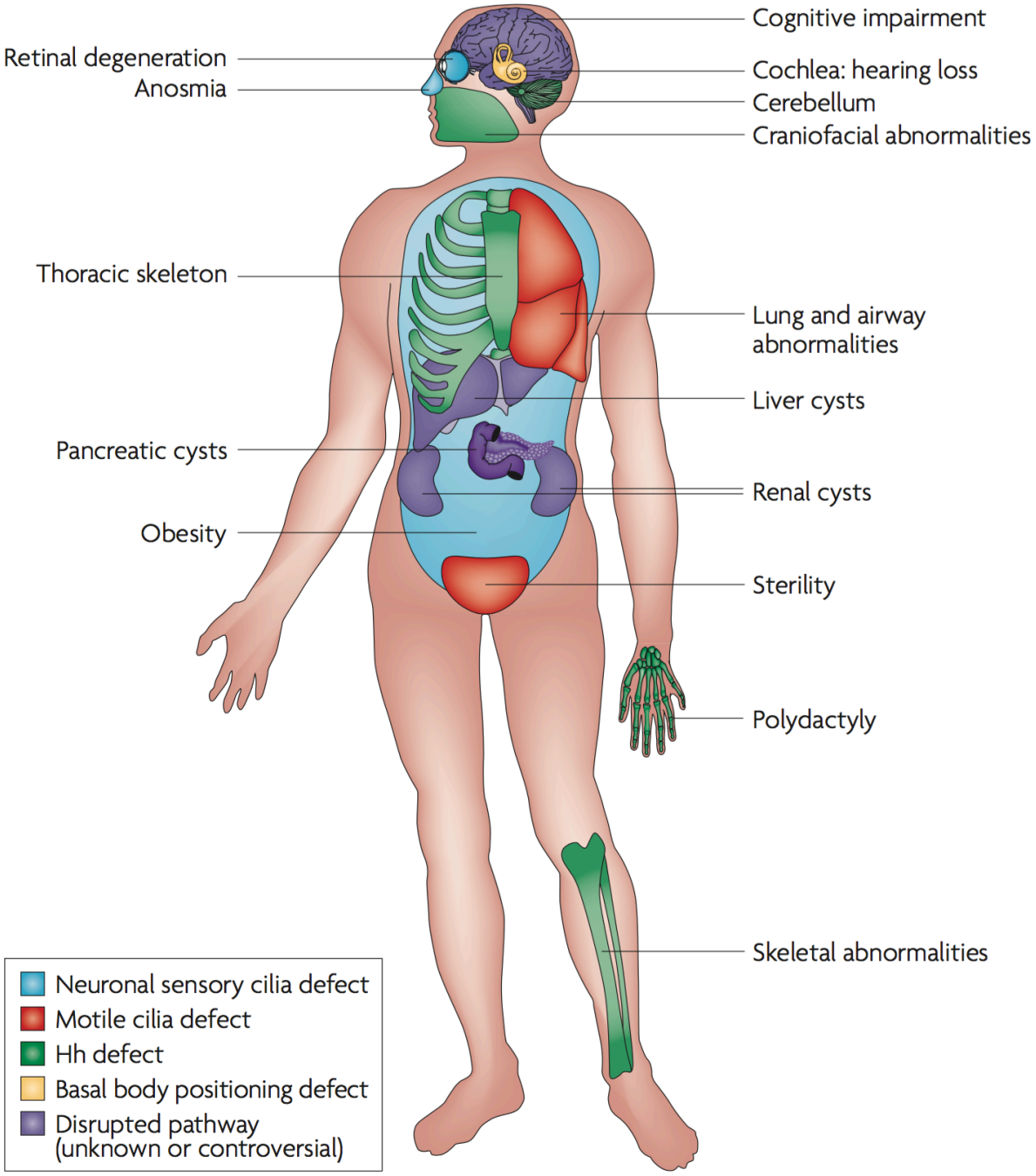

Figure 1.2 – Etiologic linkage of cilia to human disease. Defects in cilia are causative in many pleiotropic disorders in humans. Primary cilia are often linked to defects in signaling pathways, and their dysfunction results in abnormal skeletal morphology, cystic organs (pancreas, kidneys, liver), as well as cognitive impairment and obesity. Motile cilia result in defects of the airway and sterility. Many other conditions observed in ciliopathies do not have a clear causative link. (Taken from Goetz and Anderson, 2010)

1.2 - Building a cilium: ciliogenesis

Though functionally different, the underlying mechanisms of building a cilium -- ciliogenesis -- are much the same between primary cilia and motile cilia. In each, assembly is governed by a multistep pathway (Ishikawa and Marshall, 2011). Basal bodies must first form in one of two ways: either through modification of an existing centrosome or through *de novo* basal body biogenesis, the latter being common when a cell requires dozens of cilia (Garcia and Reiter, 2016; Kobayashi and Dynlacht, 2011). The basal body then docks at the surface of the cell and begins nucleation of microtubules, causing a protrusion of the cell membrane and formation of the transition zone. Protein synthesis cannot take place within the cilium, as it lacks translational machinery. Therefore, a mechanism must exist to extend microtubules as well as bring other material into the developing cilium. This process is carried out by IFT, a microtubule-motor dependent process that brings tubulin monomers to the distal end of the axoneme, as well as other various structural components (Rosenbaum and Witman, 2002; Scholey, 2003). Upon completion of ciliogenesis, the axonemal microtubule doublets exist in a steady-state, wherein tubulin at the distal end is under continuous turnover (Lechtreck *et al.* 2017).

1.2.1 - Transcriptional control of ciliogenesis

Cilia are present across many types of vertebrate tissue and their functions vary greatly between tissue types. Even cilia with seemingly similar roles adapt unique characteristics between tissues (Choksi et al., 2014). For example, airway multiciliated cells possess dozens of cilia spread evenly across their surface, whereas multiciliated cells lining ependymal tissue have longer cilia clustered towards the center of the apical cortex (Guirao et al. 2010; Worthington and Cathcart, 1963). Recent studies have evidenced that this diversity is closely linked to underlying transcriptional machinery that brings about several downstream events required for ciliogenesis.

Core to motile ciliogenesis across tissues are FOXJ1 and RFX family transcription factors. The RFX family is characterized by a winged-helix DNA-binding domain that (Gajiwala et al. 2000). In total, there are eight members of this family, but the majority are not closely related to the ciliary program. Both Rfx2 and Rfx3 are highly expressed in ciliated tissues, namely the brain, kidneys, testis, node, as well as the frog epidermis (Bisgrove et al. 2012; Chung et al., 2012) . In their absence, cilia are dysfunctional, severely truncated, and absent altogether in some cases. Further, several studies have been carried out to elucidate the downstream targets of these genes. In each, key members of ciliogenic machinery were identified as targets, including intraflagellar transport proteins, basal body proteins, and structural components of the axoneme, among others (Chung et al., 2012).

Studies concerning the forkhead-box protein Foxj1 have revealed similar functionality. Loss of Foxj1 results in complete loss of motile cilia in mice, frogs, and fish (Brody et al., 2000; Stubbs et al. 2008; Yu et al. 2008). The role of Foxj1 in induction of the cilia program is highlighted by the formation of motile monocilia on non-ciliated tissues when the transcription factor is ectopically expressed. Effectors of this transcription factor have been shown to play similar roles to those observed in Rfx2 and Rfx3, namely axoneme assembly, cytoskeletal binding, and ciliary motility (Stauber et al., 2017).

Across different tissue types, the Rfx/Foxj1 module is the result of distinct upstream transcription factors and signals. Nodal cilia are dependent on numerous inputs, including Notch and Wnt, which induce ciliogenesis at the node, and Noto, which transcriptionally activates Foxj1 and Rfx proteins (Caron et al. 2012; Lopes et al. 2010; Walentek et al. 2012) . In multiciliated cells, a transcriptional hierarchy regulates cell-fate specification and ciliogenesis. At the top of this hierarchy is Notch, which perturbs ciliation through lateral inhibition (Liu et al. 2007; Morimoto et al. 2010). Downstream of notch signaling is the transcriptional cofactor Multicilin (MCIDAS), which induces multiciliogenesis in non-ciliated cells when ectopically expressed as well as activate downstream transcription factors Myb, Rfx, Foxj1, and other genes involved in multiciliogenesis (Figure 1.3; Boon et al., 2014; Brooks and Wallingford, 2014; Stubbs et al. 2012.).

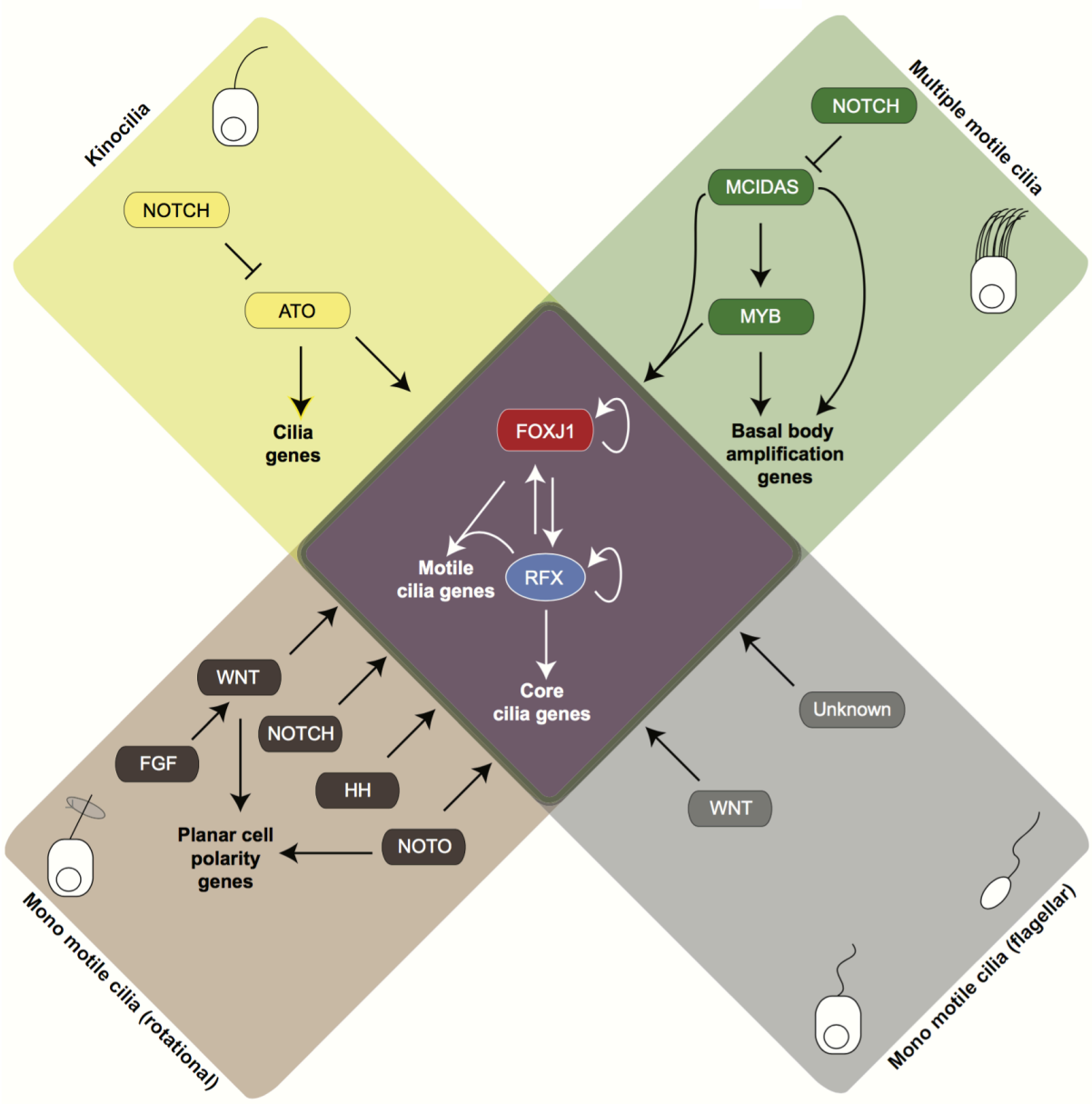

Figure 1.3 – Regulatory networks governing motile ciliogenesis.
Motile ciliogenesis is dependent on a central module composed of FOXJ1 and the RFX family of transcription factors. The formation multiciliated cells is dependent on many different inputs upstream of FOXJ1 and RFX. NOTCH inhibition initializes a cascade in which MCIDAS and MYB drive basal body biogenesis, allowing for the formation of many cilia. Nodal cilia are dependent on a complex interconnectivity of many input signals including WNT, NOTCH, Hedgehog, among others. (Taken from Choksi et al., 2014)

1.2.2 - Basal body formation and docking

Centrioles are a ubiquitous cellular structure that play central roles in cell division, cytoskeletal organization, as well as cell polarity. The cylindrical shape of these organelles is based on organization of tubulin into nine triplets (Conduit, Wainman, and Raff, 2015; Lange and Gull, 1996). During most of the cell cycle, the proximal end of the mother centriole is connected to a orthogonally-oriented daughter centriole through a linkage (Bahe et al. 2005). However, this linkage varies between ciliated cell type. For example, in monociliated cells, basal bodies usually are linked to a daughter centriole, whereas basal bodies in multiciliated cells are not paired. Surrounding the core structure of the centriole is a dense phase-separated region known as the pericentriolar material from which microtubules are nucleated through the formation of a γ-tubulin ring complex (γ-TuRC) complex (Raynaud-Messina and Merdes, 2007).

The formation of basal bodies can be formed by two different means in ciliated cells. The basal bodies of monociliated cells are typically derived from mother centrioles inherited following cell division. Multiciliated cells, on the other hand require many basal bodies to carry out ciliogenesis. To mediate biogenesis a large number of centrioles, multiciliated cells harness an electron-dense structure called the deuterosome, which is likely derived from a daughter centriole (Al Jord *et al.* 2014; Zhang and Mitchell, 2015).

Following formation of nascent basal bodies, undergo migration to the surface of the cell. This process is mediated by both vesicle traffic and actin

dependent movement, during which the centriole acquires many accessory structures, including distal appendages, basal foot, rootlets, and a distal cap (Brooks and Wallingford 2014; Dawe et al., 2006; Sorokin, 1962). The vesicle bound to the basal body then fuses with the plasma membrane, allowing the basal body to anchor to the surface of the cell, at which point microtubules will begin to polymerize to form the early axoneme.

1.2.3 - Intraflagellar transport

A challenge that exists in the formation and function of all cilia is the targeting and organization of a complex milieu of proteins within the axoneme. Proteomic studies of isolated cilia have identified over 600 proteins present within the structure (Pazour et al. 2005). However, the cilium in itself does not possess the capability to translate mRNAs. Further, protein complexes with roles in limitation of diffusion have been shown to localize to the transition zone at the base of cilia (Reiter et al. 2012). Together, these characteristics raise the problem of selective protein entry into the axoneme. Key to this problem is the bidirectional trafficking process known as IFT.

IFT was initially described in the unicellular biciliated algae *Chlamydomonas reinhardtii* in 1993 when a ciliary motility distinct from flagellar beating was described (Kozminski et al. 1993). Within the axoneme, dense particles were shown to transverse the cilium in sandwiched between the outer microtubule doublets and the ciliary membrane, which led others to hypothesize a role for this process in ciliary assembly (Kozminski et al. 1995). Further studies in *Chlamydomonas* shed light on the mechanics of particle movement within cilia, specifically the molecular motors that govern this process. A heterotrimeric complex of two kinesin II motors and an accessory protein (KIF3A, KIF3B, and KAP, respectively), were shown to be necessary for the anterograde transport of IFT proteins (Cole et al. 1993; Kosminski et al. 1995), and a cytoplasmic dynein 2 motor was found to be involved in retrograde transport (Hou et al. 2004; Pazour

et al. 1998). The specific functions of anterograde and retrograde are reflected by phenotypes during perturbation of respective motors; mutations in anterograde transport lead to the complete absence of cilia due to failure to transport precursor molecules to the distal end of the cilia, whereas loss of retrograde transport results in shortened, bulbous cilia due to accumulations of IFT particles at the ciliary tip (Pazour et al. 1998; Signor et al. 1999; Scholey, 2008).

The ciliary motor proteins serve to transport IFT particles, which are made up of two biochemically distinct complexes, IFT-A and IFT-B, that separate from one another at increased ionic strength (Cole et al. 1998). Currently, six proteins are believed to constitute the IFT-A complex (IFT144, 140, 139, 122, 121, and 43), and sixteen subunits are believed to make up the IFT-B complex (IFT172, 88, 81, 80, 74, 70, 57, 56, 54, 52, 46, 38, 27, 25, 22, and 20) (Taschner and Lorentzen, 2016). Biochemical analysis has further subdivided these complexes into core and peripheral subcomplexes based on interaction stability in various *in vitro* assays (Lucker et al. 2005; Mukhopadhyay et al., 2010; Taschner et al. 2016).

Functional studies of the IFT complexes have yielded information regarding various roles that individual subunits may play in specific processes during ciliogenesis. Disruption of the IFT-B complex yields ciliary phenotypes similar to those observed in anterograde motor defects, namely severe ciliogenesis defects (Pazour et al. 2000; Zhang et al. 2016), whereas IFT-A mutants possess phenotypes akin to defects in retrograde transport (Blacque et al., 2006; Fu et al., 2016), suggesting that the A and B complexes take on specific roles required for retrograde and anterograde transport, respectively.

Individual proteins within the IFT-A and IFT-B complexes are predicted to contain numerous domains often involved in mediating protein-protein interactions, such as WD40 repeats, coiled-coil domains, tetratricopeptide repeats, among others (Taschner et al., 2012). This raises the possibility that the IFT subunits are a platform for interaction amongst other IFT subunits, motors, as well as an array of unique cargoes. Assays such as yeast-two hybrid screening, co-immunoprecipitation, and limited crystallography have aimed to shed light on protein-protein interactions that exist within the individual complexes, as well as interactions of subunits with their respective cargoes (Bhogaraju et al., 2011; Lechtreck et al., 2009; Taschner et al. 2014; Taschner and Lorentzen, 2016).

Such assays have produced fruitful results with regard to the IFT-B complex, revealing a vast array of protein interactions that exist within the complex, eventually allowing *in vitro* reconstitution of the complex (Taschner et al., 2011; 2016). Cargo interactions have been more difficult to uncover, as the interactions are usually transient and weak. However, a handful of interactions mediating transport of motility factors, tubulins, and other axonemal precursors have been identified. For instance, transport of IDAs and ODAs has been shown to rely on IFT56 and IFT46, respectively (Hou et al. 2007; Ishikawa et al. 2014; Taschner et al. 2017). IFT25 and 27 have suggested roles in linking the IFT complex to the BBSome, a complex responsible for movement of membrane embedded signaling proteins along the cilia (Eguether et al. 2014). A well-characterized IFT-cargo interaction is that of IFT81 and 74 N-termini with tubulin monomers (Bhogaraju et al., 2013; Kubo et al., 2016).

Compared to the IFT-B complex, interactions that exist within the IFT-A complex have not been well characterized. The core of the IFT-A complex was named as such because three components -- IFT122, IFT140, and IFT 144 -- formed a stable complex independent of the three remaining members of the complex (Mukhopadhyay et al. 2010). In addition, various immunoprecipitation experiments have identified putative pairwise interactions that exist within the complex (FIGURE)(Behal et al. 2012). Though cargo interactions have not yet been uncovered, links have been made between the IFT-A complex and selective entry of membrane proteins into primary cilia (Fu et al. 2016, Mukhopadhyay et al. 2010). Of particular note concerning members of the IFT-A complex is the presence of beta-propeller domains, which have been previously shown to function in COP1-mediated vesicle transport (Beck et al. 2009). This has led to the hypothesis that these proteins may be required for vesicle fusion at the ciliary base, for which a recent study has found evidence (Fu et al. 2016).

Surrounding the basal body is a “pool” of IFT complexes that associate with one another before transport into the cilium. These complexes oligomerize with one another in an unknown stoichiometry to form IFT “trains” that transverse the cilium. The trains travel to the ciliary tip via anterograde kinesin motors along B-tubules of microtubule doublets, at which point they are disassembled then remodeled into retrograde trains of different morphology (Stepanek and Pigino, 2016). Over the course of ciliogenesis, IFT trains transport cargoes from the base of the cilium to the tip in order to mediate both the growth and organization of the

ciliary compartment. In mature cilia, this active process remains, serving as a means of structural maintenance (Figure 1.4).

However, there are exceptions to the roles of IFT in cargo transport into the cilium. Several recent studies have shed light on the ability of many proteins to enter the cilium independent of IFT. For example, tubulin and the microtubule binding protein EB1 diffuse readily into the cilium over the course of ciliogenesis (Craft et al., 2015; Harris et al., 2016). Additionally, membrane proteins localizing to the cilium, such as the Somatostatin Receptor 3 and Smoothened (a Hedgehog signal transducer) predominantly move through the compartment via IFT-autonomous diffusion (Ye et al. 2013).

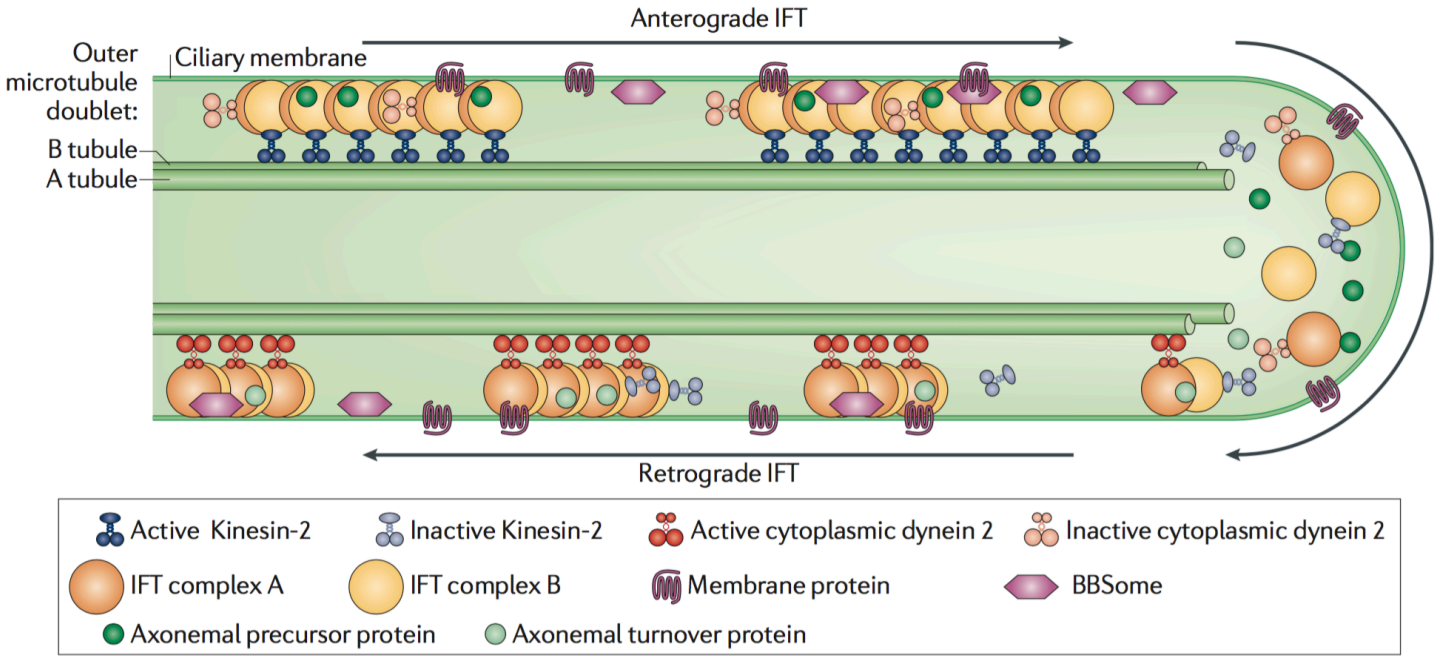

Figure 1.4 – Intraflagellar transport. Intraflagellar transport (IFT) is an active process through which molecules are shuttled through the ciliary axoneme. This bidirectional process depends on movement of motor proteins along microtubules: anterograde traffic (base to tip) is dependent on a heterotrimeric kinesin-II motor, whereas the retrograde movement (tip to base) is dependent on cytoplasmic dynein-II. Cargoes transverse the cilium attached to IFT complexes A and B, which oligomerize to form IFT "trains." IFT trains assemble at the base of the cilium, then move to the tip of the cilium via anterograde transport, at which point the trains disassemble, then restructure to form retrograde trains that are transported back to the cell body. An additional component of the IFT machinery is the BBSome, a complex of proteins that binds to IFT-B and is required for transport of transmembrane cargoes. (Taken from Ishikawa and Marshall, 2011)

1.3 - Axonemal Dynein Arms

1.3.1 - Axonemal dynein structure and function

Dynein is a cytoskeletal motor protein that is responsible for guiding organelles, proteins, and mRNAs towards the plus-end of microtubules throughout cells. The importance of this class of motor protein is underscored by the numerous cellular events they regulate, including cytosolic organization, cell division, ciliogenesis, as well as ciliary beating (Roberts et al., 2013). Force-generation by dyneins is the result of coordination of ATPase activity and regulated binding of heavy chains to microtubules to produce a power stroke (Oiwa, 2013). There are nine classes of dynein heavy chain found in metazoans: one bona fide cytoplasmic dynein, one cytoplasmic dynein that has evolved a role in intraflagellar transport (IFT dynein), and seven axonemal dyneins responsible for ciliary motility (Roberts et al., 2013).

Axonemal dynein heavy chains are half-megadalton, multidomain proteins that associate with several intermediate, intermediate-light, and light chain dyneins to form dynein arms. Studies of these arms have been primarily carried out in *Chlamydomonas*, wherein genetic screens and electron microscopy have given insight into the structure and function of the complexes. ODAs contain two different dynein heavy chains (three in *Chlamydomonas*) along with approximately fifteen to twenty accessory subunits that serve as adaptors to the A-tubule as well as interactors with various components of the ciliary ultrastructure including radial spokes (Ishikawa, 2016; King, 2016). A subset of these accessory light chains and

intermediate chains serve as adaptors for the non-catalytic regions of dynein heavy chains (Oda et al., 2016). IDAs are aligned adjacent to the ODAs on the A-tubule and are composed of eight dynein heavy chains that also interact with other motility machinery, such as the N-DRC (Bui et al., 2008).

Along axonemes, dynein arms are docked in a repeated fashion, with an ODA every 24 nm and an IDA every 96 nm (Figure 1.5). However, the composition of dynein arms at different regions of the ciliary compartment is likely to vary slightly. Evidence for this has been derived from immunofluorescence microscopy in human airway cilia as well as well as *Clamydomonas*, which shows that specific dynein arm subunits localize to distinct regions of the axoneme. Instances of this include the relationship between the human dynein heavy chains DNAH5 and DNAH9. The former localizes along the entire length of the cilium, but is replaced at the distal tip of the cilium by DNAH9 (Fliegauf et al. 2005). Another human heavy chain isoform, DNAH11, has been shown to localize only to the proximal region of airway cilia (Doughtery et al., 2016). These findings are supported by studies in *Chlamydomonas*, wherein heavy chain dyneins DHC3, DHC4, and DHC11 localized to the proximal region (Yagi et al. 2009). This variation is reflected by the fact that there are multiple representatives for some axonemal dyneins in the genome -- humans, for example have a total of 14 axonemal dynein heavy chain isoforms, potentially hinting at specialized roles in beat regulation at various regions of the cilium.

The mechanics of ciliary beating have long been debated, however, with the recent development of cryo electron tomography the various stages of ciliary

beating have been observed, illuminating potential models for this complex process. One mechanistic example that has withstood the test of time is the so-called switch point model, in which activity of dyneins at one side of the axoneme cause directional bending in one direction of the ciliary beat, whereas dynein activity on the opposite side of the axoneme cause bending in the opposite direction (Satir and Matsuoka, 1989). Genetic studies of radial spoke and central pair proteins have identified these components as critical to this coordination. They are hypothesized to carry this out by transmission of signals to other complexes to induce dynein arm activity, such as the dynein regulatory complex and the calmodulin and spoke associated complex (Dymek et al., 2011; Heuser et al. 2009; Oda et al. 2014). In the beat cycle, outer dynein arms are supposed drivers of beat frequency, whereas inner dynein arms are believed to play roles in shaping the ciliary waveform (Bui et al., 2012; Hamasaki et al., 1999).

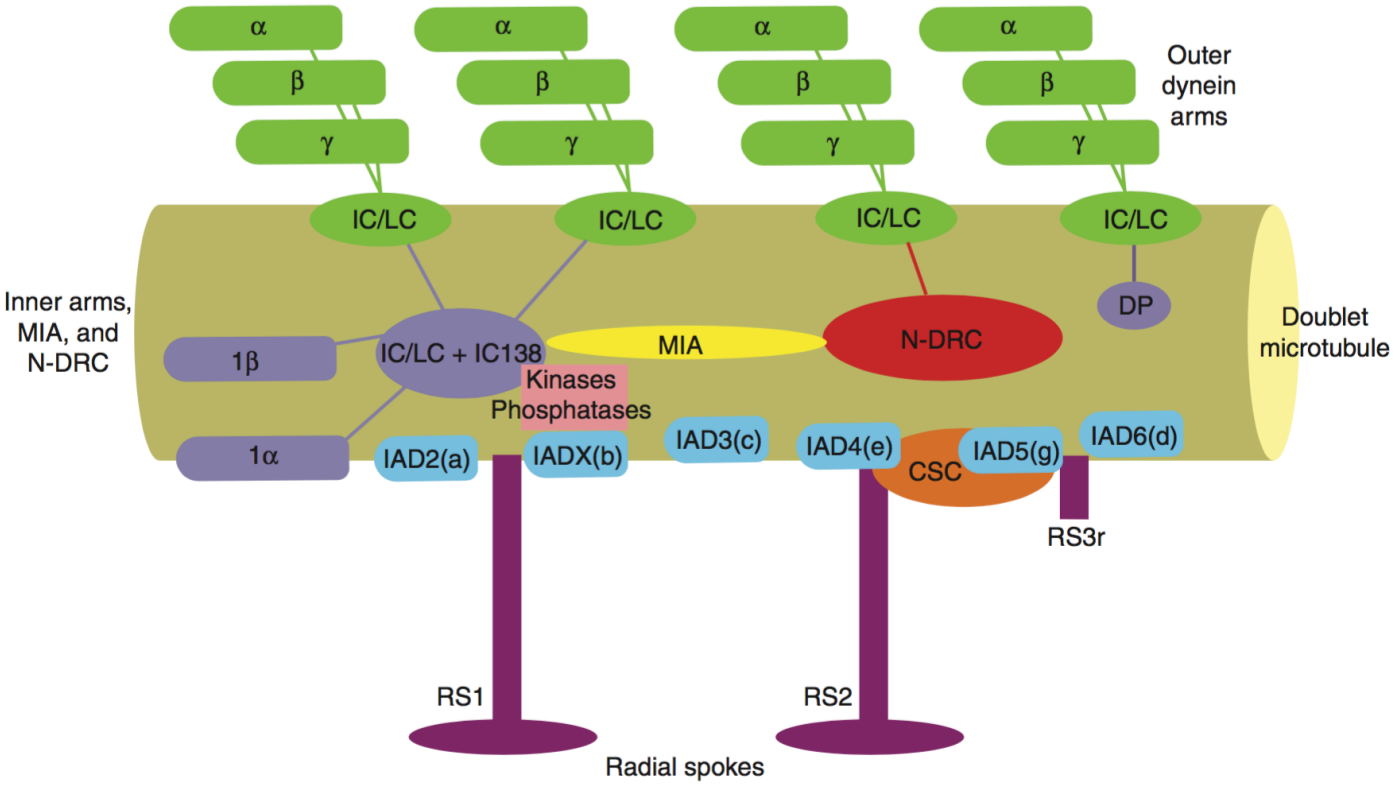

Figure 1.5 – 96-nm repeat of motile cilia. Organization of the motile ciliary axoneme is based upon a repeating structure of protein complexes that span 96 nm. Each repeat contains four outer dynein arms spaced 24 nm apart from one another (Green in figure). Inner dynein arms contain 6 monomeric dynein heavy chains (blue) along with dynein subunits I1/f (purple). This structure spans the entire repeat. The dynein regulatory complex (Red) is linked to inner dynein arms though the MIA complex (yellow). Each repeat also contains three radial spokes (maroon) as well as a calmodulin and spoke associated complex (orange) that interacts with both inner dynein arms and radial spokes. (Taken from King, 2016).

1.3.2 - Cytoplasmic preassembly of dynein arms

In order to produce motion, the cilium requires the coordination of multiple structural components. Implied in this coordination are many ciliary motility defects that arise in the absence of axonemal constituents. Over 30 human genes have been identified as causal in a ciliopathy termed primary ciliary dyskinesia (PCD), which affects approximately 1 in 10,000 live births (Praveen et al., 2015). Characterized by immotile cilia, PCD manifests in chronic respiratory infections, situs inversus, male and female infertility, and in rare cases hydrocephalus (Werner et al., 2015). In the majority of PCD cases, causal genes encode parts of the ciliary ultrastructure. Among the most common are the dynein arm subunits (DNAH5, DNAI1, DNAI2; Loges et al., 2008; Olbrich et al., 2002; Pennarun et al., 1999), central pair proteins (HYDIN; Olbrich et al., 2012), radial spoke proteins (RSPH1, RSPH4a, RSPH9; Castleman et al., 2009; Knowles et al., 2014), as well as members of the dynein regulatory complex (DRC1; Wirschell et al., 2013). However, in the last decade, a combination of human PCD genetics and forward genetic screens has led to the discovery of a population of cytoplasmically localized proteins required for the assembly of both IDAs and ODAs, which as now classified as the axonemal dynein assembly factors (DNAAFs).

The presence of proteins with this role have been long hypothesized, as immunoprecipitation of axonemal dynein subunits in cytoplasmic fractions of *Chlamydomonas* revealed that complex formation is abrogated in several dynein

arm mutants (Fowkes and Mitchell, 1998). Ten years later, a forward genetic screen in the medaka fish *Oryzias latipes* identified a mutant with left-right patterning defects and paralyzed cilia. that failed to recruit IDAs and ODAs to cilia. This phenotype was traced to a gene encoding a cytoplasmic protein, kintoun (KTU, now renamed DNAAF2), and later identified as causal in several PCD patients (Omran et al., 2008). This finding served as a catalyst for identification of similar genes. Ten other cytoplasmic proteins have been identified that lead to loss of IDAs and ODAs when perturbed, including DNAAF1 (LRRC50; Duquesnoy et al., 2009; Loges et al., 2009), DNAAF3 (Mitchison et al., 2012), DNAAF4 (DYX1C1; Tarkar et al., 2013), DNAAF5 (HEATR2; Diggle et al., 2014; Horani et al., 2012), C21orf59 (Austin-Tse et al., 2013), SPAG1 (Knowles et al., 2013), CCDC103 (King and Patel-King, 2015; Panizzi et al., 2012), LRRC6 (Horani et al., 2013; Kott et al., 2012), ZMYND10 (Moore et al., 2013; Zariwala et al., 2013), and most recently, PIH1D3 (Dong et al., 2014; Olcese et al., 2017; Tamara et al., 2017)

The necessity of these factors is reflected by the massive size of the dynein arm complexes, which are on the order of megadaltons with individual subunits exceeding 500 kDa. The large sizes of these polypeptides lead to the problem of folding -- during protein synthesis several stretches of hydrophobic residues raise the potential for aggregation in the cytoplasm. Typically, cells stabilize these stretches and folding and prevent aggregation through utilization of chaperone machinery. It is likely that many dynein assembly factors act in this fashion as evidenced by several reported interactions between this machinery and the heat shock protein 70 and 90 (Hsp70/90) complexes (Tarkar et al., 2013; Olcese et al.,

2017; Omran et al., 2008), as well as the CCT chaperonin complex (Tarkar et al., 2013). This is further reported by the decreased proteolytic of ODA heavy chains in the absence of *pf13* and *pf22*, the *Chlamydomonas* orthologs of human DNAAF2 and DNAAF3, respectively (Mitchison et al., 2013).

Further, many dynein assembly factors contain domains that often mediate protein protein interactions, including tetratricopeptide repeats (TPR; factors includie DNAAF4, SPAG1), CS (Pih1d3, DNAAF2), as well as PIH (protein interacting with Hsp90) domains (KTU, Pih1d3, and *Mot48*, a *Chlamydomonas* protein). Efforts have been made to gain mechanistic insight into dynein arm assembly, namely through utilization of protein association assays to probe interactions between dynein assembly factors as well as ubiquitous cellular machinery. Findings have included direct interactions between a multitude of factors and the intermediate chain dynein DNAI2, which serves as an attachment point for dynein heavy chains of the outer dynein arm (Diggle et al., 2014; Olcese et al., 2017; Omran et al., 2008; Tarkar et al., 2013). Further, many dynein assembly factors have been shown to associate with one another, including pairwise interactions between DNAAF2 and DNAAF4 (Tarkar et al., 2013), between LRRC6 and ZMYND10 (Zariwala et al., 2013), and between LRRC6 and C21orf59 (Jaffe et al., 2016).

Discreet PIH1 domains are believed to mediate several of these interactions (Yamomoto et al., 2010). Interestingly, the N-terminal region of DNAAF2 displays similar homology to the yeast Pih1 protein, a member of the nucleolar R2TP complex involved in pre-ribosomal RNA processing (Kakihara and Houri, 2012;

Zhao et al., 2008). In this complex, a TPR domain on the protein Tel2 binds to the CS domain of Pih1, which in turn binds to Rvb1/2 and Tel2, which activates downstream phosphoinositol-kinase like kinases (PIKKs) (Kakihara and Houri, 2012; Pal et al., 2014). Similarly, the TPR domain of DNAAF4 interacts with DNAAF2, the PIH domain of which is believed to interact with DNAI2 during ODA assembly (Olcese et al., 2017; Omran et al., 2008). Strikingly, the zebrafish ortholog of Rvb2, Ruvbl2, has been shown to interact with Lrrc6 and results in motile ciliary defects when mutated, thus drawing another similarity between the R2TP complex and cytoplasmic dynein assembly factors (Zhao et al., 2013).

The mechanism by which these proteins cooperate with one another to mediate the folding and/or assembly of dynein arms is unclear as of yet. Most of the known dynein assembly factors have been recognized as necessary for ODA and IDA formation. Specific functions that each factor serves in these individual (or paired) processes is not known, however recent experiments have hinted that individual factors may play important roles in subunit recruitment to IDAs. In *Chlamydomonas*, the PIH-domain containing protein *mot48* is required for IDA formation via recruitment of dynein heavy chains b, c, d, and e (Yamomoto et al., 2010); similarly, *pf13 (*DNAAF2 in humans), was revealed to play roles in recruitment of subunit c to IDAs (Omran et al., 2008). PIH1D3 is hypothesized to play a similar role in recruitment of dynein subunits f and g to inner dynein arms, as cryo electron tomography of human airway cilia suggests (Olcese et al., 2017).

1.4 - Liquid-liquid phase separation

A major challenge that cells have faced over the course of evolution is that of carrying out complex biochemical reactions in the crowded milieu of the cytoplasm. In many cases, certain reactions require a specialized environment that is different in many ways from the cytosol including varying pH, ionic concentration, and localized concentration of reactants. Eukaryotic cells have solved many such problems through partitioning these reactions to specialized compartments called organelles, which may contain a distinct environment required for such reactions to occur (Rothfield, 2014). Typically, this is achieved through the use of one or more phospholipid bilayers, which serve many purposes. In the lysosome, this barrier serves as a means of protecting the rest of the cell from the hazardous proteolytic molecules that reside within it (de Vuve, 1963). In the peroxisome, the membrane serves to prevent oxidants from dispersing into the rest of the cell (Deisseroth and Dounce, 1970). In mitochondria, membranes regulate local pH in order to drive ATP synthesis through utilization of electrochemical gradients (Ernster and Schatz, 1980).

However, it has recently been discovered that cells also utilize other means of compartmentalization wherein no membranes are present. Rather, these compartmentalized regions of cytoplasm or nucleoplasm are formed via molecular crowding events dependent upon weak multivalent interactions between biological macromolecules (discussed further in section 1.4.2; Hyman et al., 2014). There are many bona fide organelles in the cell that operate in this manner, including stress granules, which serve as points of RNA triage during cellular stress (Buchan

and Parker, 2009); nucleoli, the nuclear regions of ribosomal biogenesis (Hernandez-Verdun, 2006); P-bodies, sites of RNA metabolism and translational regulation (Eulalio et al., 2007); and centrosomes, the organelles responsible for microtubule nucleation and organization (Woodruff et al., 2015).

1.4.1 - Properties of biological liquid-liquid phase separations

The absence of a phospholipid bilayer raises the question of how non-membranous structures are able to remain intact as distinct entities within the aqueous, dynamic environment of the cytosol. In the past-decade, the physical nature of these structures has been described as liquid droplets that are out of phase with the remainder of the cytoplasm and arise through liquid-liquid demixing, similar to how oil forms droplets in water (Hyman and Simons, 2012). Pioneering work to uncover properties of non-membrane bound organelles was carried out in the early embryo of the nematode *Caenorhabditis elegans*, where germline P-granules help establish anteroposterior polarity by segregating specific RNAs to the posterior side of the embryo (Wang and Seydoux, 2014). Observation of these granules *in vivo* revealed that they held physical properties inherently similar to viscous liquids including fusion, rapid exchange of components with cytosol, and deformed under shear flow (figure 1.6; Brangwynne et al., 2009). This finding paved the way for observation of similar properties in now well-known liquid liquid phase separations including stress granules, nucleoli, and P-bodies (Brangwynne et al., 2011; Han et al., 2012).

Many of the above described phase-separated organelles are not simple mixtures, but complex mixtures with dozens to hundreds of component proteins. Parsing the roles of these individual proteins to identify which are required for phase separation and which are involved in higher-order functions of the compartment has been an elusive problem, but recent *in vitro* work has begun to identify the key players in many such compartments. It is well understood that

many phase separated structures are directly involved with RNA (nucleoli, P-bodies, stress granules, etc.), and many proteins within these dynamic structures contain RNA binding domains, leading many to study the role of ribonucleoproteins (RNPs) in separation (Brangwynne et al., 2011). Typically, proteins bind to RNAs through RNA-binding domains with fairly low affinity, however, many RNAs are able to bind to such domains at a time, thus increasing the total affinity (a property called multivalency). Supporting their role in this process, when RNA-binding proteins are mixed with RNA in vitro, they undergo liquid-liquid phase separation in a process dependent on low-complexity domains (stretches of protein with low amino acid variation) (Kato et al., 2012). Further supporting this notion is the finding that specific RNA-binding proteins PGL-1 and PGL-2 serve as scaffolds in the formation of *C. elegans* P-granules (Hanazawa et al., 2011). Together, these findings have led to the formation of a model that describes phase separation as dependent on three classes of molecules, multivalent protein-protein and protein-RNA interactions drive the formation of a large scaffold. The second type of molecules are proteins that bind specifically to the first class of molecules, some that may play roles regulation of properties within specific compartments. The third and most abundant class are proteins and other molecules not involved in phase-separation, but carrying out specific biochemical reactions (Hyman and Simons, 2011).

Another set of problems faced by the cell are nucleation and regulation of size of phase-separations. For example, in the *C. elegans* embryo, P-granules may have a diameter of several microns, whereas the P-bodies found in cultured cells

typically are far less than a micron in diameter. It is believed that size constraints are, in part, due to diffusive transport that occurs between the droplet and the surrounding cytoplasm. Large droplets will be able to readily exchange more material with their surrounding cytosol; however, it will take significantly longer for the processed molecule to diffuse out of the droplet to the cytosol. Supporting evidence for this has been drawn from comparison of droplets in cells of many different sizes, revealing that size does not scale linearly -- a *Xenopus laevis* oocyte for example, will favor multiple small droplets to few large (Brangwynne, 2013). Nucleation of biological structures is rarely random. Condensation of a homogenous mixture is not energetically favorable (Binder and Stauffner, 1976), and thus, nucleation of droplet organelles is likely to occur in a heterogeneous fashion, wherein a pre-existing base serves as a precursor for the entire structure. In fact, there are well studied examples of this, such as the mediation of centrosome formation by the presence of a centriole (Zwicker et al., 2014). In the case of RNP-containing organelles, the process of phase separation is believed to rely on locally concentrated RNAs that bind to proteins through multivalent interactions that preclude self-organization of higher-ordered structures.

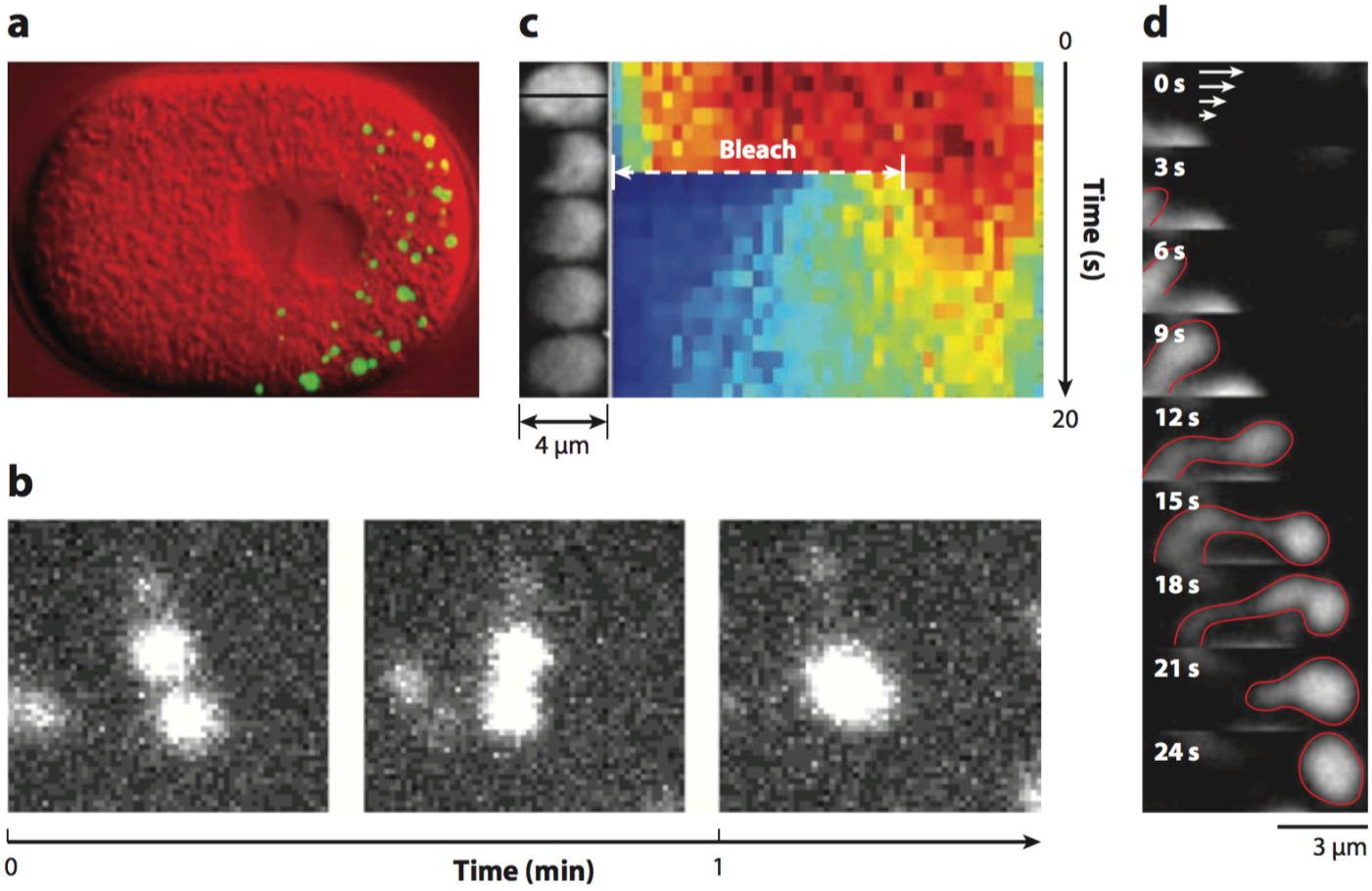

Figure 1.6 – Liquid-like properties of cytoplasmic phase separations. (a) A one-cell stage *C. elegans* embryo is shown with P-granules labeled. (b) P-granules fuse with one another when in close proximity. (c) When bleached, P-granules exhibit very quick recovery, indicating rapid exchange of molecules with the cytoplasm (red is high intensity, blue is low). (d) When shear flow is applied to P-granules, they undergo deformation. (images from Brangwynne et al., 2009; figure from Hyman et al., 2014)

1.4.2 - Functions of phase separation in biology

At the root of many biochemical processes that occur in cells is the clustering of multi-protein complexes to carry out particular tasks. The highly dynamic nature of cytosolic phase separations provides a basis for many of these processes to occur – protein complexes are allowed to cluster in close proximity with one another, and products can be easily released into the surrounding cytosol via diffusion and trafficked to other structures within cells. In recent studies, it has been observed that many different cellular processes are carried out in this manner, namely in signal transduction. Examples of this include phase separation of Dishevelled (Dvl) in Wnt signaling (Schwarz-Romond et al., 2007; Sear et al., 2007), phase separation of N-WASP, an important actin regulator (Li et al., 2012). Further, phase transitions play key roles in cytoplasmic RNA, wherein P-bodies and stress granules regulate are utilized as points of RNA metabolism and translation repression. Recently it has been observed that phase separation is important to local translation of specific RNAs in neurons and at the leading edge of migrating cells (Holt and Schuman, 2013; Willett et al., 2011).

These findings have uncovered that phase-separation may be a central principle in biology through which many biochemical processes are organized within the cytoplasm. Current biochemical and microscopy methods allow for significant progression in our understanding of droplet organelles and the many ways they may influence metabolism, signal transduction, translational regulation, and protein complex assembly, among others.

Chapter 2: Ankrd55 is a member of the IFT-B complex

2.1 - Background

Cilia are microtubule-based projections from cells that hold many functions in signaling and homeostasis in vertebrates. Formation and function of cilia is dependent on IFT, a bidirectional trafficking process composed of two multi-protein complexes, IFT-A and IFT-B (Taschner and Lorentzen, 2016). As discussed in Chapter 1, defects in cilia often lead to diverse human ailments, including skeletal abnormalities, neural tube closure defects, and cognitive impairment, among many others. To cultivate a better understanding of the molecular basis of many of ciliopathies, study of protein composition and protein interactions within the cilium have recently gained footing (Gupta et al., 2015; Ishikawa et al., 2012).

The relationship between phenotype and genotype is a central concept in molecular biology. One of the many ways to study this relationship is to gain an understanding of the relationships that exist between proteins within a cell, as these biomolecules are the major force in carrying out cellular functions. Studying protein-protein interaction is not only a critical tool in understanding biochemical processes within the cell, but also in understanding many human genetic diseases, because interacting proteins are often linked to similar phenotypes. One of the main tools that has been utilized to answer this problem is through proteomics via mass spectrometry to construct partial maps of human protein complexes through a variety of methods. Recently, work utilizing affinity purification / mass spectrometry (AP-MS) and co-fractionation / mass spectrometry (CF-MS) have expanded the known set of human

protein complexes (Hein et al., 2015; Huttlin et al., 2015; Wan et al., 2015). However, this diverse set of experiments yielded vastly different datasets that had very little overlap. This could be due to different types of cells used in each assay, variation in experimental method, and false positives. To circumvent these problems, a computational pipeline was designed and integrated to produce a novel protein complex map based upon the three aforementioned studies, termed hu.MAP, which vastly expanded coverage of human protein complexes (Drew et al., In review).

A central application of this protein complex map was its implementation to characterize biological modules relevant to human disease, namely ciliopathies. Here, efforts to identify and characterize novel ciliogenic machinery, namely those involved in the process of IFT, are discussed. Using the *Xenopus* epithelium as a model ciliated tissue, we describe and characterize a new IFT-B complex member, ANKRD55.

2.2 – Results

2.2.1 hu.MAP identifies ANKRD55 as an IFT-B interactor

The use of hu.MAP as a means of identifying ciliary proteins was fruitful. Of interest to us, hu.MAP was able to recapitulate many known protein-protein interactions within in both IFT-B and IFT-A complexes. Not only did the map identify interactions that exist within each complex, but it also revealed interactions of subcomplexes within IFT-B including parts of the IFT-B1 complex containing members IFT22, IFT46, IFT74, and IFT81. Additionally, the map identified interactions recently reported to make up the IFT-B2 complex, including members IFT38, IFT54, IFT57, and IFT172 (Taschner, 2016). Further, the map also identified interactions between each of the members of the anterograde motor complex of IFT, including members KIF3A, KIF3B, and KAP (Scholey et al., 2008). Interestingly, no interactions were identified between IFT-A and IFT-B complex members, presumably because the interaction between the two complexes is not stable, and thus would not be identified by methods used to generate interaction data.

In addition to well-characterized ciliary machinery, hu.MAP also identified interactions between known IFT components and uncharacterized proteins. For example, members of the IFT-A complex were predicted to bind the proteins METL21B and C11orf74, and members of the IFT-B complex were predicted to bind to EHBP1, HSBP1, and RABEP2. Intriguingly, RABEP2, a member of the endosomal sorting complex, has recently been implicated in ciliogenesis and hedgehog signaling defects (Airik et al., 2016).

Another interesting prediction was that between the IFT-B members IFT70 (paralogs TTC30a and TTC30b), IFT52, and IFT27 with the poorly characterized protein ANKRD55 (Figure 2.1a, b). ANKRD55 is a 68 kDa protein containing 9 ankyrin repeats, a common domain that is important for mediation of protein-protein interactions in a variety of contexts (Figure 2.1c; Mosavi et al., 2004). Previously, ANKRD55 has been identified as a candidate multiple sclerosis risk gene, however, no link has been drawn between this protein and the ciliogenic machinery (Lopez de Lapuente et al., 2016).

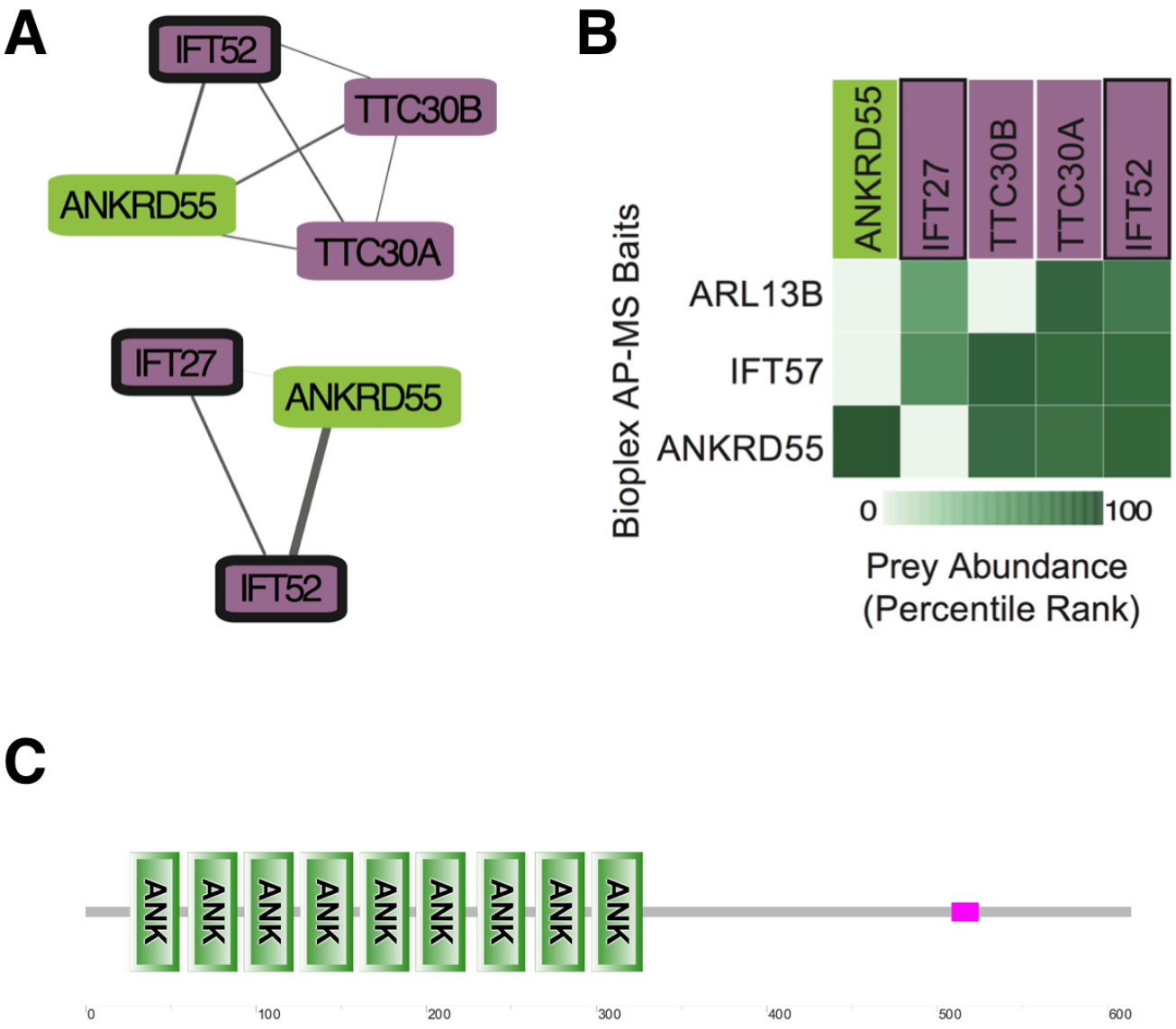

Figure 2.1 – ANKRD55 interacts with IFT-B proteins (A) Network view of known IFT proteins interacting with ANKRD55 as predicted by hu.MAP. (B) Matrix of AP-MS experiments show strong support for interactions between ANKRD55 with IFT70, and IFT52. (C) Domain prediction for human ANKRD55 reveal nine ankyrin repeats within the protein. (domain prediction was done using SMART; Letunic et al., 2014). Interaction data from hu.MAP courtesy of Kevin Drew.

2.2.2 ANKRD55 displays characteristics of other IFT-B members

In cilia, IFT complexes transverse the axoneme along microtubules to transport ciliary proteins the axonemal tip via anterograde transport and move back to the cell body via retrograde transport. As such, when observed via high-speed time lapse microscopy, IFT proteins typically move up and down axonemes in a punctate pattern.

To assess whether ANKRD55 exhibits characteristic dynamic behavior of other IFT proteins, *Xenopus* ANKRD55 was cloned and fused to green fluorescent protein (GFP) and transcribed mRNAs were injected into ventral blastomeres of 4-cell stage *Xenopus* embryos. Live imaging of epidermal multiciliated cells revealed that ANKRD55-GFP localized to axonemes in a punctate pattern, similar to that observed in other IFT-B proteins (Figure 2.2a). *In vivo* High-speed time lapse confocal microscopy was then utilized to track ANKRD55-GFP over time (Brooks and Wallingford, 2012), revealing that ANKRD55 is dynamic in axonemes and traffics throughout cilia with both anterograde and retrograde trajectories (Figure 2.2b**)**. Because ANKRD55 moved along axonemes, we hypothesized that it would traffic alongside another member of the IFT-B complex, CLUAP1 (IFT38). Indeed, kymographs produced from two-color confocal microscopy revealed that ANKR55-GFP puncta colocalized with CLUAP1-RFP puncta as they moved along axonemes (Figure 2.3**)**.

Typically, genes that play roles multiciliated cells, IFT proteins in particular, display a clear expression pattern in *Xenopus*. *In situ* hybridization of ciliary genes shows clear patterns in ciliated tissues – along the epidermis there is typically a “salt and pepper” pattern indicating multiciliated cells, as well as staining of nephrostomes, another multiciliated tissue. (Hayes et al., 2007). To assay the specificity of expression

of ANKRD55 to ciliated cells, we carried out *in situ* hybridization and found distinct expression in nephrostomes, as well as strong expression in the notochord and ventral neural tube, similar to the expression pattern observed in the IFT-B complex member IFT81 (Figure 2.4).

In previous studies, it has been observed that perturbation of certain cilia genes leads to disrupted localization of other ciliary machinery. Of particular note, it has been observed that loss of retrograde transport, either by disruption of IFT dynein or IFT-A proteins leads to accumulation of IFT-B complex proteins within the axoneme. We assessed whether ANKRD55 would accumulate in the axonemes under IFT-A disruption by knockdown of the ciliopathy gene JBTS17, which was recently shown to elicit buildup of IFT-B, but not IFT-A (Toriyama et al., 2016). Under JBTS17-KD, we observed a buildup of ANKRD55 within the cilium, consistent with its predicted interaction with other IFT-B proteins (Figure 2.5).

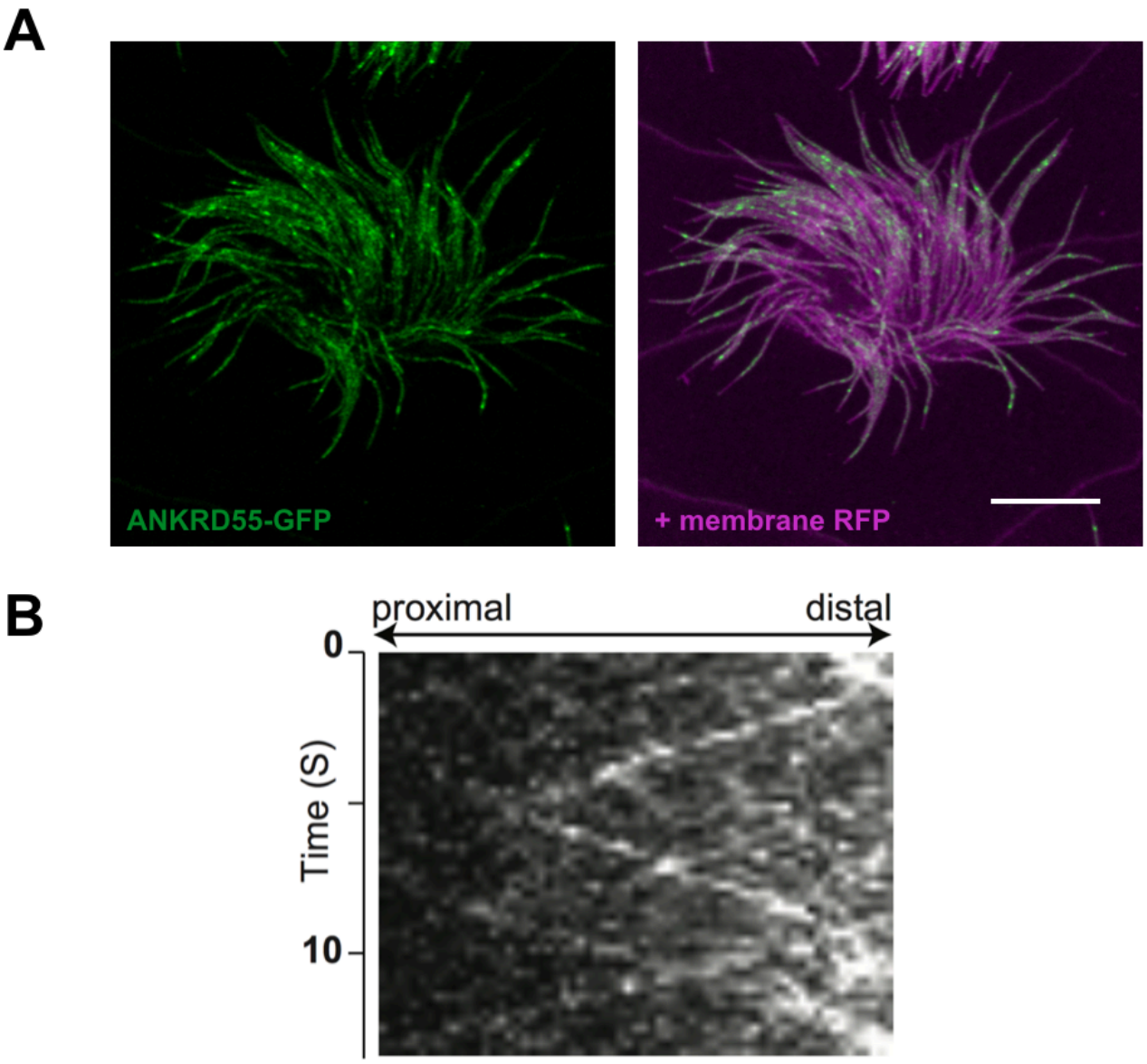

Figure 2.2 – **ANKRD55 localizes to and traffics within axonemes.** (A)Two-color fluorescent image shows localization of ANKRD55-GFP to axonemes of *Xenopus* multiciliated cells. (B) Kymograph made from time lapse movie of ANKRD55-GFP traffic within ciliary axonemes.

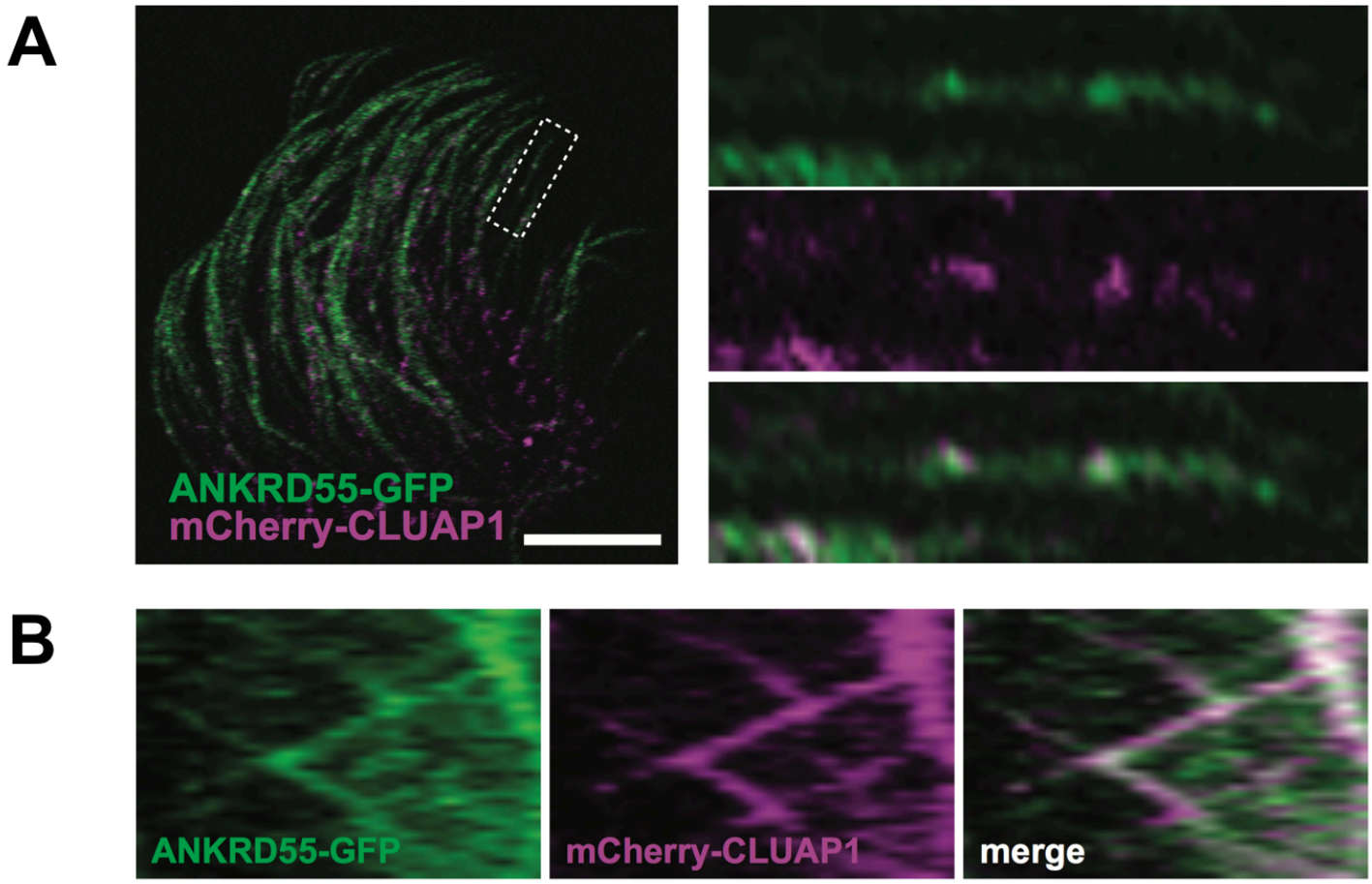

Figure 2.3 – ANKRD55 moves along axonemes with the IFT-B member CLUAP1. (A) Two-color confocal imaging shows that ANKRD55 colocalizes with CLUAP1 in puncta along axonemes. Scale bar: 10μm. (B) Two-color kymographs generated from time lapse movie of cell in panel A. Proximal to the left, Distal to the right. Data courtesy of Chanjae Lee.

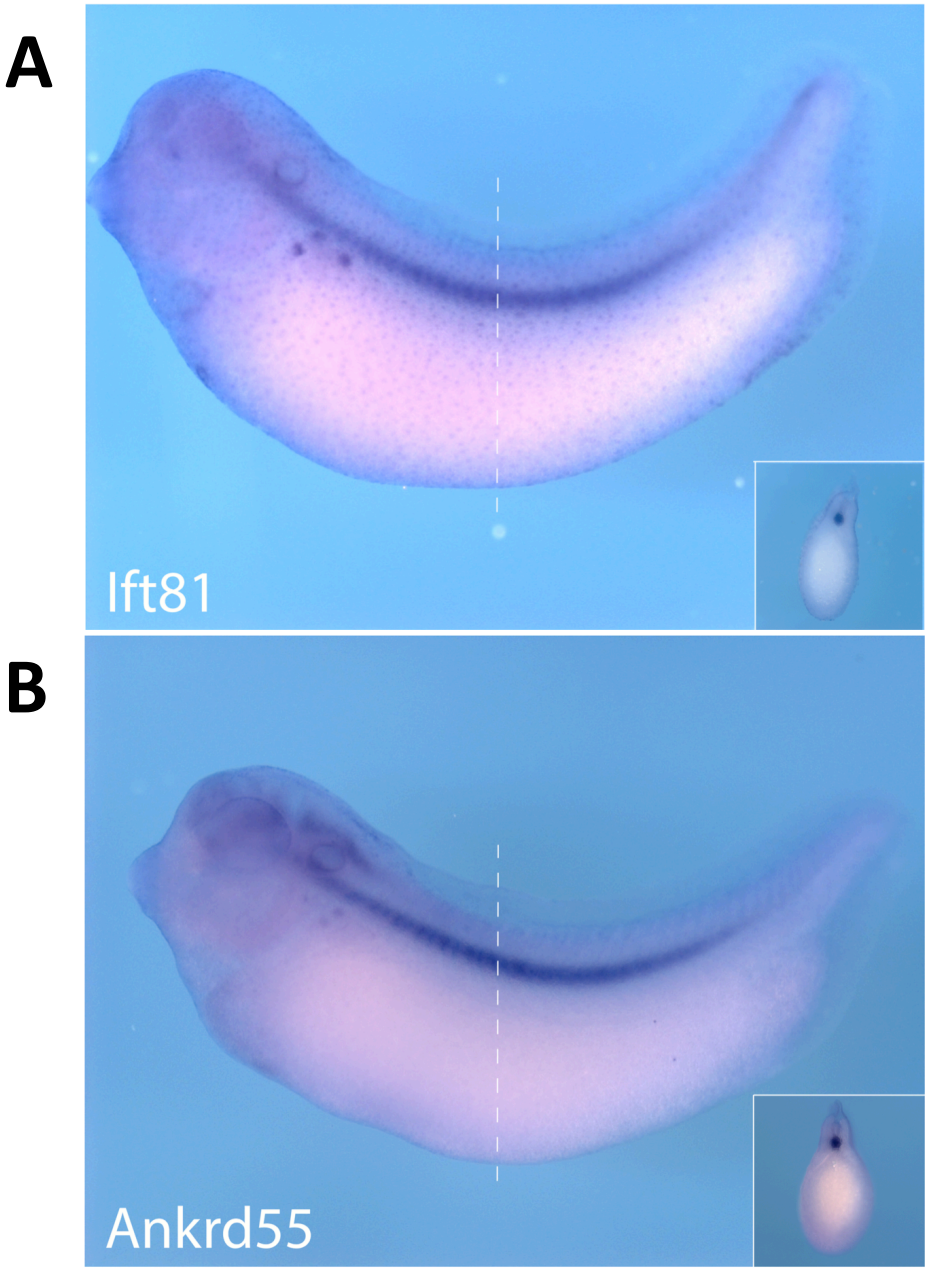

Figure 2.4 – Expression pattern of ANKRD55 is similar to other IFT genes. (A) Whole mount in situ hybridization of IFT81, an IFT-B complex member. (B) Whole mount in situ hybridization of ANKRD55. Insets show transverse sections of embryos

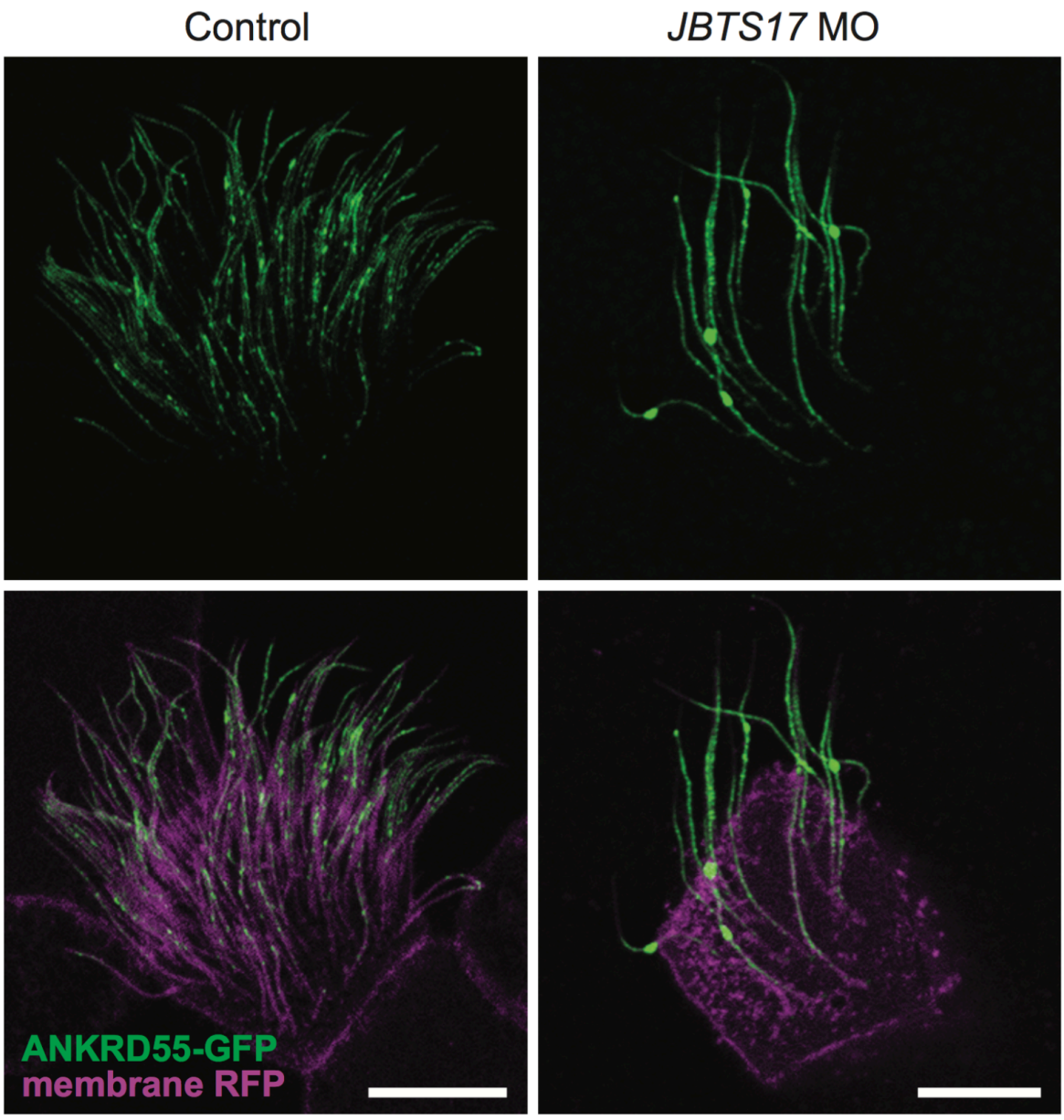

Figure 2.5 – ANKRD55 accumulates in axonemes in JBTS17 knockdown. Morpholino-mediated knockdown of JBTS17 is known to specifically affect localization of IFT-B components. JBTS17 knockdown results in buildup of ANKRD55 in axonemes. Scale bar 10 μm.

2.2.3 ANKRD55 is required for ciliogenesis and neural tube closure

IFT is a process required for signal transduction of important signals during embryonic development and homeostasis. As such, mutations in IFT subunits often elicit severe birth defects across vertebrates (Hildebrandt et al., 2011). We expected that abrogation of ANKRD55 function would result in ciliary defects as well as early embryonic phenotypes. To assess this, we utilized *in vivo* experiments to characterize the functions of ANKRD55.

In many IFT mutants, complex formation is disrupted, and ciliogenesis defects are almost always lost. One such member that elicits this phenotype is IFT52, a predicted interactor of ANKRD55 (Zhang et al., 2016). Splice-blocking morpholino-antisense oligonucleotides (MO) against ANKRD55 and IFT52 were injected into 4-cell stage embryos that were later tested for ciliary phenotypes. We observed that both morphants for both genes elicited ciliogenesis defects in epidermal multiciliated cells (Figure 2.6), giving further indication of a link between ANKRD55 and the IFT-B complex.

Vertebrates mutant for IFT genes often possess the phenotype of delayed or failed neural tube closure, resulting in defects such as exencephaly, anencephaly, and spina bifida (Hildebrandt et al., 2011). Underlying these defects is a failed transduction of signal transduction of sonic hedgehog from the notochord to the floor plate, thus resulting in failure of dorsoventral patterning of the neural tube (Murdoch and Copp, 2010). Therefore, we hypothesized that knockdown of ANKRD55 in *Xenopus* would elicit similar phenotypes. Assuredly, ANKRD55 embryos injected dorsally with ANKRD55-MO displayed severe neural tube closure phenotypes. The specificity of the

ability of the MO to knockdown ANKRD55 RNA was reflected by rescued neural tube closure phenotype when co-injected with ANKRD55 mRNA (Figure 2.7). Taken together, these results indicate that ANKRD55 interacts physically and functionally and may play roles in human ciliopathies.

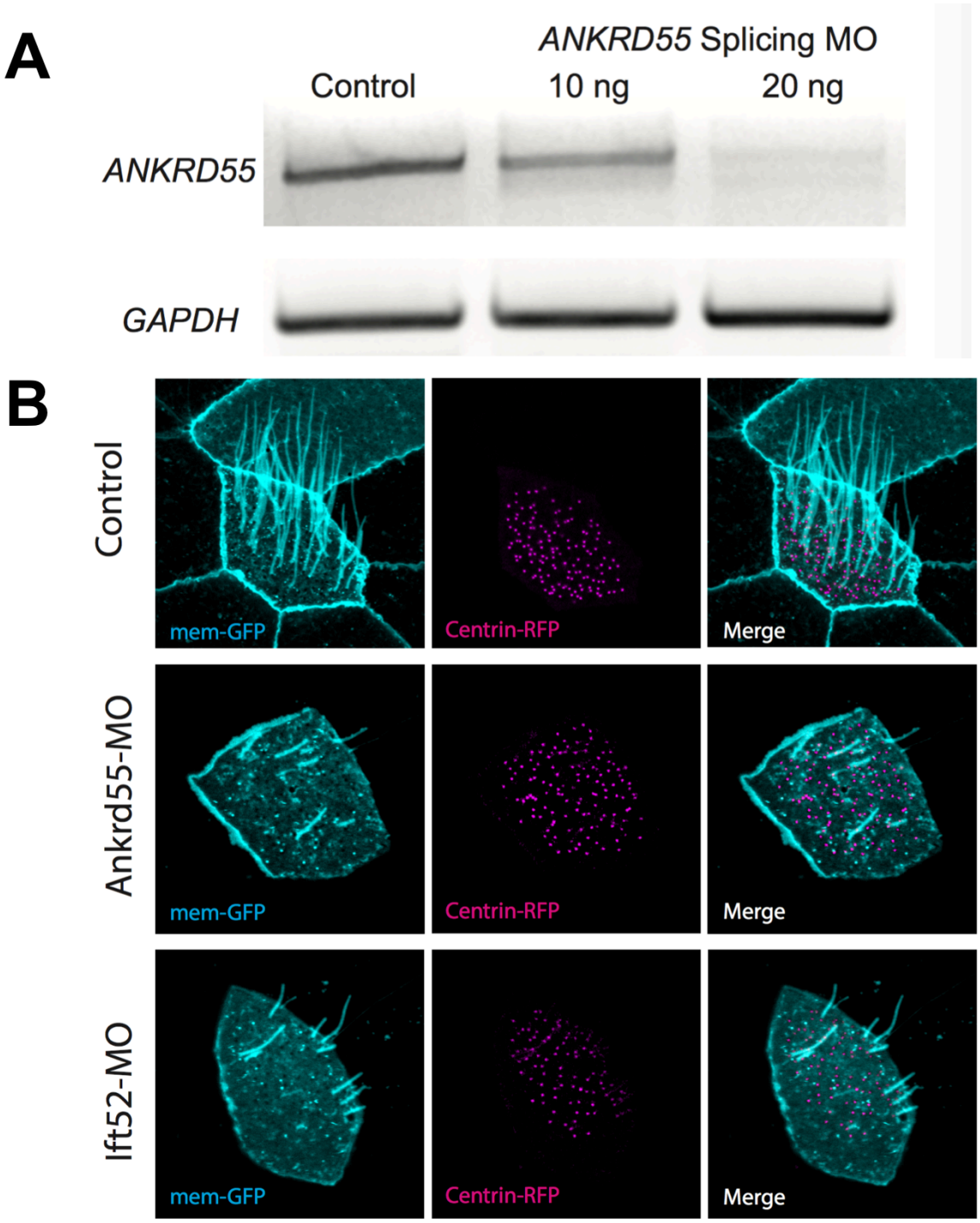

Figure 2.6 – ANKRD55 knockdown results in ciliogenesis defects. (A) RT-PCR demonstrates the efficiency of ANKRD55 morpholino to abrogate splicing of ANKRD55 RNA in *Xenopus* embryos. GAPDH used as control. (B) ANKRD55 knockdown results in loss/shortening of cilia in a manner similar to IFT52 knockdown.

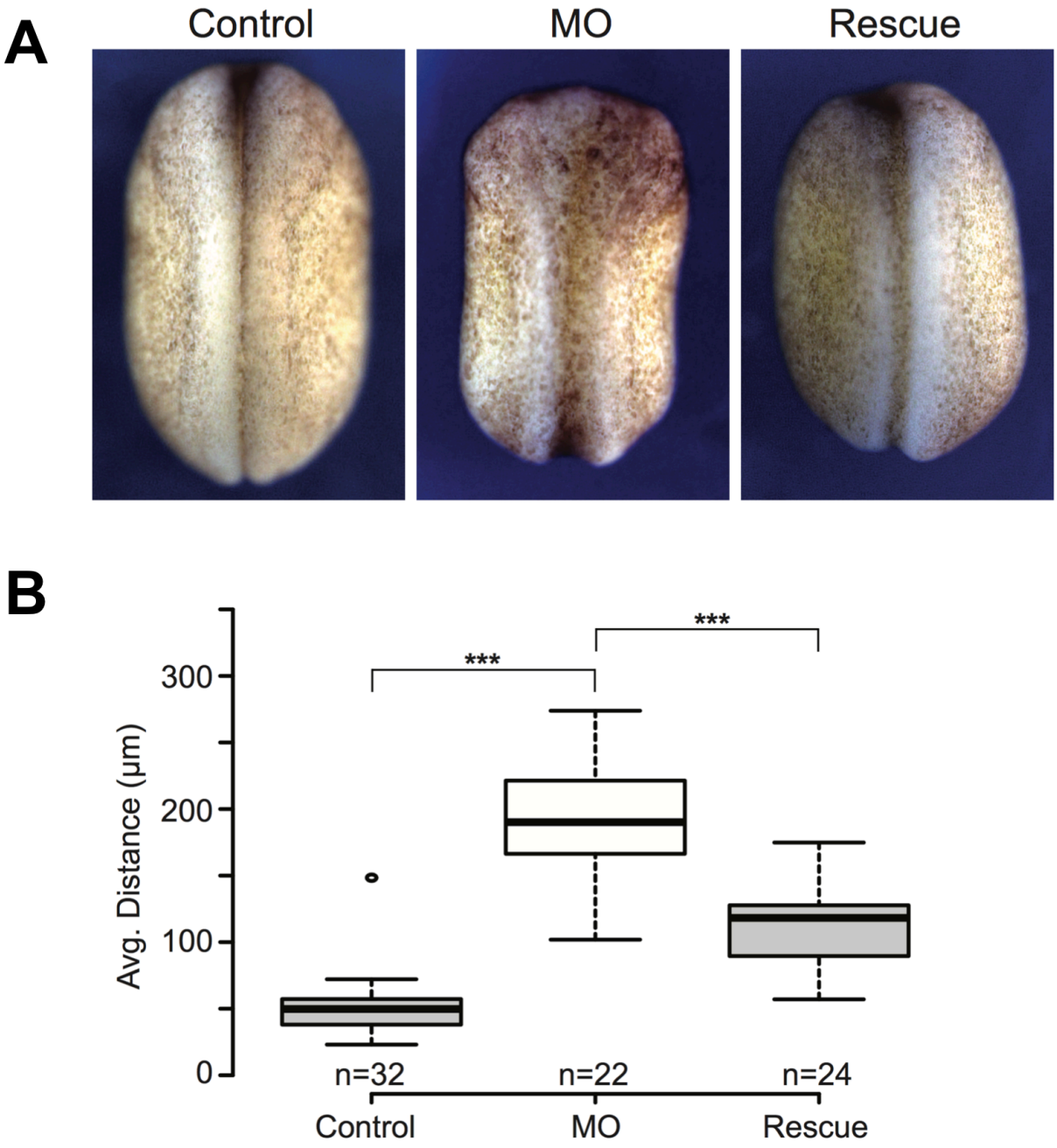

Figure 2.7 – ANKRD55 knockdown causes neural tube closure defects. (A) Dorsal view of stage 19 *Xenopus* embryos shows that ANKRD55 morphants have neural tube closure defects that are rescued by ANKRD55. (B) Quantification of neural tube closure defects in A. The box plot displays average distance between neural folds in control, morphant and rescue embryos. *** ($P < 0.0001$)

2.2.4 ANKRD55 mutations identified in short rib polydactyly patients

The combination of localization, loss of function phenotype, and physical interaction with IFT-B prompted a search for human mutations in this gene. In humans, skeletal defects such as short rib polydactyly often arise in ciliopathies due to impaired hedgehog signaling, (Baldridge et al., 2010). Through collaboration with the International Skeletal Dysplasia Registry, we identified three cases (registry numbers R98-413A, R95-149, and R98-017) that possessed rare variants of ANKRD55 as revealed by exome sequencing, however, no cases were either homozygous or compound heterozygotes for these variants. From these variants, two point mutations were identified: 383G>C, resulting in an amino acid change from arginine to proline at position 126 and 528A>T, resulting in an amino acid change glutamine to histidine at position 176 (Figure 2.8a). RaptorX structural prediction (Peng and Xu, 2011) identified that Arg126Pro mutation was likely in a constituent alpha helix of an ankyrin repeat and the Gln176His mutation was in a loop between helices (Figure 2.8b).

To better understand if these variants have the potential to contribute to human ailments, we modeled these mutations in *Xenopus* by making point mutants in ANKRD55 and fusing them to GFP. *In vivo* confocal imaging identified that the Gln169His variant displayed similar localization to the wild type ANKRD55 -- it localized to puncta along axonemes which moved both anterograde and retrograde. The Arg126Pro variant (Arg121Pro in *Xenopus*) displayed notable reduction of fluorescence in the cytosol and complete loss of localization to axonemes. This prompted us to identify if this variant was degraded and thus prevented from carrying out its function. Western blotting against GFP tagged variants showed a marked reduction in ANKRD55-R121P

levels, but comparable levels of ANKRD55-Q169H and wild-type ANKRD55, possibly indicating that the R121P variant is degraded. Taken together, these results indicate that ANKRD55 may contribute to the etiology of human ciliopathies.

Patient	Gene	DNA Change	Protein Change
R98-413A	ANKRD55	528A>T	Gln176His
R95-149	ANKRD55	383G>C	Arg126Pro
R98-017	ANKRD55	383G>C	Arg126Pro

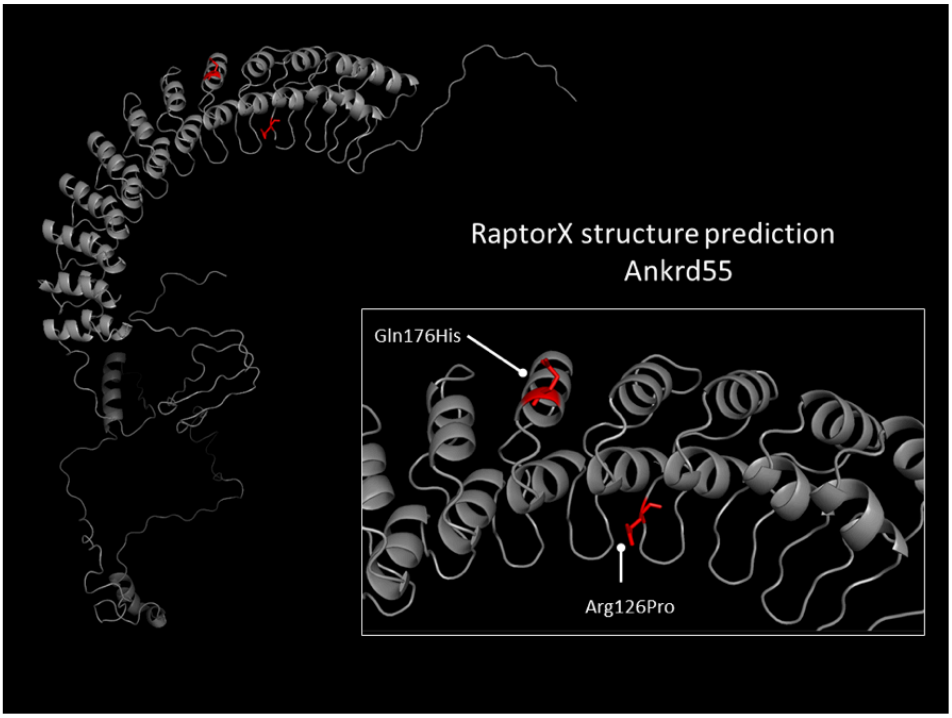

Figure 2.8 – Identified ANKRD55 variants in short rib polydactyly patients. Two variants were identified in data from short rib polydactyly patients from the International Skeletal Dysplasia Consortium. Amino acid changes are highlighted in the RaptorX structural prediction of ANKRD55. Data from Krakow group, UCLA. Structural prediction courtesy of Claire McWhite.

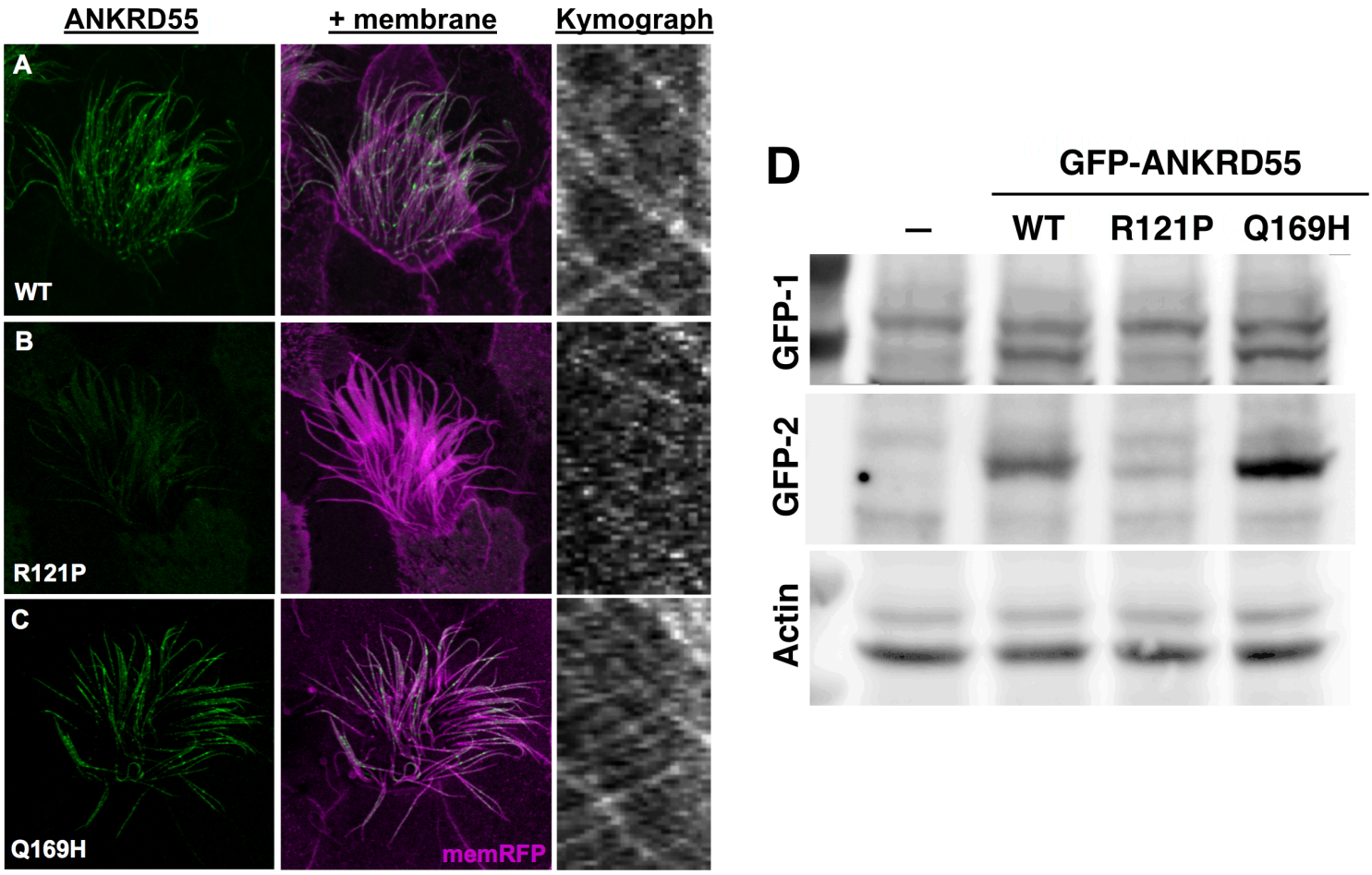

Figure 2.9 – Modeling human ANKRD55 variants in *Xenopus*. (A-C) Localization of ANKRD55-GFP fusion proteins in *Xenopus* epidermal multiciliated cells. Kymographs generated from time-lapse movies of ANKRD55 movement in axoneme. Wild type and Q169H localize and traffic normally, however, the R121P variant is markedly reduced. (D) Western blot of whole-embryo lysates from embryos injected with either wild type, Q169H or R121P variants of ANKRD55-GFP. R121P levels are drastically reduced when compared to wild type or Q169H ANKRD55. Two GFP antibodies were used to confirm result. Actin used as control. Kymographs and western blot courtesy of Chanjae Lee.

2.3 - Discussion

ANKRD55 is a protein containing multiple ankyrin repeat domains and is conserved across vertebrates. ANKRD55 has been implicated in human disease, namely multiple sclerosis (Lapuente et al., 2016), however the exact function of the protein is not well understood. Here, using proteomic analysis, ANKRD55 is identified as an interactor of the IFT-B complex with specific interactions between proteins IFT70, IFT52, and IFT27. Additional support for this interaction comes from the known structure of the IFT-B1 complex, wherein IFT70 and IFT52 bind one another as a module extending from the IFT81-IFT74 C-termini. These two proteins were predicted to be the strongest interactors of ANKRD55, and IFT27 was predicted to be a much weaker interaction. Support for this notion lies in the placement of the IFT25/27 module as an independent region of the B1 complex wherein they serve to bind the BBSome through the adaptor protein LZTFL1 (Lechtreck, 2015). Based on our data as well as the known interactions between members of the IFT-B complex, placement of ANKRD55 as a member of the B1 complex is a compelling inference.

Disruption of specific IFT often lead to characteristic ciliary phenotypes. For example, disruption of many IFT-B proteins often lead to abrogation of ciliogenesis, as retrograde transport cannot proceed. Mutations in IFT-A proteins often lead to the failure of retrograde transport and thus cause a buildup of ciliary molecules within the axoneme, leading to short, bulbous cilia. Interestingly, some subunits do not have a ciliary phenotype, but rather result in sole roles in signaling, these include the small GTPases of IFT-B -- IFT25 and 27. In knockdown of ANKRD55, we observed a marked reduction of ciliogenesis in multiciliated cells of the *Xenopus* epidermis, giving further evidence of

the protein's participation in the IFT-B complex. Additional evidence for this notion came the protein's behavior *in vivo*. ANKRD55 was observed to traffic through axonemes alongside the IFT-B protein CLUAP1. Additionally, there are many embryonic phenotypes that manifested in ANKRD55 morphants that give further evidence that this protein is a protein involved in IFT. Neural tube closure defects are a common defect observed due to failure of sonic hedgehog transduction and thus, failure to pattern the central nervous system. Additionally, early evidence from human patients suggest that ANKRD55 may govern human ciliopathies including short rib polydactyly.

To better understand the function of this protein in the context of intraflagellar transport, investigation into its developmental importance in other vertebrate system will likely be employed. Utilization of a mouse knockout line will allow significant leaps to be made in the understanding of ANKRD55 in identifying specific ciliopathic phenotypes, such as skeletal anomalies and CNS patterning defects. Further studies in *Xenopus* could shed light on how ANKRD55 interacts with other components of intraflagellar transport. In its absence, does the IFT complex fail to assemble or do certain cargoes fail to enter the cilium? An interesting point of future is the role of ANKRD55 in processes at the basal body. Many components of IFT display strong localization to a peri-basal body pool where they are recruited into complexes before transport into the cilium. Contrastingly, ANKRD55 does not localize strongly to basal bodies, and shows preference for localization at distal ends of cilia (data not shown). This is similar trafficking to that displayed in the *C. elegans* anterograde IFT motor OSM3, which moves cargoes along the distal end of cilia (Pan et al., 2006). No vertebrate ortholog of

this gene, nor spatially-distinct components of IFT been identified in vertebrates, making ANKRD55 an interesting target for future studies.

In addition to identification of ANKRD55 as a novel member of the IFT-B complex, this study serves as a testament to the power of computation to identify and better understand elements of human disease. Here, a high-confidence protein complex map base upon over 9000 mass spectrometry experiments has been utilized to successfully identify potential ciliopathic genes. These results indicate the potential of this integrated human protein complex map to identify candidate genes in a wide range of human diseases.

Chapter 3 - Axonemal dynein arms are assembled at cytosolic phase-separated organelles.

3.1 - Background

Motile cilia are complex cellular organelles that drive fluid propulsion and movement across eukaryotes. In humans, motile cilia function in the transport of fluids (such as in mucociliary clearance in the airway) or in directed movement of individual cells (such as sperm). The movement of these organelles is dependent solely on a group of protein complexes aligned along microtubule doublets within axonemes, including radial spokes, central pair, nexin-dynein regulatory complexes, inner dynein arms, and outer dynein arms. Dynein arms are the machinery that underlies ciliary beating, wherein dynein heavy chain subunits bind and release microtubules in an ATP-dependent fashion in order to slide microtubules relative to one another and induce beating.

Dynein arms are highly complex protein complexes that are on the order of megadaltons, with individual heavy chains that can exceed 500 kDa. Assembling these protein complexes prior to ciliary transport is a problem that ciliated cells face in that there is massive potential for aggregation during protein folding. In addition, joining the individual components with one another is a complex process that may necessitate specialized cellular machinery. Indeed, recent studies have unveiled the role of many cytoplasmically localized (but not in axonemes) proteins that are required for the assembly of axonemal dynein arms. Their specific roles in this process are not well understood, but there are several lines of evidence that point to their role in the folding process of dynein heavy chains, as well as specific recruitment of certain components of inner dynein arms. This has led many to hypothesize a chaperone-like function for

many of these so-called axonemal dynein assembly factors (DNAAFs). In fact, many DNAAFs have been shown to directly interact with cellular chaperone machinery, including Hsp70, Hsp90, and CCT.

A coupling of biochemistry and human genetics has led to a better understanding of how individual DNAAFs work in the process of dynein arm assembly as well as given insight into potential new cytoplasmic factors that play roles in this process. However, studies regarding the cell biological basis of this process have been limited. In cultures of human nasal epithelial cells, immunofluorescence microscopy has been used to describe localization of DNAAFs as “thick, fibrous granules”, but the structures themselves have not been described. Further, another limitation of many studies is a lack of live imaging to describe the process of cytoplasmic dynein preassembly as it occurs. Here, we attempt to better characterize cytoplasmic preassembly of axonemal dynein arms by utilizing the multiciliated epidermis of *Xenopus laevis* as a model. We hypothesize that this assembly takes place at cytoplasmic liquid-liquid phase separations, and test this notion using various live imaging techniques.

3.2 - Results

3.2.1 - Dynein assembly factors colocalize at multiciliated cell-specific cytosolic foci

In previous studies regarding DNAAFs, localization has been described using immunofluorescence, and reports of subcellular localization have ranged from diffuse cytosolic to trans-golgi. In addition, several studies have aimed to identify interactions that exist between various DNAAFs and dynein arm subunits. However, spatial relationships that exist between multiple DNAAFs have not yet been probed.

In attempt to better define where in the cell these factors localize, and if they colocalize with one another, several known DNAAFs were cloned and fused to either eGFP or mCherry tags, including DNAAF2 (KTU), DNAAF3, DNAAF4 (DYX1C1), DNAAF5 (HEATR2), LRRC6, and PIH1D3. To assay subcellular localization, each of these constructs were transcribed *in vitro* and mRNAs were injected into ventral blastomeres of 4-cell stage *Xenopus* embryos and multiciliated cells on the epidermis of later stage embryos were imaged using two-color confocal microscopy. It was identified that every dynein assembly factor cloned colocalized with one another at subcellular foci at the periphery of multiciliated cells (Figure 3.1). Previous studies indicate that axonemal dynein subunits also colocalize with some dynein assembly factors. To test this, the intermediate chain axonemal dynein DNAI2 was assayed for subcellular localization, revealing that it also localizes to the same cytosolic foci (Figure 3.2).

Because these factors have been reported to govern a highly-specialized cell process that occurs only in cells that possess motile cilia, we hypothesized that the foci we identified were also multiciliated cell specific. Indeed, injection of KTU revealed that

foci were present in the cytosol of multiciliated cells, but absent from the cytosol of other cell types of the *Xenopus* epidermis (Figure 3.3). In order to further clarify the specificity of these foci, we turned to overexpression of ciliated cell transcriptional machinery. First, we co-injected KTU-GFP with the transcription factor FOXJ1, which, in the *Xenopus* epidermis induces growth of a node-like cilium on the surface of non-multiciliated cells (Stubbs et al., 2008). We found that in addition to multiciliated cells, other cell types that possessed node-like cilia also formed small KTU+ cytoplasmic foci (Figure 3.4).

Additionally, we were able to utilize a hormone inducible version of the multiciliated cell transcriptional co-factor multicilin (Multicilin-HGR), which will induce most cells along the epidermis to undergo multiciliated cell differentiation upon treatment with dexamethasone (DEX) by activating genes responsible for basal body biogenesis and ciliogenesis (Ma et al., 2014). Upon co-injection of KTU-GFP with multicilin-HGR, animal caps were removed from embryos (which develop into epidermal tissue) and later treated with DEX to induce multiciliated cell specification. Confocal microscopy revealed that all multiciliated cells along the epidermis contained KTU+ foci (Figure 3.3).

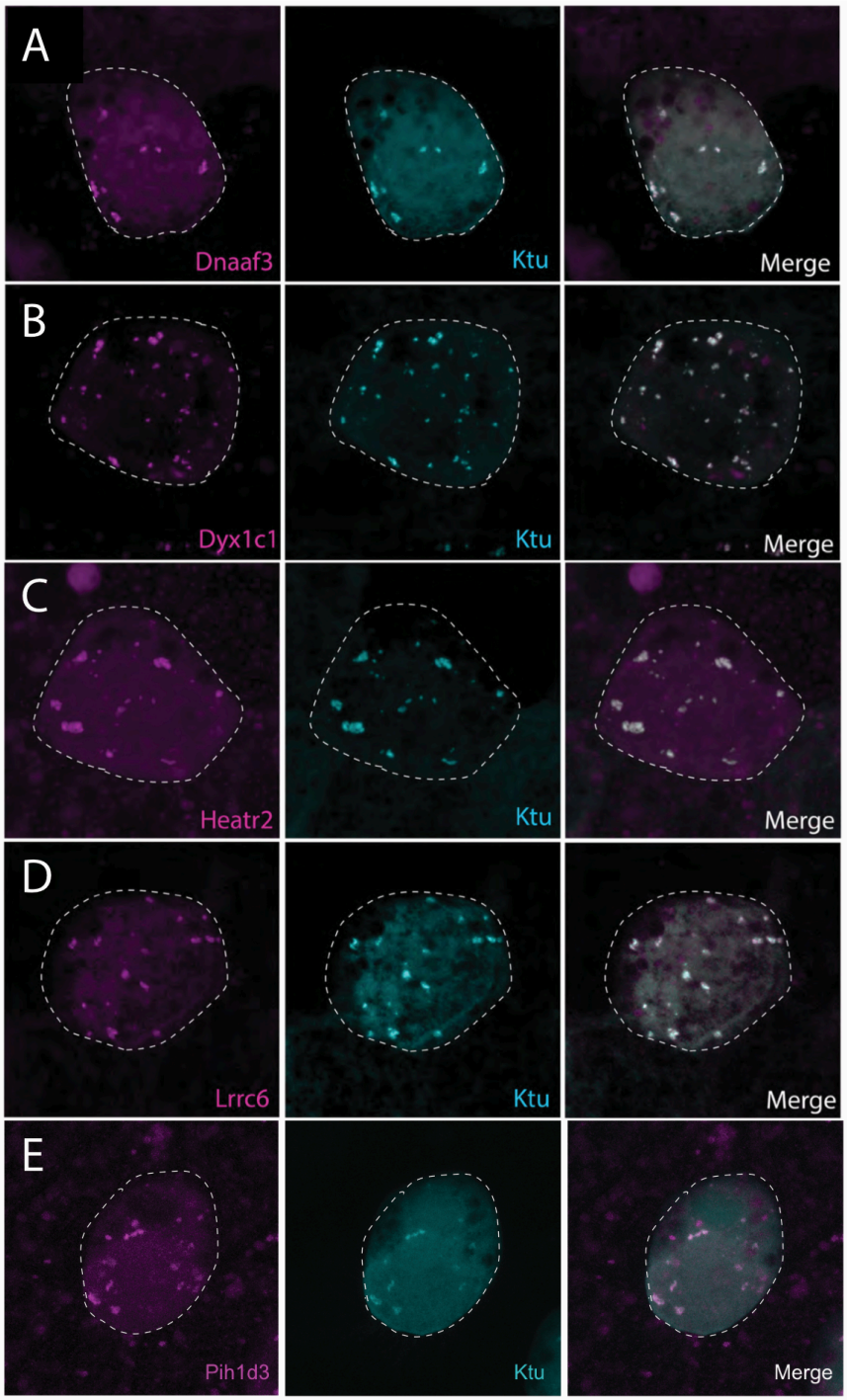

Figure 3.1 – Axonemal dynein assembly factors colocalize at cytoplasmic foci. Two color imaging of GFP-tagged KTU (middle panel) with mCherry-tagged DNAAF3 (A), DYX1C1 (B), HEATR2 (C), LRRC6 (D), or PIH1D3(E) (left panel). Dashed lines represent cell boundary.

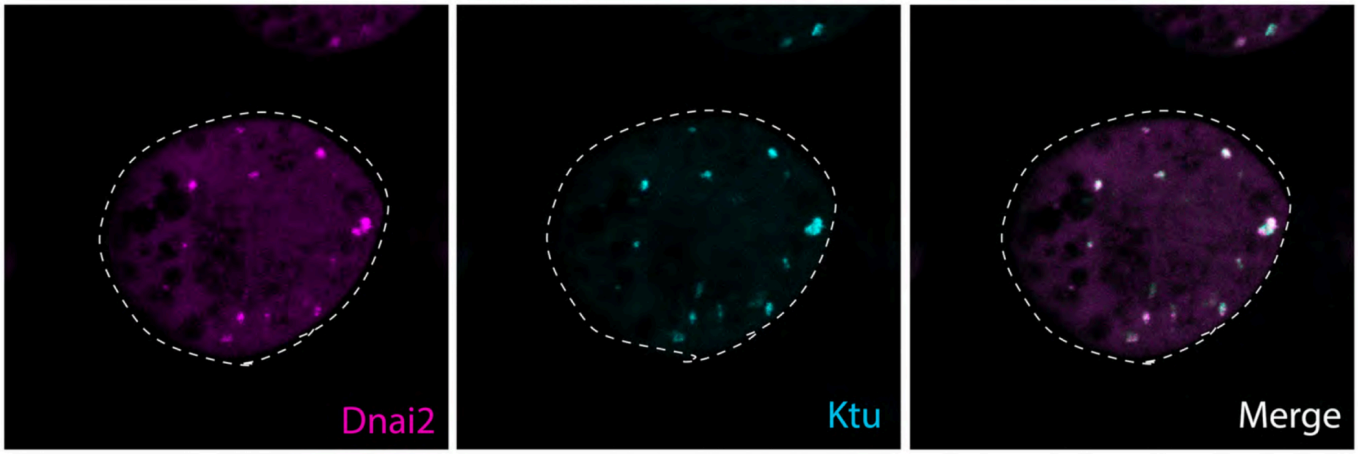

Figure 3.2 – The axonemal dynein intermediate chain DNAI2 colocalizes with KTU at cytoplasmic foci. mCherry-DNAI2 colocalizes with GFP-KTU at cytoplasmic foci in *Xenopus* epidermal multiciliated cells. Dashed line indicates cell boundary.

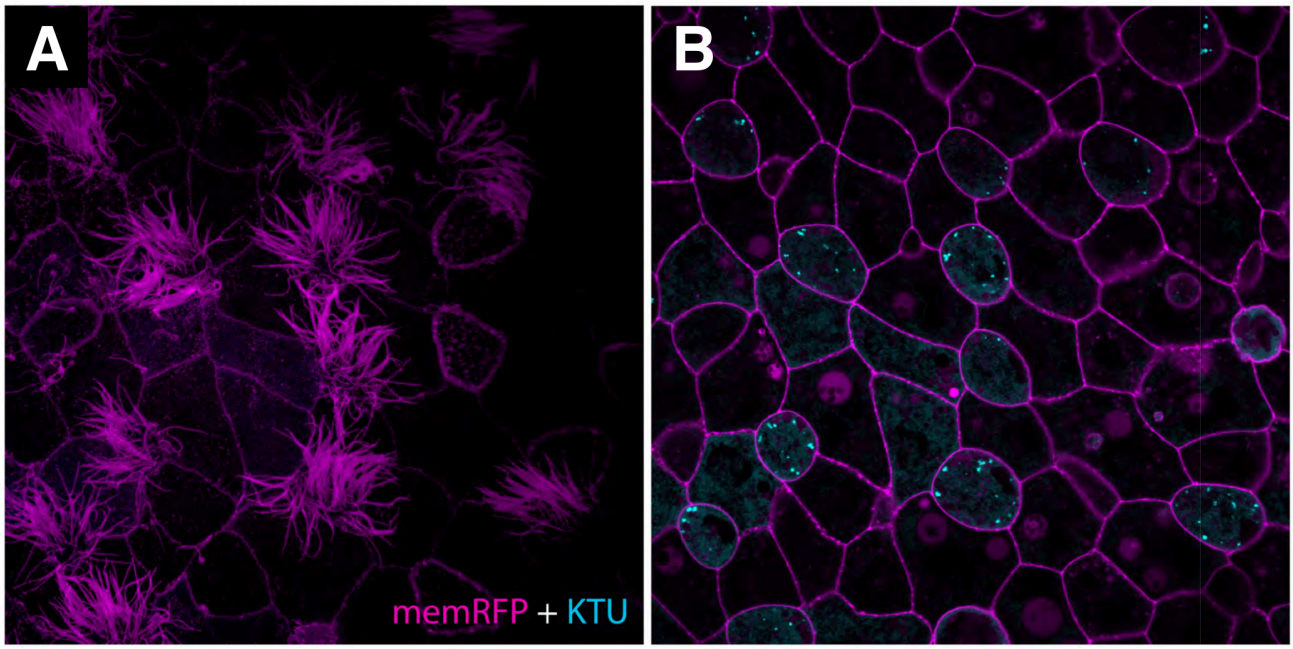

Figure 3.3 – Dynein assembly particles are multiciliated cell specific. (A) Superficial image of *Xenopus* epidermis decorated with multiciliated cells. (B) Subapical slice of same tissue shown in A. Foci are only present in multiciliated cells. Membrane labeled with membrane-RFP, Foci labeled with KTU-GFP.

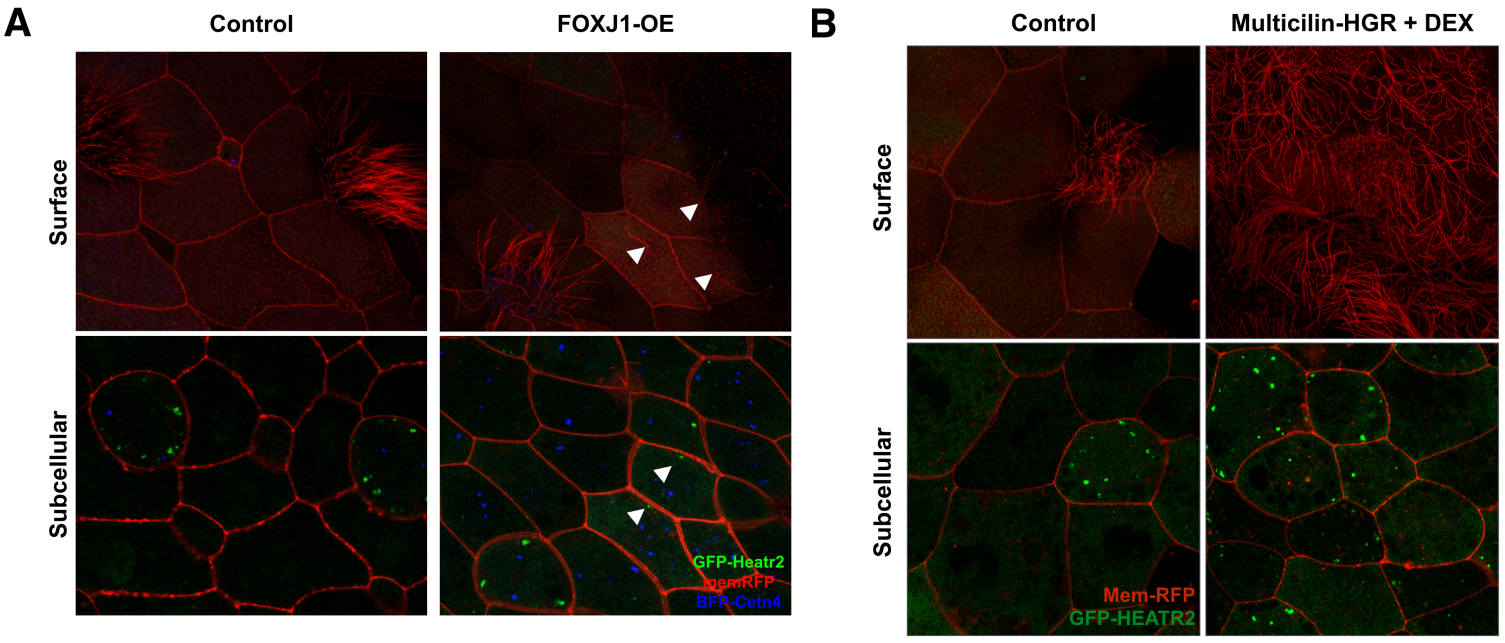

Figure 3.4 – Ciliogenic transcription factors are sufficient to induce formation of dynein assembly particles. (A) FOXJ1 overexpression induces growth of single node-like cilium in non-multiciliated cells of the epidermis. Membrane labelled with memRFP, foci labeled with GFP-HEATR2, and basal bodies labeled with BFP-Cetn4. Arrows indicate monocilia in top panel, foci in non-MCCs in bottom panel. (B) Multicilin-HGR injected embryos treated with dexamethasone (DEX) induce multiciliated cell specification in epidermal cell types. Membrane labeled with mem-RFP, foci labeled with GFP-HEATR2. Images courtesy of Chanjae lee

3.2.2- DynAPs are physically and compositionally similar to liquid-liquid phase separated organelles.

We next attempted to define the cellular compartment at which DNAAFs colocalized with one another. To answer this question, we utilized markers for cellular compartments that have been implicated axonemal dynein assembly, namely the *trans* golgi (Olcese et al., 2017). Co-injection of KTU with GALT, a marker of the *trans* golgi, revealed that the multiciliated cell-specific foci were independent of golgi (Figure 3.5). In we also looked at markers of several other membrane bound compartments by either overexpressing a GFP-tagged CAAX membrane localization domain or staining live embryos with BODIPY-ceramide. In either case, there was no colocalization with reported dynein assembly factors (data not shown).

These results prompted us to search for other cellular compartments to which cytosolic preassembly of axonemal dyneins could take place. The highly variable morphology of the cytosolic foci was reminiscent of the shape of stress granules, cytosolic phase-separated organelles that function as triage points for cytoplasmic RNAs. Stress granules are nucleated in a manner that utilizes the protein G3BP1, which we chose to use as a marker to assay for colocalization. Co-expression of G3BP1 with the dynein assembly factor HEATR2 revealed that the two colocalized (Figure 3.6A). Further, co-expression of another stress granule-localized protein TIA1 with KTU revealed colocalization as well (Figure 3.6B), giving additional evidence for the compositional similarity between stress granules and sites of cytosolic preassembly of axonemal dynein arms, which we term DynAPs (Dynein Assembly Particles). Interestingly, imaging of TIA1 and G3BP1 revealed that in numerous DynAPs, there

were spherical, concentrated regions of these proteins directly adjacent. This could potentially indicate exchange of material between two independent bodies, similar to the process by which P-bodies and stress granules exchange RNAs with one another (Decker and Parker, 2012). As stated in Chapter 1, stress granules are liquid-liquid phase separations that rely, in part, on increased local concentration RNAs. To test whether this principle holds true for DynAPs, we stained whole embryos with an RNA-selective stain, which revealed that there were increased cytoplasmic RNA concentrations where HEATR2 localized in the cytoplasm (Figure 3.6C).

The parallels between stress granules and DynAPs, coupled with the lack of colocalization of DNAAFs with markers of membrane-bound compartments argued that these structures may be cytoplasmic phase separations. In previous studies, phase-separated organelles possess liquid-like properties, including fusion events between particles, rapid exchange of material with the cytosol, and deformation under various forces (Brangwynne et al., 2009). We were able to utilize a number of microscopy techniques to test for liquid-like characteristics *in vivo*. Firstly, we utilized time lapse microscopy of HEATR2 in multiciliated cells to identify potential fusion events. DynAPs displayed highly dynamic behavior in multiciliated cells, in some cases moving rapidly across the cell. This indicated that these particles may be trafficked through some cytoskeletal mechanism. In addition, we were able to note several interactions between particles. In many cases, DynAPs would briefly come into contact with one another before moving apart. In other cases, however, two particles would contact and then fuse to form larger entities in approximately two minutes (Figure 3.7).

To probe how material was exchanged between DynAPs and the cytoplasm, fluorescence recovery after photobleaching (FRAP) was utilized, wherein a whole or partial bleach of a particle was carried out, and the recovery over time was charted. Because multiciliated cells are surrounded by other cell types in the *Xenopus* epidermis, we were able to observe recovery of the stress granule protein G3BP1 in both goblet cell stress granules as well as KTU+ DynAPs. In both cell types, G3BP1 exhibited similar recovery curves in both complete and partial bleach, with a half recovery time of approximately one second (Figure 3.8). This rapid recovery also serves as further evidence of the absence of a membrane surrounding DynAPs. FRAP of GALT, a luminal protein of the *trans* golgi, displays recovery rates exceeding a one minute half-time.

Despite these similarities, there are some characteristics of DynAPs that deviate from stress granules. For example, some proteins that normally localize in stress granules fail to localize to DynAPs, including FUS, a protein that in part makes up the phase-separated matrix of stress granules, as well as several of the translation initiation factors (EIF4E, EIF4G). In addition, DynAPs contain many ubiquitous components not previously reported to localize to stress granules, but have been demonstrated to interact with various dynein assembly factors. These include Hsp70, Hsp90, and Hsp40 family co-chaperones (data not shown). These results indicate that while similar in some facets, DynAPs are distinct in composition, arguing that the highly specialized multiciliated cell may have adopted some of the core machinery required for phase separation in stress granules, and applied it to carry out a novel task -- carrying out biochemical processes to mediate the folding and assembly of axonemal dynein complexes.

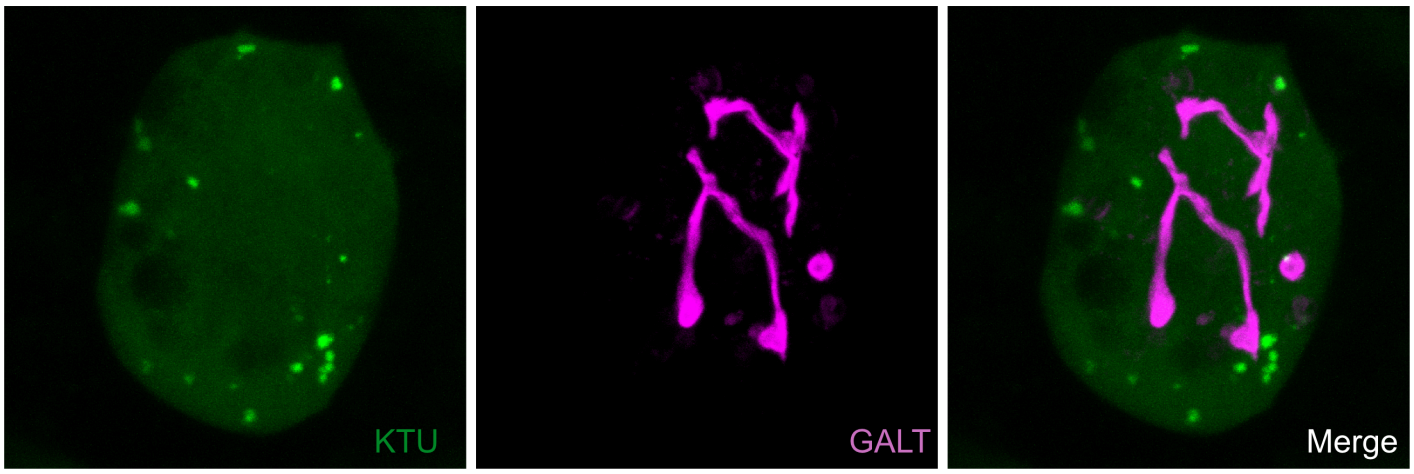

Figure 3.5 – Dynein assembly factors do not localize to *trans* golgi. Maximum projection of multiciliated cells expressing both KTU-GFP and GALT-RFP, a trans golgi localized protein. There is no overlap between the two, implying localization to independent cellular compartments.

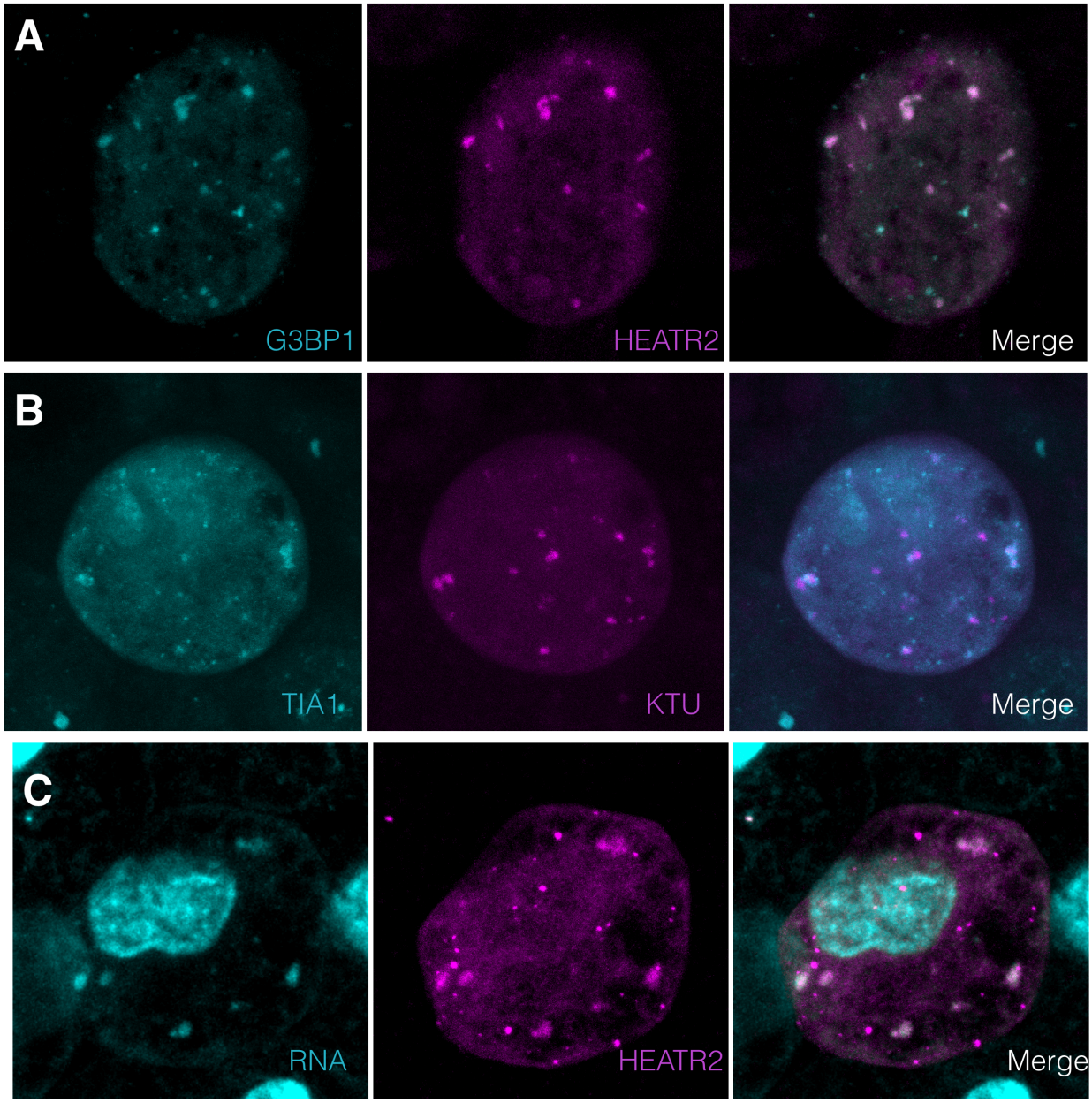

Figure 3.6 – Stress granule components colocalize with axonemal dynein assembly factors. (A) G3BP1-GFP colocalizes with the axonemal dynein assembly factor HEATR2-mCherry. (B) TIA1-GFP colocalizes with KTU-mCherry. (C) In fixed embryos, HEATR2 colocalizes with cytoplasmic RNA, shown with an RNA-selective fluorescent dye (Thermo Fisher)

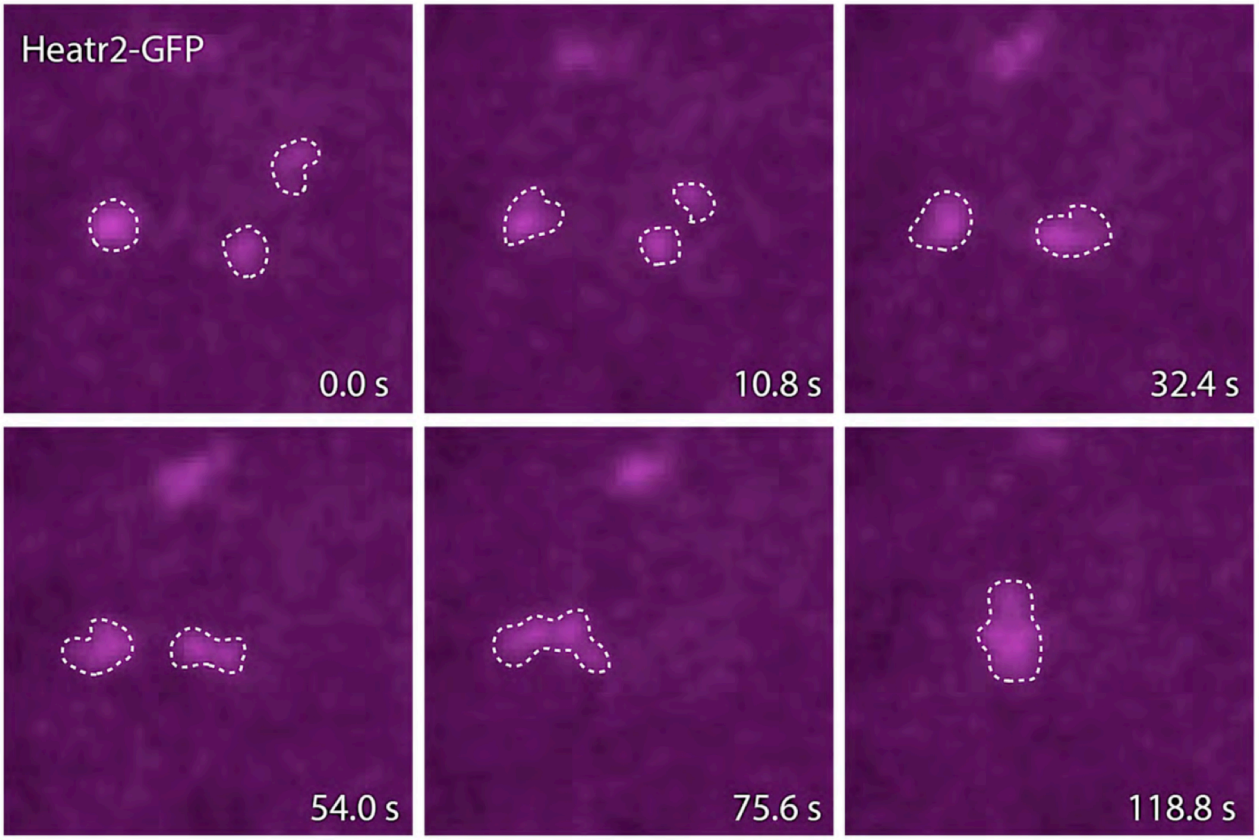

Figure 3.7 – Dynein assembly particles fuse with one another *in vivo*. Time lapse confocal images of subcellular HEATR2 foci. An initial fusion event between two foci is shown at 54 s. Another fusion event is observed at 75.6 s, then relaxation at 118.8 s. Dashed lines represent boundaries around dynein assembly particles.

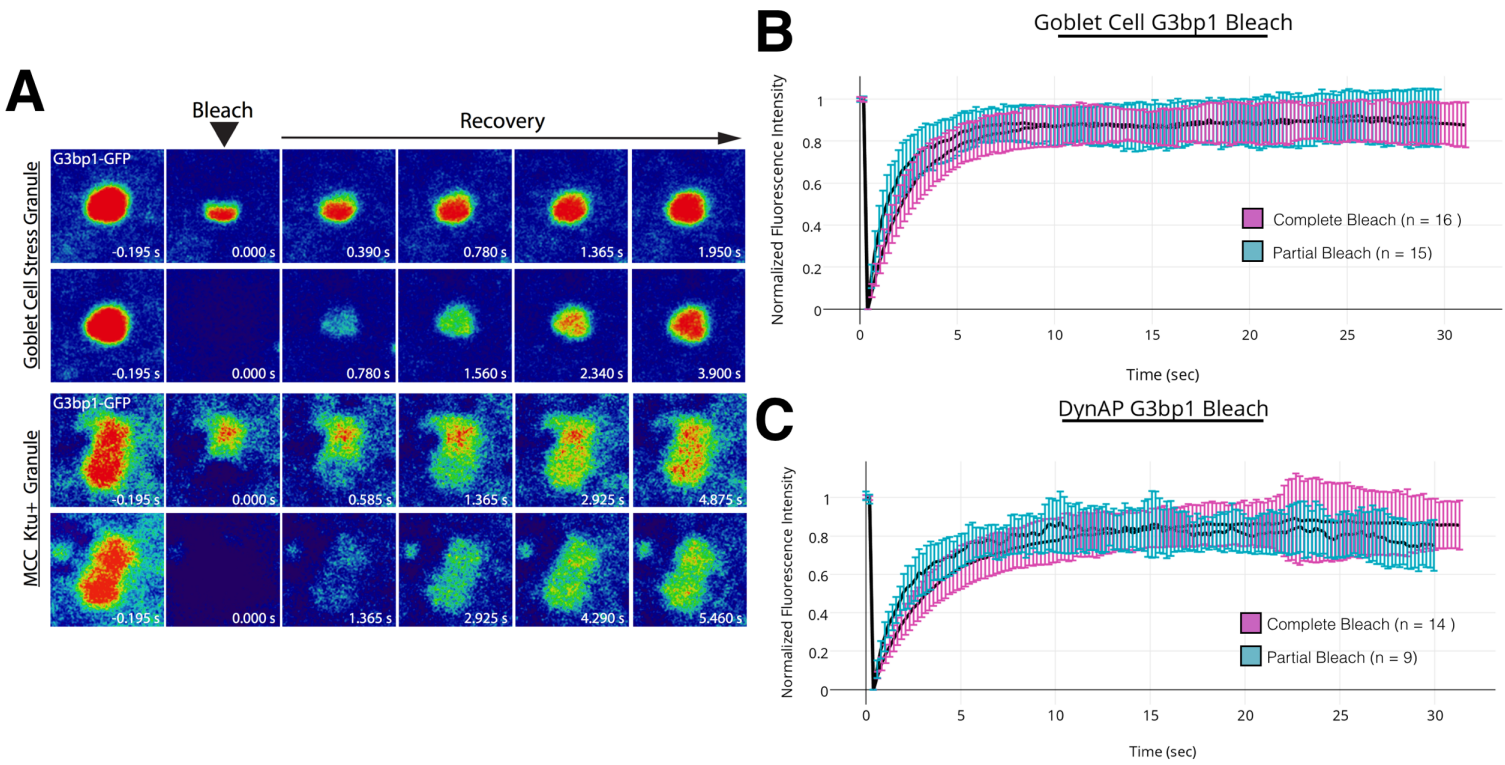

Figure 3.8 – G3BP1 in dynein assembly particles rapidly exchange with cytoplasmic G3BP1. (A) G3BP1 in both stress granules in goblet cells (Top) and dynein assembly particles in multiciliated cells (Bottom) exhibit rapid recovery rates following photo bleach. Partial and complete bleach were carried out to assess diffusion within each particle. Red indicates high intensity, blue indicates low intensity. (B) FRAP curve for partial and complete bleach of goblet cell stress granules (magenta indicates complete bleach, cyan indicates partial bleach). (C) FRAP curve for partial and complete bleach of multiciliated cell dynein assembly particles (magenta indicates complete bleach, cyan indicates partial bleach).

3.2.3 - Stress granule machinery is required for DynAP formation and axonemal dynein localization

In many phase separated organelles, assembly is mediated in a manner wherein local concentrations of particular molecules, such as RNA and RNA binding proteins, are increased such that a scaffold made of many components forms for specific biochemical processes to take place. In stress granules, a multi-step process involving phosphorylation of the translation initiation factor EIF2α which induces the multimerization of the RNA binding protein G3BP1 (Matsuki et al., 2013). Because of the similarities in makeup between stress granules and DynAPs, we hypothesized that G3BP1 may play a similar role in DynAP formation. To test this, we utilized a morpholino antisense oligonucleotide against G3BP1 in the *Xenopus* epidermis by injection into ventral blastomeres at the 4-cell stage. Following injection, there were a number of clear multiciliated cell phenotypes observed.

When G3BP1 and G3BP2 are knocked down in cultured cells, there is a resulting marked reduction in stress granule number. Following knockdown of G3BP1 in *Xenopus*, we noticed a similar reduction in the number of DynAPs in multiciliated cells. In wild-type cells, foci usually decorated the periphery of the cell, whereas in the G3BP1 knockdown embryos, the distribution was sparse or altogether absent. Additionally, when DynAPs were present in knockdown cells, their size was drastically reduced (Figure 3.9) when compared to wild type. The involvement of these foci in the process of axonemal dynein assembly was made apparent by loss of the dynein intermediate chain subunit DNAI2 in ciliary axonemes upon knockdown (Figure 3.10). This subunit has been shown to bind DNAAFs and is required for addition of heavy chain dyneins in

outer dynein arm assembly. As in many other models, the loss of outer dynein arms in the axoneme resulted in static cilia. This phenotype served as compelling evidence that the cytoplasmic preassembly of axonemal dyneins uses a core machinery similar to stress granules in order to carry out the chaperone-mediated folding and assembly of dynein arms.

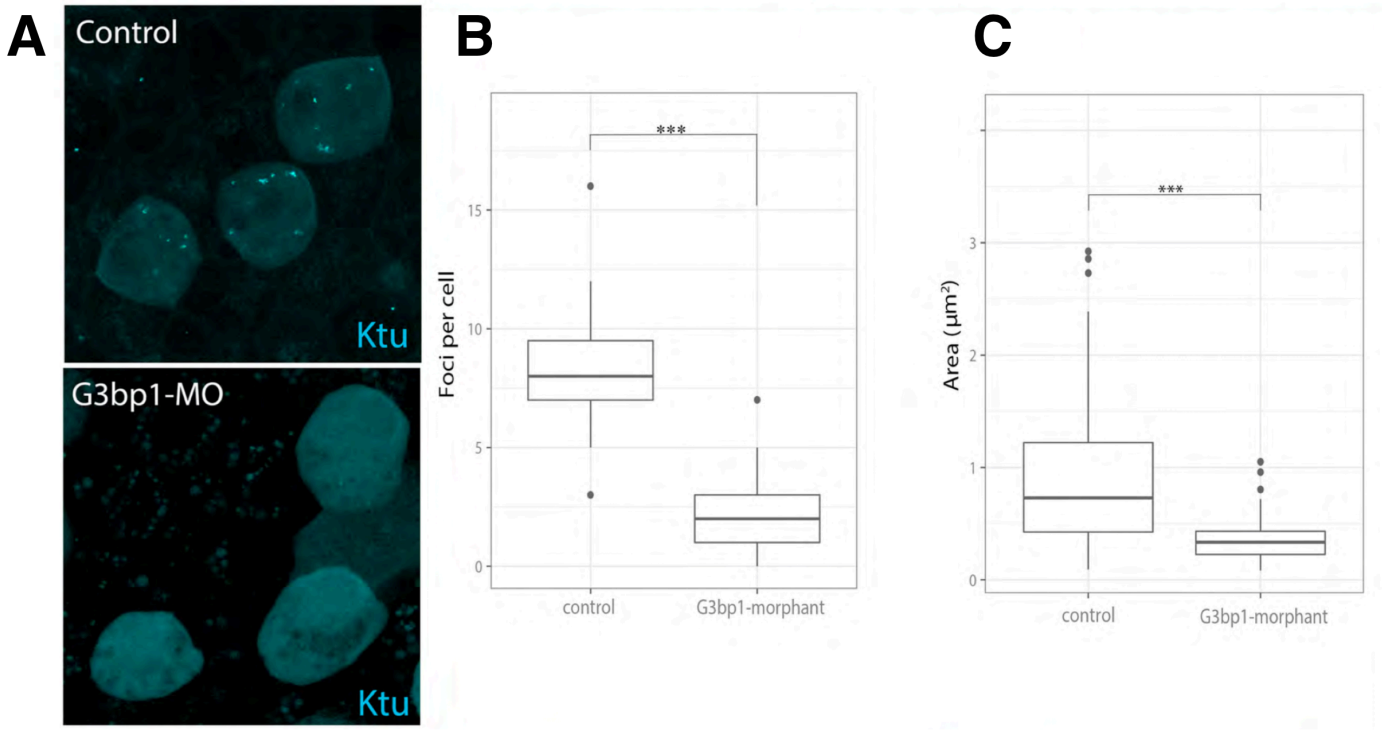

Figure 3.9 – G3BP1 knockdown affects size and number of dynein assembly particles in multiciliated cells. (A) In control cells, dynein assembly particles are normally distributed around the periphery of multiciliated cells. In G3BP1 morphants, particles are no longer present. (B) Box plot quantifying number of dynein assembly particles per multiciliated cell in control and G3BP1 morphants *** (P > 0.001 by two-sample Kolmogorov-Smirnov test). (C) Box plot quantifying area of foci in control and G3BP1 morphant multiciliated cells. *** (P > 0.001 by two-sample Kolmogorov-Smirnov test).

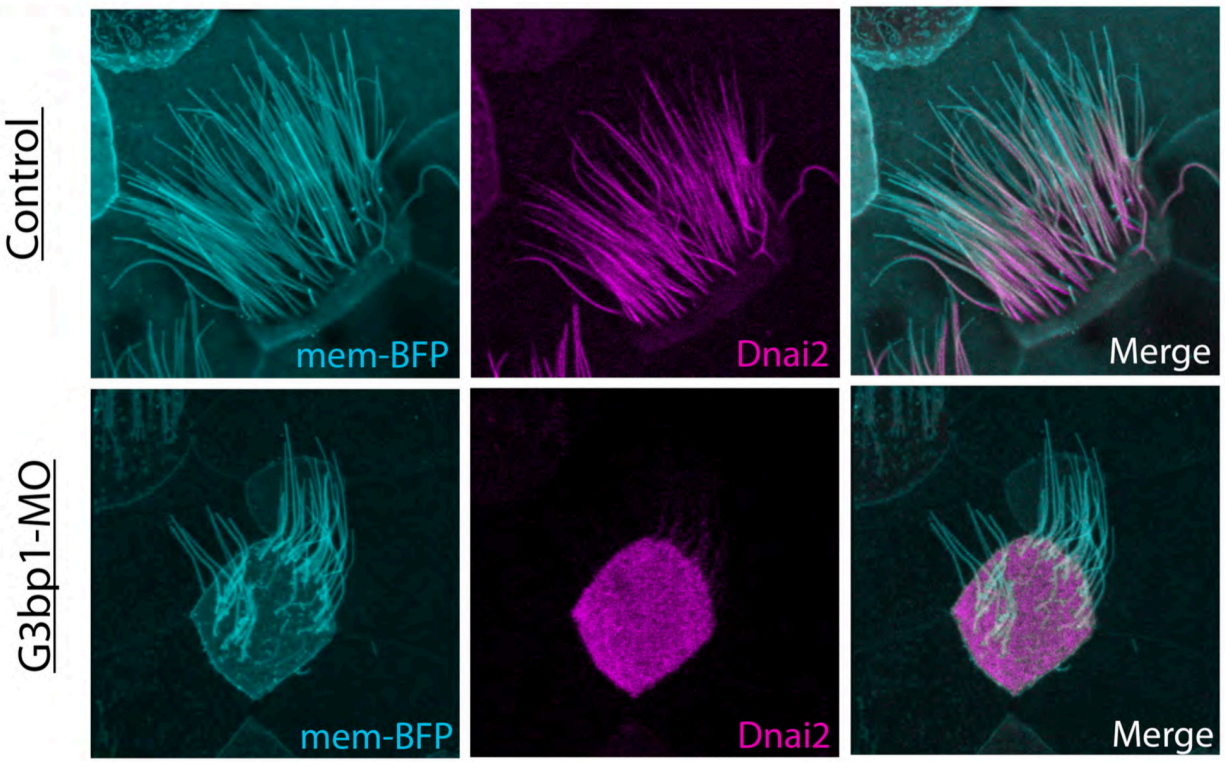

Figure 3.10 – G3BP1 knockdown results in failure to recruit outer dynein arms to cilia. In control multiciliated cells, the outer dynein arm subunit DNAI2 is normally localized to axonemes. In G3BP1 knockdown, this distribution is lost. Membrane labeled by mBFP, outer dynein arms marked by the intermediate chain subunit mCherry-DNAI2.

3.3 - Discussion

Motile cilia beat in a fashion that requires a coordination of many large protein complexes within the axoneme. How these complexes are synthesized, assembled, and transported has been an elusive problem. Work concerning both the inner and outer dynein arms suggests that these complexes are assembled in the cytosol of ciliated cells prior to their transport via intraflagellar transport and docking along microtubule doublets. This process is mediated by a group of cytosolic assembly factors known as DNAAFs that are believed to mediate both the folding of large dynein subunits as well as assembly of complexes through coordination with various chaperones including Hsp70 and Hsp90. Mutations of any of these factors result in a heterogeneous human disease called primary ciliary dyskinesia, which is characterized by immotile cilia. EM of motile cilia from these patients suggests that loss of function in dynein assembly factors leads to complete loss of both inner and outer dynein arms from axonemes (Praveen et al., 2015). These factors are conserved across organisms containing motile cilia, from the algae *Chlamydomonas Reinhardtii* to mammals (Omran et al., 2008). This implies that the cytoplasmic assembly of axonemal dynein likely has its roots far back in the evolutionary history of eukaryotes, potentially dating back to the last eukaryotic common ancestor. The pairing of the interesting evolutionary history, paired with the physiological implications of the process make cytoplasmic assembly of axonemal dyneins a fascinating point of study.

DNAAFs have been reported to have an array of interactions with both one another as well as various other cellular components, however, reports of the subcellular localization of these proteins has been varied. Some have been reported to

localize diffusely in the cytoplasm, while others were reported to localize to the golgi. A varied localization such as this would not be optimal for carrying out this multi-step process. Here, we reported colocalization of many known factors, including KTU, DNAAF3, DYX1C1, HEATR2, LRRC6, and PIH1D3. DNAAFs localized to subcellular foci with odd morphology, suggesting that stochastic interactions between dynein subunits and DNAAFs do not govern this process, but rather, they localize with one another at concentrated regions of cytoplasm to carry out assembly.

Further investigation revealed that the cytoplasmic foci to which DNAAFs localized were not membrane bound, but rather liquid-like cytoplasmic phase separations similar in composition to stress granules. This was revealed by *in vivo* properties of the structures, including observations of fusion, fission, and rapid exchange of material with the cytosol. Additionally, perturbation of a stress granule assembly factor, G3BP1, abrogated the formation of DynAPs as well as failure to recruit axonemal dynein to cilia. However, there were several properties that deviated the DynAPs from previously identified phase-separated organelles, namely in that they lacked many factors known to be present in stress granules, and also contained many different chaperone proteins. Further, stress granules have been reported to form in times of cellular stress, then disassemble when favorable conditions are met (Protter and Parker, 2016); this was not observed in DynAPs. A model was developed to describe these observations in conjunction with previously identified characteristics of this process, wherein unfolded axonemal dynein peptides are shuttled into a phase separated matrix, where DNAAFs work in conjunction with chaperones such as Hsp70 and 90 to mediate the folding and assembly of axonemal dynein arms (Figure 3.11)

These observations imply that the DynAPs were distinct cellular structures carrying out a highly-specialized cellular process built upon a core cellular machinery.

These observations bring up many other questions that necessitate further investigation. For example, we noted that within DynAPs were enriched for RNAs, however the identity of these molecules is unknown, but could potentially give insight into the processes occurring within the granules. The RNAs within these structures could be nonspecific, serving only as a means of binding to RNA-binding domains in order to mediate the phase-separation process, or they could be increased local concentrations of dynein RNAs that are present to localize translation. In addition, recent studies have indicated that stress granules are assembled through a multistep process wherein a “core” structure is first assembled then various components are recruited to form a “shell” surrounding it (Wheeler et al., 2016). Super resolution microscopy could be implemented to designate substructural elements such as these in the DynAP. The data presented here imply that the cytoplasmic assembly of axonemal dynein arms is dependent on both ciliated cell-specific elements (i.e. dynein assembly factors) paired with ubiquitous cellular machinery (i.e. stress granule components) working together in a phase-separated matrix to carry out a highly-specialized process. This suggests that various other processes may utilize phase-separation to compartmentalize certain cell type-specific biochemical events.

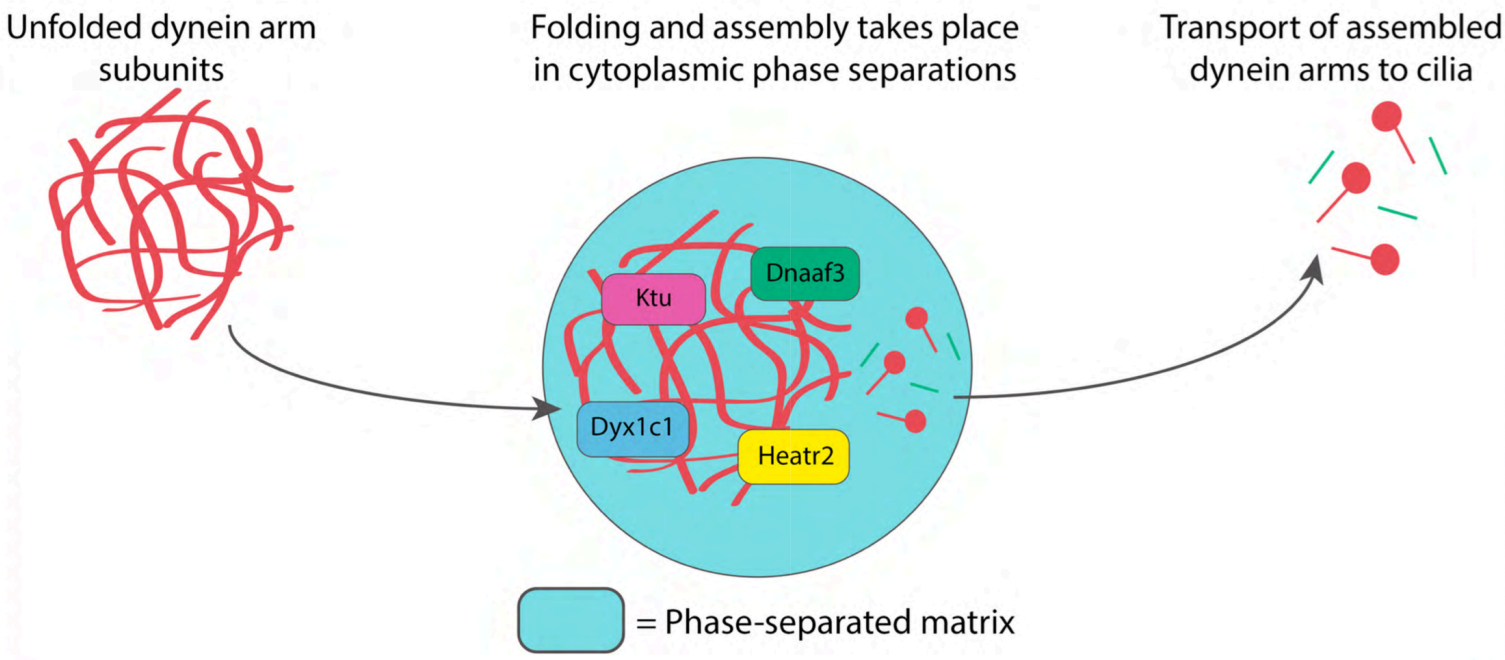

Figure 3.11 – Putative model for cytoplasmic preassembly of axonemal dynein arms. Based on our data, a model has been developed for axonemal dynein arm assembly, where unfolded axonemal dynein subunits are shuttled in to a phase-separated matrix composed in part by stress granule components. In this matrix, axonemal dynein assembly factors and ubiquitous cellular chaperones mediate the folding of dynein subunits as well as the assembly of dynein arm complexes. After the dynein arms have been assembled, they are shuttled out of the phase-separated organelles and transported into cilia via intraflagellar transport.

Chapter 4: Summary and conclusions

Ciliogenesis is governed by coordination of many different cellular processes to regulate the formation and function of cilia. Proper organization of these events is critical across eukaryotes, as cilia serve multiple roles: in single cells, they serve as a means of propulsion, in multicellular organisms, they line certain tissues to generate fluid flow, and in vertebrates, they serve as a signaling center (Goetz and Anderson, 2010). In humans, failure to produce cilia results in a pleiotropic ailments, including skeletal dysplasias, neural tube closure defects, mental retardation, and blindness, among others (Hildebrandt et al., 2011). In this thesis, I have defined novel machinery required for two processes governing ciliogenesis: intraflagellar transport, a bidirectional process responsible for the transport of materials into the cilium (Rosenbaum and Witman, 2002), and cytoplasmic preassembly of axonemal dynein arms, the machinery that generates force required for ciliary motility (King, 2016).

First, using a computationally curated map of human protein complexes, hu.MAP, the ankyrin repeat protein ANKRD55 was identified as an interactor of intraflagellar transport proteins. Specifically, we found that it interacted with IFT70, IFT52, and IFT27, three components of the previously described IFT-B1 complex (Drew et al., In review; Taschner et al., 2016). Using *Xenopus laevis* as a vertebrate model, ANKRD55 was functionally characterized. A GFP tagged version of this protein localized to axonemes in a punctate pattern, and trafficked along cilia, colocalizing with another IFT-B subunit CLUAP1 as revealed by high-speed time lapse microscopy (Figure 2.2, 2.3). ANKRD55 also showed expression restricted to ciliated tissues including nephrostomes and ventral neural tube, similar to the pattern observed in the IFT-B1 component IFT81 (Figure 2.4).

Previously observed IFT-B buildup in JBTS17 morphant multiciliated cells was utilized to further assay ANKRD55 for IFT-B-like behavior. Indeed, ANKRD55-GFP accumulated in cilia in JBTS17 knockdown (Figure 2.5).

Consistent with the observed behavior of ANKRD55 in cilia, its knockdown resulted in phenotypes identified in other IFT morphants. ANKRD55 morphant multiciliated cells showed depleted or absent ciliogenesis with normal basal body docking, a phenotype akin to that observed in knockdown of its predicted binding partner IFT52 (Figure 2.6). Often, IFT mutations result in neural tube closure defects in vertebrates (Hildebrandt et al., 2011). Indeed, ANKRD55 knockdown embryos neural tubes were splayed open, indicating a likely failure of sonic hedgehog transduction in the ventral neural tube due to loss of cilia (Figure 2.7). Often, skeletal abnormalities are observed in humans with pathogenic variants of IFT (Baldridge et al., 2010). Patients with variants in ANKRD55 were identified and *Xenopus* versions of these genes were produced and expressed. One of the two variants identified showed immensely reduced fluorescence in axonemes and within the cell body of multiciliated cells, and protein levels were greatly reduced indicating that degradation of protein or mRNA was likely (Figure 2.8-2.9). These findings together imply that ANKRD55 is a novel member of the IFT-B1 complex that likely underlies human ciliopathies.

Second, the process of cytoplasmic assembly of axonemal dynein arms was characterized. Previous studies have shed light on the role of several cytoplasmic factors in the folding of axonemal dynein subunits in the cytoplasm prior to their shipment and docking along microtubule doublets in axonemes. However, the cellular compartment to which this process occurs has not been identified -- reports have ranged

from diffuse cytosolic localization to *trans* golgi localization. Several dynein assembly factors were cloned and tagged with fluorescent proteins in order to points of subcellular localization in multiciliated cells of the *Xenopus* epidermis. I found that every dynein assembly factor tightly colocalized with one another to amorphous cytosolic foci (Figure 3.1). These factors are believed to interact with various axonemal dynein subunits, and thus, I hypothesized that they would colocalize at these cytosolic foci. Indeed, the intermediate chain axonemal dynein DNAI2 also localized to the same cytoplasmic foci (Figure 3.2). These foci, which we term dynein assembly particles (DynAPs), were found to be non-membrane bound and displayed liquid like properties, including fusion and exchange of material with the cytoplasm (Figure 3.7-3.8). Further, DynAPs displayed compositional similarity to stress granules as they contained many of the same proteins, as well as RNA (Figure 3.6). However, there were many deviations from this, for example, no translation initiation factors were found in DynAPs, and many chaperones were enriched in DynAPs, which are absent from stress granules. In knockdown embryos for one of these components, G3BP1, a stress granule nucleator, DynAPs failed to form and the outer dynein arm subunit DNAI2 was no longer recruited to cilia (Figure 3.9, 3.10). From these results I proposed a model wherein unfolded axonemal dynein subunits are shuttled into a phase separated matrix, wherein they are folded and assembled by dynein assembly factors before being transported out and docked within axonemes.

To conclude, using the well-defined model system of the *Xenopus* epidermis, this thesis has presented findings that further characterize events that contribute to the formation and function of cilia. First, using a computational map of human protein

complexes, ANKRD55 was identified was a novel member of the IFT-B complex. Second, dynein arms are assembled at distinct, phase-separated organelles specific to the cytoplasm of multiciliated cells that are structurally similar to eukaryotic stress granules. Though the work presented here has begun to uncover new players in ciliogenic processes, the molecular mechanisms that govern both axonemal dynein assembly and intraflagellar transport are largely unknown and merit further study.

Appendix A: Materials and Methods

Plasmids and cloning

Specific DNA regions were amplified from *Xenopus* cDNA or plasmid DNA by polymerase chain reaction. Xenopus gene sequences were obtained from Xenbase and primers were subsequently designed either by hand or through the use of Invitrogen's OligoPerfect primer design software (Thermo Fisher). Primers used for the work presented in this thesis are contained in Table 5.1. For PCR of cDNA, Phusion High-Fidelity Polymerase was used (NEB), for amplification of plasmid DNA, Taq DNA polymerase was used. PCRs typically contained 0.5U polymerase, 0.2mM dNTPs (NEB), 0.5μM each primer, 1X of reaction buffer, and variable amounts of template DNA/cDNA. Reactions were carried out in thermocycler (Eppendorf). PCR products were purified using the QIAquick PCR Purification Kit (Qiagen) in accordance with manufacturer's instructions.

Linear or plasmid DNA was digested with restriction endonucleases in CutSmart buffer (both supplied by NEB). 5-10 μg DNA was added to 20-50U restriction enzyme in 1X buffer. Digestions were carried out at 37°C for a minimum 3 hours.

Agarose gel electrophoresis was used to analyze DNA samples. Gels ranging between 1-1.5% agarose in 1/3X TAE (w/v). To prepare gels, agarose was added to TAE and dissolved by microwave. Ethidium bromide was added at a concentration of 0.5 μg/ml. 5X loading buffer was added to DNA samples before loading, and DNA ladders were loaded as size reference. Samples were run at constant voltage (80-120V) and gels were later visualized via UV transilluminator. Following gel electrophoresis,

desired fragments were removed from the gel by cutting with a clean razor blade. DNA was then extracted from this gel with the QIAquick Gel Extraction Kit (Qiagen) in accordance with manufacturer's instructions.

To ligate a DNA insert into a vector of interest, typically containing an eGFP, mRFP, or mCherry tag at the N or C terminus of the encoded protein. 100 ng of digested vector was combined with 3 molar equivalents of DNA insert. 1U of T4 DNA ligase (NEB), 1X T4 ligase buffer (NEB) were added and samples were incubated at room temperature for .5 - 1 hour. ANKRD55, KTU, HEATR2, LRRC6, PIH1D3, DNAI2, G3BP1, and TIA1 inserts were placed in a pCS10R-GFP or mCherry vectors (derived from pCs107). DNAAF3 and DYX1C1 were cloned into pCS2+ Gateway destination vector containing an RFP tag and and alpha tubulin promoter from Gateway ENTRY clones via Gateway LR Clonase II Enzyme mix (Life Technologies).

Plasmid DNA was added to 100 µL chemically competent DH5-α cells and incubated on ice for 30 minutes before a 45 second heat shock at 42°C. Cells were then placed back on ice for 5 minutes to recover and ~60 µL cells were plated on LB-agar plates containing antibiotics corresponding to the selection marker within the plasmid. Transformations were incubated 16-18 hours at 37°C. From previously plated transformation, a single colony was selected and used to inoculate 5 mL of LB medium with antibiotic added. Cultures were incubated for 16-18 hours at 37°C with shaking then cells were collected via centrifugation. DNA was harvested from cells using the QIAprep Miniprep Kit (Qiagen) according to manufacturer's instructions. All plasmids were verified through Sanger sequencing of insert.

Primer Name	*Sequence (5'-->3')*
DNAAF3 F	GGGGTCGACATGGCTGCTGCTGCTGGTAGAAGAATG
DNAAF3 R	GGGGCGGCCGCTCATTGGGCAGTTTGCAGTTCTACAGA
KTU F	GGGGTCGACATGGCGGAAAAACTTCAGAATCTGGAA
KTU R	GGGGCGGCCGCTCAGTCTAGGTCAAACAGCAATGAATT
HEATR2 F	GGGGTCGACATGGCGGCGGAGGGTGAGCAGCGTGCG
HEATR2 R	GGGGCGGCCGCCTACGTGCATTCTGTAGGAGTCGGGCT
DYX1C1 F	GGGGTCGACATGCCTATCATAGCGAATGATTATACG
DYX1C! R	GGGGCGGCCGCTCACAAGTCCTTGATGTCCAACATGAT
LRRC6 F	GGGGTCGACATGGTGCGAGTTAGTGAAGATCTGATC
LRRC6 R	GGGGCGGCCGCTCACATGAGTGGCGGAACGTCTGTGTT
ANKRD55 F	GGGGTCGACCTAGCTGTTAGAATCGGAGTTGTTTTC
ANKRD55 R	GGGACTAGTATGGATTTCAGCAACTCGTCTGTGTTT
G3BP1 F	GGGGTCGACATGATGCTGCTGCCATCTTCTGGTCCG
G3BP1 R	GGGGCGGCCGCTCACTGGCGTGGGCCTTGATTACCCCT
DNAI2 F	GGGGTCGACATGGAGATTGTCTATGTGTATACACGG
DNAI2 R	GGGGCGGCCGCTTATTCATGTACAATTTTCTCCTCAGA
TIA1 F	GGGGTCGACATGGAGGAAGAATTACCCAGAACGCTG
TIA1 R	GGGGCGGCCGCTCATTGTGTTTGGTATCCAGCCATCCG
PIH1D3 F	GGGGTCGACATGGAACTGGCACTGGGTGAGTTTACA
PIH1D3 R	GGGGCGGCCGCTCAAAGGAAGTTGATGAAATCTAATTC
GAPDH F	ATGGTGAAGGTTGGAATTAACGGATTT
GAPDH R	TTATTCCTTAGATGCCATGTGACACAC

Table 5.1 – Primers used in this thesis. Primers used for cloning and RT-PCR from *Xenopus* cDNA are listed. In each case, 5' ends of primers are on the left, and 3' ends are on the right.

Xenopus embryo manipulations

Female adult *Xenopus* were induced to ovulate via injection of human chorionic gonadotropin, and oocytes were gathered via squeezing frogs the following day. Testes were gathered from adult male frogs by euthanization in 0.05% benzocaine, followed by surgical removal of testes. *In vitro* fertilization was carried out by cutting and homogenizing a small fraction of a testis in .33X Marc's modified Ringer's (MMR;0.1 M Nacl, 2.0mM KCL, 1mM $MgSO_4$, 2mM $CaCl_2$, 5mM HEPES (pH 7.8) in double distilled H2O, pH to 7.4) and added to each clutch of oocytes. At the two-cell stage, embryos were dejellied in 3% cysteine and subsequently moved to 1/3x MMR.

For microinjection, *Xenopus* embryos were placed in a 2.0% solution of Ficoll (w/v) in .33X MMR, injected using Dumont forceps and an Oxford universal micromanipulator. Embryos were then reared in 2% Ficoll in 0.33X MMR to gastrulation, then washed and reared in 0.33X MMR alone. Washes were repeated twice per day until optimal stage was reached.

Morpholino and mRNAs

Morpholinos targeting ANKRD55, G3BP1 long and short alloalleles, IFT52, and JBTS17 were obtained from Gene Tools. Sequences of these morpholinos are as follows:

ANKRD55 5'- TCTGAATCACCTTGAAGCACAAAGA -3';

JBTS17 5'- TCTTCTTGATCCACTTACTTTTCCC-3';

IFT52 5'-AAGCAATCTGTTTGTTGACTCCCAT-3';

G3BP1.S 5' – GGGTTTGTTTTTACGCATACCTTCT -3';

G3BP1.L 5’ - TTTCTTTTACCACATACCTTCTGGA -3’.

Capped, polyadenylated mRNA was produced from PCS10R plasmids linearized by AscI digestion using the SP6 mMessage mMachine kit (Ambion) following manufacturer's instructions. mRNAs and morpholinos were injected into 4-cell stage embryos in either the ventral blastomeres (to target epidermis) or dorsal blastomeres (to target neural tissue). Dosages of plasmids, mRNA, and Morpholinos used in experiments presented in Table 5.2.

RT-PCR

ANKRD55 morpholino was injected into all four blastomeres of a 4-cell stage embryo at varying doses. Embryos were reared until stage 20, then RNAs were isolated using TRIzol reagent (Invitrogen). A stage 20 cDNA library was produced M-MLV reverse transcriptase (Invitrogen) with random hexamers. ANKRD55 and GAPDH were amplified using Phusion High-fidelity DNA Polymerase (NEB) with the primers listed in.

In situ hybridization

Whole-mount in situ hybridization of Xenopus embryos was performed as described previously (Sive et al., 2000) using digoxigenin-labeled antisense RNA probes against ANKRD55 and IFT81 made using an mMessage mMachine T7 kit (Ambion) . Bright-field images were obtained using a Zeiss Axiozoom V16 stereomicroscope.

Embryo fixation and RNA staining

For quantification of ANKRD55 neural tube closure experiments, embryos were arrested at stage 19 by fixation in MEMFA for two hours at room temperature after removing the vitelline envelope, then washed repeatedly with PBST (1X PBS with 0.05% Triton X-100). RNA staining of stage 26 *Xenopus* embryos was carried out by using Dent's Fix (20% DMSO, 80% methanol) for two hours, washing with PBST, then staining with SYTO RNAselect green fluorescent stain (Thermo Fisher).

Injected Molecule	*Dosage*	*Usage*
ANKRD55-GFP mRNA	75 pg	Localization
ANKRD55 mRNA	350 pg	Neural tube closure rescue
ANKRD55 MO	40 ng	ANKRD55 Knockdown
CETN4-BFP	40 pg	Localization
CLUAP1-mCherry	100 pg	Localization
DNAAF3-RFP Plasmid	35 pg	Localization
mCherry-DNAI2 mRNA	100 pg	Localization
DYX1C1-RFP Plasmid	40 pg	Localization
FOXJ1 mRNA	200 pg	Ciliogenesis induction
GFP-G3BP1 mRNA	75 pg	Localization, FRAP
*G3BP1.S MO**	30 pg	G3BP1 knockdown
*G3BP1.L MO**	30 pg	G3BP1 knockdown
GALT-RFP mRNA	60 pg	Localization
GFP-HEATR2 mRNA	75 pg	Localization
mCherry-HEATR2	75 pg	Localization
IFT52 MO	40 ng	IFT52 knockdown
JBTS17 MO	20 ng	JBTS17 knockdown
GFP-KTU	75 pg	Localization
mCherry-KTU	75 pg	Localization
GFP-LRRC6	100 pg	Localization
membrane-GFP	50 pg	Localization
membrane-RFP	50 pg	Localization
membrane-BFP	75 pg	Localization
Multicilin-HGR	100 pg	Ciliogenesis induction
GFP-TIA1	100 pg	Localization

Table 5.2 – Dosage listing for mRNAs, plasmids, and morpholinos used in this thesis. * G3BP1.S and G3BP1.L morpholinos were used in conjunction with one another to target both alloalleles.

Live imaging of Xenopus embryo epidermis

For *in vivo* experiments, stage 25-28 *Xenopus* embryos were anesthetized in 0.005% benzocaine, then placed between cover glass in circular imaging disks as previously described (Keiserman et al., 2010). Fluorescent images of the *Xenopus* epidermis were obtained using an LSM700 confocal microscope (Carl Zeiss) with a 63x oil-immersion objective. High-speed time-lapse microscopy was carried out on a Nikon eclipse confocal microscope using a 63x oil-immersion objective. Kymographs were produced from IFT movies using the Kymograph Fiji plugin.

Fluorescence Recovery after Photobleaching and Analysis

For fluorescence recovery after photobleaching (FRAP), embryos were anesthetized in 0.005% benzocaine and placed between cover glass and imaged using an LSM700 inverted confocal microscope (Carl Zeiss) with a 63x oil-immersion objective. Time lapse movies were taken with simultaneous photobleaching of either stress granules (labeled with G3BP1 but not KTU) or DynAPs (containing both G3BP1 and KTU). Images were corrected for drift with the StackReg plugin in Fiji, and subsequent intensity measurement and recovery curve generation were carried out using the Jython FRAP script (http://imagej.net/Analyze_FRAP_movies_with_a_Jython_script). Intensity measurements of G3BP1-GFP were normalized to background cytoplasmic intensity.

References

Afzelius, B.A. (1976). A human syndrome caused by immotile cilia. Science *193*, 317–319.

Airik, R., Schueler, M., Airik, M., Cho, J., Ulanowicz, K.A., Porath, J.D., Hurd, T.W., Bekker-Jensen, S., Schrøder, J.M., Andersen, J.S., et al. (2016). SDCCAG8 Interacts with RAB Effector Proteins RABEP2 and ERC1 and Is Required for Hedgehog Signaling. PLOS ONE *11*, e0156081.

Al Jord, A., Lemaître, A.-I., Delgehyr, N., Faucourt, M., Spassky, N., and Meunier, A. (2014). Centriole amplification by mother and daughter centrioles differs in multiciliated cells. Nature *516*, 104–107.

Arafa, S.Z., and Reda, E.S. (2012). Surface features of the monogenean gill parasites Pseudodactylogyrus anguillae and Pseudodactylogyrus bini from the European eel Anguilla anguilla in Egypt. Parasitol Res *110*, 127–133.

Austin-Tse, C., Halbritter, J., Zariwala, M.A., Gilberti, R.M., Gee, H.Y., Hellman, N., Pathak, N., Liu, Y., Panizzi, J.R., Patel-King, R.S., et al. (2013). Zebrafish Ciliopathy Screen Plus Human Mutational Analysis Identifies C21orf59 and CCDC65 Defects as Causing Primary Ciliary Dyskinesia. The American Journal of Human Genetics *93*, 672–686.

Baccetti, B., and Dallai, R. (1976). The spermatozoon of arthropoda. XXVII. Uncommon axoneme patterns in different species of the cecidomyid flies. Journal of Ultrastructure Research *55*, 50–69.

Bahe, S., Stierhof, Y.-D., Wilkinson, C.J., Leiss, F., and Nigg, E.A. (2005). Rootletin forms centriole-associated filaments and functions in centrosome cohesion. J Cell Biol *171*, 27–33.

Baldridge, D., Shchelochkov, O., Kelley, B., and Lee, B. (2010). Signaling pathways in human skeletal dysplasias. Annu Rev Genomics Hum Genet *11*, 189–217.

Beck, R., Ravet, M., Wieland, F.T., and Cassel, D. (2009). The COPI system: Molecular mechanisms and function. FEBS Letters *583*, 2701–2709.

Behal, R.H., Miller, M.S., Qin, H., Lucker, B.F., Jones, A., and Cole, D.G. (2012). Subunit Interactions and Organization of the Chlamydomonas reinhardtii Intraflagellar Transport Complex A Proteins. J. Biol. Chem. *287*, 11689–11703.

Bhogaraju, S., Taschner, M., Morawetz, M., Basquin, C., and Lorentzen, E. (2011). Crystal structure of the intraflagellar transport complex 25/27. The EMBO Journal *30*, 1907–1918.

Bhogaraju, S., Cajanek, L., Fort, C., Blisnick, T., Weber, K., Taschner, M., Mizuno, N., Lamla, S., Bastin, P., Nigg, E.A., et al. (2013a). Molecular Basis of Tubulin Transport Within the Cilium by IFT74 and IFT81. Science *341*, 1009–1012.

Bhogaraju, S., Engel, B.D., and Lorentzen, E. (2013b). Intraflagellar transport complex structure and cargo interactions. Cilia *2*, 10.

Binder, K., and Stauffer, D. (1976). Statistical theory of nucleation, condensation and coagulation. Advances in Physics *25*, 343–396.

Bisgrove, B.W., Makova, S., Yost, H.J., and Brueckner, M. (2012). RFX2 is essential in the ciliated organ of asymmetry and an RFX2 transgene identifies a population of ciliated cells sufficient for fluid flow. Developmental Biology *363*, 166–178.

Blacque, O.E., Li, C., Inglis, P.N., Esmail, M.A., Ou, G., Mah, A.K., Baillie, D.L., Scholey, J.M., and Leroux, M.R. (2006). The WD Repeat-containing Protein IFTA-1 Is Required for Retrograde Intraflagellar Transport. Mol Biol Cell *17*, 5053–5062.

Boon, M., Wallmeier, J., Ma, L., Loges, N.T., Jaspers, M., Olbrich, H., Dougherty, G.W., Raidt, J., Werner, C., Amirav, I., et al. (2014). MCIDAS mutations result in a mucociliary clearance disorder with reduced generation of multiple motile cilia. Nature Communications *5*, 4418.

Brangwynne, C.P. (2013). Phase transitions and size scaling of membrane-less organelles. J Cell Biol *203*, 875–881.

Brangwynne, C.P., Eckmann, C.R., Courson, D.S., Rybarska, A., Hoege, C., Gharakhani, J., Jülicher, F., and Hyman, A.A. (2009). Germline P Granules Are Liquid Droplets That Localize by Controlled Dissolution/Condensation. Science *324*, 1729–1732.

Brangwynne, C.P., Mitchison, T.J., and Hyman, A.A. (2011). Active liquid-like behavior of nucleoli determines their size and shape in Xenopus laevis oocytes. PNAS *108*, 4334–4339.

Brody, S.L., Yan, X.H., Wuerffel, M.K., Song, S.-K., and Shapiro, S.D. (2000). Ciliogenesis and Left–Right Axis Defects in Forkhead Factor HFH-4–Null Mice. Am J Respir Cell Mol Biol *23*, 45–51.

Brooks, E.R., and Wallingford, J.B. (2012). Control of vertebrate intraflagellar transport by the planar cell polarity effector Fuz. J Cell Biol *198*, 37–45.

Brooks, E.R., and Wallingford, J.B. (2014). Multiciliated Cells. Current Biology *24*, R973–R982.

Buchan, J.R., and Parker, R. (2009). Eukaryotic Stress Granules: The Ins and Outs of Translation. Molecular Cell *36*, 932–941.

Bui, K.H., Sakakibara, H., Movassagh, T., Oiwa, K., and Ishikawa, T. (2008). Molecular architecture of inner dynein arms in situ in Chlamydomonas reinhardtii flagella. J Cell Biol *183*, 923–932.

Bui, K.H., Yagi, T., Yamamoto, R., Kamiya, R., and Ishikawa, T. (2012). Polarity and asymmetry in the arrangement of dynein and related structures in the Chlamydomonas axoneme. J Cell Biol *198*, 913–925.

Caron, A., Xu, X., and Lin, X. (2012). Wnt/β-catenin signaling directly regulates Foxj1 expression and ciliogenesis in zebrafish Kupffer's vesicle. Development *139*, 514–524.

Carvalho-Santos, Z., Azimzadeh, J., Pereira-Leal, J.B., and Bettencourt-Dias, M. (2011). Tracing the origins of centrioles, cilia, and flagella. J Cell Biol *194*, 165–175.

Castleman, V.H., Romio, L., Chodhari, R., Hirst, R.A., de Castro, S.C.P., Parker, K.A., Ybot-Gonzalez, P., Emes, R.D., Wilson, S.W., Wallis, C., et al. (2009). Mutations in Radial Spoke Head Protein Genes RSPH9 and RSPH4A Cause Primary Ciliary Dyskinesia with Central-Microtubular-Pair Abnormalities. The American Journal of Human Genetics *84*, 197–209.

Choksi, S.P., Lauter, G., Swoboda, P., and Roy, S. (2014). Switching on cilia: transcriptional networks regulating ciliogenesis. Development *141*, 1427–1441.

Chung, M.-I., Peyrot, S.M., LeBoeuf, S., Park, T.J., McGary, K.L., Marcotte, E.M., and Wallingford, J.B. (2012). RFX2 is broadly required for ciliogenesis during vertebrate development. Developmental Biology *363*, 155–165.

Cole, D.G., Chinn, S.W., Wedaman, K.P., Hall, K., Vuong, T., and Scholey, J.M. (1993). Novel heterotrimeric kinesin-related protein purified from sea urchin eggs. Nature *366*, 268–270.

Conduit, P.T., Wainman, A., and Raff, J.W. (2015). Centrosome function and assembly in animal cells. Nat Rev Mol Cell Biol *16*, 611–624.

Craft, J.M., Harris, J.A., Hyman, S., Kner, P., and Lechtreck, K.F. (2015). Tubulin transport by IFT is upregulated during ciliary growth by a cilium-autonomous mechanism. J Cell Biol *208*, 223–237.

Czarnecki, P.G., and Shah, J.V. (2012). The ciliary transition zone: from morphology and molecules to medicine. Trends in Cell Biology *22*, 201–210.

Dawe, H.R., Farr, H., and Gull, K. (2007). Centriole/basal body morphogenesis and migration during ciliogenesis in animal cells. Journal of Cell Science *120*, 7–15.

Decker, C.J., and Parker, R. (2012). P-Bodies and Stress Granules: Possible Roles in the Control of Translation and mRNA Degradation. Cold Spring Harb Perspect Biol *4*.

Deisseroth, A., and Dounce, A.L. (1970). Catalase: Physical and chemical properties, mechanism of catalysis, and physiological role. Physiological Reviews *50*, 319–375.

Diggle, C.P., Moore, D.J., Mali, G., Lage, P. zur, Ait-Lounis, A., Schmidts, M., Shoemark, A., Munoz, A.G., Halachev, M.R., Gautier, P., et al. (2014). HEATR2 Plays a Conserved Role in Assembly of the Ciliary Motile Apparatus. PLOS Genetics *10*, e1004577.

Dong, F., Shinohara, K., Botilde, Y., Nabeshima, R., Asai, Y., Fukumoto, A., Hasegawa, T., Matsuo, M., Takeda, H., Shiratori, H., et al. (2014). Pih1d3 is required for cytoplasmic preassembly of axonemal dynein in mouse sperm. J Cell Biol *204*, 203–213.

Dougherty, G.W., Loges, N.T., Klinkenbusch, J.A., Olbrich, H., Pennekamp, P., Menchen, T., Raidt, J., Wallmeier, J., Werner, C., Westermann, C., et al. (2016). DNAH11 Localization in the Proximal Region of Respiratory Cilia Defines Distinct Outer Dynein Arm Complexes. Am J Respir Cell Mol Biol *55*, 213–224.

Drew, K., Lee, C., Huizar, R.L., Tu, F., Borgeson, B., McWhite, C.D., Ma, Y., Wallingford, J.B., and Marcotte, E.M. (2016). A synthesis of over 9,000 mass spectrometry experiments reveals the core set of human protein complexes. bioRxiv 92361.

Duquesnoy, P., Escudier, E., Vincensini, L., Freshour, J., Bridoux, A.-M., Coste, A., Deschildre, A., de Blic, J., Legendre, M., Montantin, G., et al. (2009). Loss-of-Function Mutations in the Human Ortholog of Chlamydomonas reinhardtii ODA7 Disrupt Dynein Arm Assembly and Cause Primary Ciliary Dyskinesia. The American Journal of Human Genetics *85*, 890–896.

de Duve, C. (1963). The Lysosome Concept. In Ciba Foundation Symposium - Anterior Pituitary Secretion (Book I of Colloquia on Endocrinology), A.V.S. de R.M.S. A.R.C.S D.I.C., and rgrate P.C. M.A, eds. (John Wiley & Sons, Ltd), pp. 1–35.

Dymek, E.E., Heuser, T., Nicastro, D., and Smith, E.F. (2011). The CSC is required for complete radial spoke assembly and wild-type ciliary motility. Mol. Biol. Cell *22*, 2520–2531.

Eguether, T., San Agustin, J.T., Keady, B.T., Jonassen, J.A., Liang, Y., Francis, R., Tobita, K., Johnson, C.A., Abdelhamed, Z.A., Lo, C.W., et al. (2014). IFT27 Links the BBSome to IFT for Maintenance of the Ciliary Signaling Compartment. Developmental Cell *31*, 279–290.

Ernster, L., and Schatz, G. (1981). Mitochondria: a historical review. J Cell Biol *91*, 227s–255s.

Essner, J.J., Vogan, K.J., Wagner, M.K., Tabin, C.J., Yost, H.J., and Brueckner, M. (2002). Left–right development: Conserved function for embryonic nodal cilia. Nature *418*, 37–38.

Eulalio, A., Behm-Ansmant, I., and Izaurralde, E. (2007). P bodies: at the crossroads of post-transcriptional pathways. Nat Rev Mol Cell Biol *8*, 9–22.

Fliegauf, M., Olbrich, H., Horvath, J., Wildhaber, J.H., Zariwala, M.A., Kennedy, M., Knowles, M.R., and Omran, H. (2005). Mislocalization of DNAH5 and DNAH9 in Respiratory Cells from Patients with Primary Ciliary Dyskinesia. Am J Respir Crit Care Med *171*, 1343–1349.

Fowkes, M.E., and Mitchell, D.R. (1998). The Role of Preassembled Cytoplasmic Complexes in Assembly of Flagellar Dynein Subunits. Mol. Biol. Cell *9*, 2337–2347.

Fu, W., Wang, L., Kim, S., Li, J., and Dynlacht, B.D. (2016). Role for the IFT-A Complex in Selective Transport to the Primary Cilium. Cell Rep *17*, 1505–1517.

Gajiwala, K.S., Chen, H., Cornille, F., Roques, B.P., Reith, W., Mach, B., and Burley, S.K. (2000). Structure of the winged-helix protein hRFX1 reveals a new mode of DNA binding. Nature *403*, 916–921.

Goetz, S.C., and Anderson, K.V. (2010). The primary cilium: a signalling centre during vertebrate development. Nat Rev Genet *11*, 331–344.

Guirao, B., Meunier, A., Mortaud, S., Aguilar, A., Corsi, J.-M., Strehl, L., Hirota, Y., Desoeuvre, A., Boutin, C., Han, Y.-G., et al. (2010). Coupling between hydrodynamic forces and planar cell polarity orients mammalian motile cilia. Nat Cell Biol *12*, 341–350.

Gupta, G.D., Coyaud, É., Gonçalves, J., Mojarad, B.A., Liu, Y., Wu, Q., Gheiratmand, L., Comartin, D., Tkach, J.M., Cheung, S.W.T., et al. (2015). A Dynamic Protein Interaction Landscape of the Human Centrosome-Cilium Interface. Cell *163*, 1484–1499.

Hamasaki, T. (1999). Regulation of outer-arm-dynein activity by phosphorylation and control of ciliary beat frequency. Protoplasma *206*, 241–244.

Han, T.W., Kato, M., Xie, S., Wu, L.C., Mirzaei, H., Pei, J., Chen, M., Xie, Y., Allen, J., Xiao, G., et al. (2012). Cell-free Formation of RNA Granules: Bound RNAs Identify Features and Components of Cellular Assemblies. Cell *149*, 768–779.

Hao, L., and Scholey, J.M. (2009). Intraflagellar transport at a glance. Journal of Cell Science *122*, 889–892.

Harris, J.A., Liu, Y., Yang, P., Kner, P., and Lechtreck, K.F. (2016). Single-particle imaging reveals intraflagellar transport–independent transport and accumulation of EB1 in Chlamydomonas flagella. Mol. Biol. Cell *27*, 295–307.

Hayes, J.M., Kim, S.K., Abitua, P.B., Park, T.J., Herrington, E.R., Kitayama, A., Grow, M.W., Ueno, N., and Wallingford, J.B. (2007). Identification of novel ciliogenesis factors using a new in vivo model for mucociliary epithelial development. Developmental Biology *312*, 115–130.

Hein, M.Y., Hubner, N.C., Poser, I., Cox, J., Nagaraj, N., Toyoda, Y., Gak, I.A., Weisswange, I., Mansfeld, J., Buchholz, F., et al. (2015). A Human Interactome in Three Quantitative Dimensions Organized by Stoichiometries and Abundances. Cell *163*, 712–723.

Hernandez-Verdun, D. (2006). Nucleolus: from structure to dynamics. Histochem Cell Biol *125*, 127–137.

Heuser, T., Raytchev, M., Krell, J., Porter, M.E., and Nicastro, D. (2009). The dynein regulatory complex is the nexin link and a major regulatory node in cilia and flagella. The Journal of Cell Biology *187*, 921–933.

Hildebrandt, F., Benzing, T., and Katsanis, N. (2011). Ciliopathies. New England Journal of Medicine *364*, 1533–1543.

Holt, C.E., and Schuman, E.M. (2013). The Central Dogma Decentralized: New Perspectives on RNA Function and Local Translation in Neurons. Neuron *80*, 648–657.

Horani, A., Druley, T.E., Zariwala, M.A., Patel, A.C., Levinson, B.T., Van Arendonk, L.G., Thornton, K.C., Giacalone, J.C., Albee, A.J., Wilson, K.S., et al. (2012). Whole-Exome Capture and Sequencing Identifies HEATR2 Mutation as a Cause of Primary Ciliary Dyskinesia. The American Journal of Human Genetics *91*, 685–693.

Horani, A., Ferkol, T.W., Shoseyov, D., Wasserman, M.G., Oren, Y.S., Kerem, B., Amirav, I., Cohen-Cymberknoh, M., Dutcher, S.K., Brody, S.L., et al. (2013). LRRC6 Mutation Causes Primary Ciliary Dyskinesia with Dynein Arm Defects. PLOS ONE *8*, e59436.

Hou, Y., Pazour, G.J., and Witman, G.B. (2004). A Dynein Light Intermediate Chain, D1bLIC, Is Required for Retrograde Intraflagellar Transport. Mol. Biol. Cell *15*, 4382–4394.

Hou, Y., Qin, H., Follit, J.A., Pazour, G.J., Rosenbaum, J.L., and Witman, G.B. (2007). Functional analysis of an individual IFT protein: IFT46 is required for transport of outer dynein arms into flagella. The Journal of Cell Biology *176*, 653–665.

Hoyer-Fender, S. (2010). Centriole maturation and transformation to basal body. Seminars in Cell & Developmental Biology *21*, 142–147.

Huttlin, E.L., Ting, L., Bruckner, R.J., Gebreab, F., Gygi, M.P., Szpyt, J., Tam, S., Zarraga, G., Colby, G., Baltier, K., et al. (2015). The BioPlex Network: A Systematic Exploration of the Human Interactome. Cell *162*, 425–440.

Hyman, A.A., and Simons, K. (2012). Beyond Oil and Water—Phase Transitions in Cells. Science *337*, 1047–1049.

Hyman, A.A., Weber, C.A., and Jülicher, F. (2014). Liquid-Liquid Phase Separation in Biology. Annual Review of Cell and Developmental Biology *30*, 39–58.

Ishikawa, T. (2016). Axoneme Structure from Motile Cilia. Cold Spring Harb Perspect Biol a028076.

Ishikawa, H., and Marshall, W.F. (2011). Ciliogenesis: building the cell's antenna. Nat Rev Mol Cell Biol *12*, 222–234.

Ishikawa, H., Thompson, J., Yates III, J.R., and Marshall, W.F. (2012). Proteomic Analysis of Mammalian Primary Cilia. Current Biology *22*, 414–419.

Jiang, J., and Hui, C. (2008). Hedgehog Signaling in Development and Cancer. Developmental Cell *15*, 801–812.

Jord, A.A., Spassky, N., and Meunier, A. (2016). Abstract B26: Centriole amplification during mammalian multiciliated cell development reveals a novel centrosome asymmetry. Mol Cancer Res *14*, B26–B26.

Kakihara, Y., and Houry, W.A. (2012). The R2TP complex: Discovery and functions. Biochimica et Biophysica Acta (BBA) - Molecular Cell Research *1823*, 101–107.

Khayyeri, H., Barreto, S., and Lacroix, D. (2015). Primary cilia mechanics affects cell mechanosensation: A computational study. Journal of Theoretical Biology *379*, 38–46.

Kieserman, E.K., Lee, C., Gray, R.S., Park, T.J., and Wallingford, J.B. (2010). High-Magnification In Vivo Imaging of Xenopus Embryos for Cell and Developmental Biology. Cold Spring Harb Protoc *2010*, pdb.prot5427.

King, S.M. (2016). Axonemal Dynein Arms. Cold Spring Harb Perspect Biol *8*, a028100.

King, S.M., and Patel-King, R.S. (2015). The Oligomeric Outer Dynein Arm Assembly Factor CCDC103 Is Tightly Integrated within the Ciliary Axoneme and Exhibits Periodic Binding to Microtubules. J. Biol. Chem. *290*, 7388–7401.

Knowles, M.R., Ostrowski, L.E., Loges, N.T., Hurd, T., Leigh, M.W., Huang, L., Wolf, W.E., Carson, J.L., Hazucha, M.J., Yin, W., et al. (2013). Mutations in SPAG1 Cause Primary Ciliary Dyskinesia Associated with Defective Outer and Inner Dynein Arms. The American Journal of Human Genetics *93*, 711–720.

Knowles, M.R., Ostrowski, L.E., Leigh, M.W., Sears, P.R., Davis, S.D., Wolf, W.E., Hazucha, M.J., Carson, J.L., Olivier, K.N., Sagel, S.D., et al. (2014). Mutations in RSPH1 Cause Primary Ciliary Dyskinesia with a Unique Clinical and Ciliary Phenotype. Am J Respir Crit Care Med *189*, 707–717.

Kobayashi, T., and Dynlacht, B.D. (2011). Regulating the transition from centriole to basal body. The Journal of Cell Biology *193*, 435–444.

Kott, E., Duquesnoy, P., Copin, B., Legendre, M., Dastot-Le Moal, F., Montantin, G., Jeanson, L., Tamalet, A., Papon, J.-F., Siffroi, J.-P., et al. (2012). Loss-of-Function Mutations in LRRC6, a Gene Essential for Proper Axonemal Assembly of Inner and Outer Dynein Arms, Cause Primary Ciliary Dyskinesia. The American Journal of Human Genetics *91*, 958–964.

Kozminski, K.G., Beech, P.L., and Rosenbaum, J.L. (1995). The Chlamydomonas kinesin-like protein FLA10 is involved in motility associated with the flagellar membrane. The Journal of Cell Biology *131*, 1517–1527.

Kubo, T., Brown, J.M., Bellve, K., Craige, B., Craft, J.M., Fogarty, K., Lechtreck, K.F., and Witman, G.B. (2016). Together, the IFT81 and IFT74 N-termini form the main module for intraflagellar transport of tubulin. J Cell Sci *129*, 2106–2119.

Lange, B.M.H., and Gull, K. (1996). Structure and function of the centriole in animal cells: progress and questions. Trends in Cell Biology *6*, 348–352.

Lapuente, A.L. de, Feliú, A., Ugidos, N., Mecha, M., Mena, J., Astobiza, I., Riera, J., Carillo-Salinas, F., Comabella, M., Montalban, X., et al. (2016). Novel Insights into the Multiple Sclerosis Risk Gene ANKRD55. The Journal of Immunology *196*, 4553–4565.

Lechtreck, K.F. (2015). IFT–Cargo Interactions and Protein Transport in Cilia. Trends in Biochemical Sciences *40*, 765–778.

Lechtreck, K.F., Van De Weghe, J.C., Harris, J.A., and Liu, P. (2017). Protein transport in growing and steady-state cilia. Traffic *18*, 277–286.

Letunic, I., Doerks, T., and Bork, P. (2015). SMART: recent updates, new developments and status in 2015. Nucleic Acids Res *43*, D257–D260.

Li, P., Banjade, S., Cheng, H.-C., Kim, S., Chen, B., Guo, L., Llaguno, M., Hollingsworth, J.V., King, D.S., Banani, S.F., et al. (2012). Phase transitions in the assembly of multivalent signalling proteins. Nature *483*, 336–340.

Loges, N.T., Olbrich, H., Fenske, L., Mussaffi, H., Horvath, J., Fliegauf, M., Kuhl, H., Baktai, G., Peterffy, E., Chodhari, R., et al. (2008). DNAI2 Mutations Cause Primary Ciliary Dyskinesia with Defects in the Outer Dynein Arm. The American Journal of Human Genetics *83*, 547–558.

Loges, N.T., Olbrich, H., Becker-Heck, A., Häffner, K., Heer, A., Reinhard, C., Schmidts, M., Kispert, A., Zariwala, M.A., Leigh, M.W., et al. (2009). Deletions and Point Mutations of LRRC50 Cause Primary Ciliary Dyskinesia Due to Dynein Arm Defects. The American Journal of Human Genetics *85*, 883–889.

Lopes, S.S., Lourenço, R., Pacheco, L., Moreno, N., Kreiling, J., and Saúde, L. (2010). Notch signalling regulates left-right asymmetry through ciliary length control. Development *137*, 3625–3632.

Ma, L., Quigley, I., Omran, H., and Kintner, C. (2014). Multicilin drives centriole biogenesis via E2f proteins. Genes Dev. *28*, 1461–1471.

Matsuki, H., Takahashi, M., Higuchi, M., Makokha, G.N., Oie, M., and Fujii, M. (2013). Both G3BP1 and G3BP2 contribute to stress granule formation. Genes Cells *18*, 135–146.

Mitchell, D.R. (2007). The Evolution of Eukaryotic Cilia and Flagella as Motile and Sensory Organelles. In Eukaryotic Membranes and Cytoskeleton, (Springer New York), pp. 130–140.

Mitchison, H.M., Schmidts, M., Loges, N.T., Freshour, J., Dritsoula, A., Hirst, R.A., O'Callaghan, C., Blau, H., Al Dabbagh, M., Olbrich, H., et al. (2012). Mutations in axonemal dynein assembly factor DNAAF3 cause primary ciliary dyskinesia. Nat Genet *44*, 381–389.

Moore, D.J., Onoufriadis, A., Shoemark, A., Simpson, M.A., zur Lage, P.I., de Castro, S.C., Bartoloni, L., Gallone, G., Petridi, S., Woollard, W.J., et al. (2013). Mutations in ZMYND10, a Gene Essential for Proper Axonemal Assembly of

Inner and Outer Dynein Arms in Humans and Flies, Cause Primary Ciliary Dyskinesia. The American Journal of Human Genetics *93*, 346–356.

Morimoto, M., Liu, Z., Cheng, H.-T., Winters, N., Bader, D., and Kopan, R. (2010). Canonical Notch signaling in the developing lung is required for determination of arterial smooth muscle cells and selection of Clara versus ciliated cell fate. J Cell Sci *123*, 213–224.

Mosavi, L.K., Cammett, T.J., Desrosiers, D.C., and Peng, Z. (2004). The ankyrin repeat as molecular architecture for protein recognition. Protein Sci *13*, 1435–1448.

Mukhopadhyay, S., Wen, X., Chih, B., Nelson, C.D., Lane, W.S., Scales, S.J., and Jackson, P.K. (2010). TULP3 bridges the IFT-A complex and membrane phosphoinositides to promote trafficking of G protein-coupled receptors into primary cilia. Genes Dev. *24*, 2180–2193.

Murdoch, J.N., and Copp, A.J. (2010). The relationship between Sonic hedgehog signalling, cilia and neural tube defects. Birth Defects Res A Clin Mol Teratol *88*, 633–652.

Nauli, S.M., Alenghat, F.J., Luo, Y., Williams, E., Vassilev, P., Li, X., Elia, A.E.H., Lu, W., Brown, E.M., Quinn, S.J., et al. (2003). Polycystins 1 and 2 mediate mechanosensation in the primary cilium of kidney cells. Nat Genet *33*, 129–137.

Nicastro, D., Schwartz, C., Pierson, J., Gaudette, R., Porter, M.E., and McIntosh, J.R. (2006). The Molecular Architecture of Axonemes Revealed by Cryoelectron Tomography. Science *313*, 944–948.

Norris, D.P. (2012). Cilia, calcium and the basis of left-right asymmetry. BMC Biol *10*, 102.

Oda, T., Yanagisawa, H., Yagi, T., and Kikkawa, M. (2014). Mechanosignaling between central apparatus and radial spokes controls axonemal dynein activity. J Cell Biol *204*, 807–819.

Oda, T., Abe, T., Yanagisawa, H., and Kikkawa, M. (2016). Structure and function of outer dynein arm intermediate and light chain complex. Mol. Biol. Cell mbc.E15-10-0723.

Oiwa, K. (2013). Dynein Motility: Mechanism. In Encyclopedia of Biophysics, G.C.K. Roberts, ed. (Springer Berlin Heidelberg), pp. 558–572.

Olbrich, H., Häffner, K., Kispert, A., Völkel, A., Volz, A., Sasmaz, G., Reinhardt, R., Hennig, S., Lehrach, H., Konietzko, N., et al. (2002). Mutations in DNAH5 cause primary ciliary dyskinesia and randomization of left–right asymmetry. Nat Genet *30*, 143–144.

Olcese, C., Patel, M.P., Shoemark, A., Kiviluoto, S., Legendre, M., Williams, H.J., Vaughan, C.K., Hayward, J., Goldenberg, A., Emes, R.D., et al. (2017). X-linked primary ciliary dyskinesia due to mutations in the cytoplasmic axonemal dynein assembly factor PIH1D3. Nature Communications *8*, 14279.

Omran, H., Kobayashi, D., Olbrich, H., Tsukahara, T., Loges, N.T., Hagiwara, H., Zhang, Q., Leblond, G., O'Toole, E., Hara, C., et al. (2008). Ktu/PF13 is required for cytoplasmic pre-assembly of axonemal dyneins. Nature *456*, 611–616.

Paff, T., Loges, N.T., Aprea, I., Wu, K., Bakey, Z., Haarman, E.G., Daniels, J.M.A., Sistermans, E.A., Bogunovic, N., Dougherty, G.W., et al. (2017). Mutations in PIH1D3 Cause X-Linked Primary Ciliary Dyskinesia with Outer and Inner Dynein Arm Defects. The American Journal of Human Genetics *100*, 160–168.

Pal, M., Morgan, M., Phelps, S.E.L., Roe, S.M., Parry-Morris, S., Downs, J.A., Polier, S., Pearl, L.H., and Prodromou, C. (2014). Structural Basis for Phosphorylation-Dependent Recruitment of Tel2 to Hsp90 by Pih1. Structure *22*, 805–818.

Pan, X., Ou, G., Civelekoglu-Scholey, G., Blacque, O.E., Endres, N.F., Tao, L., Mogilner, A., Leroux, M.R., Vale, R.D., and Scholey, J.M. (2006). Mechanism of transport of IFT particles in C. elegans cilia by the concerted action of kinesin-II and OSM-3 motors. The Journal of Cell Biology *174*, 1035–1045.

Panizzi, J.R., Becker-Heck, A., Castleman, V.H., Al-Mutairi, D.A., Liu, Y., Loges, N.T., Pathak, N., Austin-Tse, C., Sheridan, E., Schmidts, M., et al. (2012). CCDC103 mutations cause primary ciliary dyskinesia by disrupting assembly of ciliary dynein arms. Nat Genet *44*, 714–719.

Pazour, G.J., and Bloodgood, R.A. (2008). Chapter 5 Targeting Proteins to the Ciliary Membrane. B.-C.T. in D. Biology, ed. (Academic Press), pp. 115–149.

Pazour, G.J., Wilkerson, C.G., and Witman, G.B. (1998). A Dynein Light Chain Is Essential for the Retrograde Particle Movement of Intraflagellar Transport (IFT). The Journal of Cell Biology *141*, 979–992.

Pazour, G.J., Dickert, B.L., Vucica, Y., Seeley, E.S., Rosenbaum, J.L., Witman, G.B., and Cole, D.G. (2000). Chlamydomonas IFT88 and Its Mouse Homologue, Polycystic Kidney Disease Gene Tg737, Are Required for Assembly of Cilia and Flagella. The Journal of Cell Biology *151*, 709–718.

Peng, J., and Xu, J. (2011). RaptorX: exploiting structure information for protein alignment by statistical inference. Proteins *79*, 161–171.

Praveen, K., Davis, E.E., and Katsanis, N. (2015). Unique among ciliopathies: primary ciliary dyskinesia, a motile cilia disorder. F1000Prime Rep *7*.

Protter, D.S.W., and Parker, R. (2016). Principles and Properties of Stress Granules. Trends in Cell Biology *26*, 668–679.

Pugh, E.N. (2015). Photoreceptor disc morphogenesis: The classical evagination model prevails. J Cell Biol *211*, 491–493.

Raynaud-Messina, B., and Merdes, A. (2007). γ-tubulin complexes and microtubule organization. Current Opinion in Cell Biology *19*, 24–30.

Reiter, J.F., Blacque, O.E., and Leroux, M.R. (2012). The base of the cilium: roles for transition fibres and the transition zone in ciliary formation, maintenance and compartmentalization. EMBO Reports *13*, 608–618.

Roberts, A.J., Kon, T., Knight, P.J., Sutoh, K., and Burgess, S.A. (2013). Functions and mechanics of dynein motor proteins. Nat Rev Mol Cell Biol *14*, 713–726.

Rohatgi, R., and Snell, W.J. (2010). The ciliary membrane. Current Opinion in Cell Biology *22*, 541–546.

Rosenbaum, J.L., and Witman, G.B. (2002). Intraflagellar transport. Nat Rev Mol Cell Biol *3*, 813–825.

Rothfield, L.I. (2014). Structure and Function of Biological Membranes (Academic Press).

Satir, P., and Matsuoka, T. (1989). Splitting the ciliary axoneme: Implications for a "Switch-Point" model of dynein arm activity in ciliary motion. Cell Motil. Cytoskeleton *14*, 345–358.

Scholey, J.M. (2008). Intraflagellar transport motors in cilia: moving along the cell's antenna. The Journal of Cell Biology *180*, 23–29.

Schwarz-Romond, T., Fiedler, M., Shibata, N., Butler, P.J.G., Kikuchi, A., Higuchi, Y., and Bienz, M. (2007). The DIX domain of Dishevelled confers Wnt signaling by dynamic polymerization. Nat Struct Mol Biol *14*, 484–492.

Sear, R.P. (2007). Dishevelled: a protein that functions in living cells by phase separating. Soft Matter *3*, 680–684.

Shinohara, K., Chen, D., Nishida, T., Misaki, K., Yonemura, S., and Hamada, H. (2015). Absence of Radial Spokes in Mouse Node Cilia Is Required for Rotational Movement but Confers Ultrastructural Instability as a Trade-Off. Developmental Cell *35*, 236–246.

Signor, D., Wedaman, K.P., Orozco, J.T., Dwyer, N.D., Bargmann, C.I., Rose, L.S., and Scholey, J.M. (1999). Role of a Class Dhc1b Dynein in Retrograde Transport of Ift Motors and Ift Raft Particles along Cilia, but Not Dendrites, in

Chemosensory Neurons of Living Caenorhabditis elegans. The Journal of Cell Biology *147*, 519–530.

Singla, V., and Reiter, J.F. (2006). The Primary Cilium as the Cell's Antenna: Signaling at a Sensory Organelle. Science *313*, 629–633.

Sive, H.L., Grainger, R.M., and Harland, R.M. (2000). Early Development of Xenopus Laevis: A Laboratory Manual (Cold Spring Harbor Laboratory Press).

Sorokin, S. (1962). Centrioles and the Formation of Rudimentary Cilia by Fibroblasts and Smooth Muscle Cells. The Journal of Cell Biology *15*, 363–377.

Stepanek, L., and Pigino, G. (2016). Microtubule doublets are double-track railways for intraflagellar transport trains. Science *352*, 721–724.

Stubbs, J.L., Oishi, I., Izpisúa Belmonte, J.C., and Kintner, C. (2008). The forkhead protein Foxj1 specifies node-like cilia in Xenopus and zebrafish embryos. Nat Genet *40*, 1454–1460.

Stubbs, J.L., Vladar, E.K., Axelrod, J.D., and Kintner, C. (2012). Multicilin promotes centriole assembly and ciliogenesis during multiciliate cell differentiation. Nat Cell Biol *14*, 140–147.

Tarkar, A., Loges, N.T., Slagle, C.E., Francis, R., Dougherty, G.W., Tamayo, J.V., Shook, B., Cantino, M., Schwartz, D., Jahnke, C., et al. (2013). DYX1C1 is required for axonemal dynein assembly and ciliary motility. Nat Genet *45*, 995–1003.

Taschner, M., and Lorentzen, E. (2016). The Intraflagellar Transport Machinery. Cold Spring Harb Perspect Biol *8*, a028092.

Taschner, M., Bhogaraju, S., Vetter, M., Morawetz, M., and Lorentzen, E. (2011). Biochemical mapping of interactions within the intraflagellar transport (IFT) B core complex IFT52 binds directly to four other IFT-B subunits. J. Biol. Chem. *286*, 26344–26352.

Taschner, M., Bhogaraju, S., and Lorentzen, E. (2012). Architecture and function of IFT complex proteins in ciliogenesis. Differentiation *83*, S12–S22.

Taschner, M., Kotsis, F., Braeuer, P., Kuehn, E.W., and Lorentzen, E. (2014). Crystal structures of IFT70/52 and IFT52/46 provide insight into intraflagellar transport B core complex assembly. J Cell Biol *207*, 269–282.

Taschner, M., Weber, K., Mourão, A., Vetter, M., Awasthi, M., Stiegler, M., Bhogaraju, S., and Lorentzen, E. (2016). Intraflagellar transport proteins 172, 80, 57, 54,

38, and 20 form a stable tubulin-binding IFT-B2 complex. The EMBO Journal *35*, 773–790.

Toriyama, M., Lee, C., Taylor, S.P., Duran, I., Cohn, D.H., Bruel, A.-L., Tabler, J.M., Drew, K., Kelly, M.R., Kim, S., et al. (2016). The ciliopathy-associated CPLANE proteins direct basal body recruitment of intraflagellar transport machinery. Nat Genet *48*, 648–656.

Walentek, P., Beyer, T., Thumberger, T., Schweickert, A., and Blum, M. (2012). ATP4a Is Required for Wnt-Dependent Foxj1 Expression and Leftward Flow in Xenopus Left-Right Development. Cell Reports *1*, 516–527.

Wan, C., Borgeson, B., Phanse, S., Tu, F., Drew, K., Clark, G., Xiong, X., Kagan, O., Kwan, J., Bezginov, A., et al. (2015). Panorama of ancient metazoan macromolecular complexes. Nature *525*, 339–344.

Werner, C., Onnebrink, J.G., and Omran, H. (2015). Diagnosis and management of primary ciliary dyskinesia. Cilia *4*, 2.

Wheatley, D.N. (1969). Cilia in cell-cultured fibroblasts. I. On their occurrence and relative frequencies in primary cultures and established cell lines. J Anat *105*, 351–362.

Wheeler, J.R., Matheny, T., Jain, S., Abrisch, R., and Parker, R. (2016). Distinct stages in stress granule assembly and disassembly. eLife *5*, e18413.

Wheway, G., Parry, D.A., and Johnson, C.A. (2014). The role of primary cilia in the development and disease of the retina. Organogenesis *10*, 69–85.

Willett, M., Brocard, M., Davide, A., and Morley, S.J. (2011). Translation initiation factors and active sites of protein synthesis co-localize at the leading edge of migrating fibroblasts. Biochemical Journal *438*, 217–227.

Woodruff, J.B., Wueseke, O., Viscardi, V., Mahamid, J., Ochoa, S.D., Bunkenborg, J., Widlund, P.O., Pozniakovsky, A., Zanin, E., Bahmanyar, S., et al. (2015). Regulated assembly of a supramolecular centrosome scaffold in vitro. Science *348*, 808–812.

Woolley, D.M. (1998). Studies on the eel sperm flagellum. 3. Vibratile motility and rotatory bending. Cell Motil. Cytoskeleton *39*, 246–255.

Worthington, W.C., and Cathcart, R.S. (1963). Ependymal Cilia: Distribution and Activity in the Adult Human Brain. Science *139*, 221–222.

Yagi, T., Uematsu, K., Liu, Z., and Kamiya, R. (2009). Identification of dyneins that localize exclusively to the proximal portion of Chlamydomonas flagella. J Cell Sci *122*, 1306–1314.

Yamamoto, R., Hirono, M., and Kamiya, R. (2010). Discrete PIH proteins function in the cytoplasmic preassembly of different subsets of axonemal dyneins. The Journal of Cell Biology *190*, 65–71.

Yu, X., Ng, C.P., Habacher, H., and Roy, S. (2008). Foxj1 transcription factors are master regulators of the motile ciliogenic program. Nat Genet *40*, 1445–1453.

Zariwala, M.A., Gee, H.Y., Kurkowiak, M., Al-Mutairi, D.A., Leigh, M.W., Hurd, T.W., Hjeij, R., Dell, S.D., Chaki, M., Dougherty, G.W., et al. (2013). ZMYND10 Is Mutated in Primary Ciliary Dyskinesia and Interacts with LRRC6. The American Journal of Human Genetics *93*, 336–345.

Zhang, S., and Mitchell, B.J. (2015). Chapter 7 - Centriole biogenesis and function in multiciliated cells. In Methods in Cell Biology, R.B. and K. Oegema, ed. (Academic Press), pp. 103–127.

Zhang, W., Taylor, S.P., Nevarez, L., Lachman, R.S., Nickerson, D.A., Bamshad, M., Krakow, D., and Cohn, D.H. (2016). IFT52 mutations destabilize anterograde complex assembly, disrupt ciliogenesis and result in short rib polydactyly syndrome. Hum Mol Genet *25*, 4012–4020.

Zhao, L., Yuan, S., Cao, Y., Kallakuri, S., Li, Y., Kishimoto, N., DiBella, L., and Sun, Z. (2013). Reptin/Ruvbl2 is a Lrrc6/Seahorse interactor essential for cilia motility. PNAS *110*, 12697–12702.

Zimmerman, K., and Yoder, B.K. (2015). SnapShot: Sensing and Signaling by Cilia. Cell *161*, 692–692.

Zwicker, D., Decker, M., Jaensch, S., Hyman, A.A., and Jülicher, F. (2014). Centrosomes are autocatalytic droplets of pericentriolar material organized by centrioles. PNAS *111*, E2636–E2645.